ANTIOXIDANT WITH ANTIMELANOGENIC ACTIVITIES OF SERICIN HYDROLYSATES
OPTIMIZED BY RESPONSE SURFACE METHODOLOGY IN HUMAN MELANIN-GENERATING
MNT-1 CELLS

Mr. Keerati Joyjamras

A Dissertation Submitted in Partial Fulfillment of the Requirements
for the Degree of Doctor of Philosophy in Pharmaceutical Sciences and Technology
Common Course
FACULTY OF PHARMACEUTICAL SCIENCES
Chulalongkorn University
Academic Year 2021
Copyright of Chulalongkorn University

ฤทธิ์ต้านออกซิเดชันร่วมกับฤทธิ์ยับยั้งการผลิตเมลานินของเซริซินไฮโดรไลเสทที่เพิ่มประสิทธิภาพ
ด้วยระเบียบวิธีพื้นผิวตอบสนองในเซลล์ผลิตเมลานินของมนุษย์ ชนิดเอ็มเอ็นที-1

นายกีรติ จ้อยจำรัส

วิทยานิพนธ์นี้เป็นส่วนหนึ่งของการศึกษาตามหลักสูตรปริญญาวิทยาศาสตรดุษฎีบัณฑิต
สาขาวิชาเภสัชศาสตร์และเทคโนโลยี ไม่สังกัดภาควิชา/เทียบเท่า
คณะเภสัชศาสตร์ จุฬาลงกรณ์มหาวิทยาลัย
ปีการศึกษา 2564

Thesis Title   ANTIOXIDANT WITH ANTIMELANOGENIC ACTIVITIES OF SERICIN

                             HYDROLYSATES OPTIMIZED BY RESPONSE SURFACE

                             METHODOLOGY IN HUMAN MELANIN-GENERATING MNT-1 CELLS
By   Mr. Keerati Joyjamras
Field of Study   Pharmaceutical Sciences and Technology
Thesis Advisor   Professor PITHI CHANVORACHOTE, Ph.D.
Thesis Co Advisor   Assistant Professor CHATCHAI CHAOTHAM, Ph.D.

        Accepted by the FACULTY OF PHARMACEUTICAL SCIENCES, Chulalongkorn University in
Partial Fulfillment of the Requirement for the Doctor of Philosophy

-- Dean of the FACULTY OF

                                                   PHARMACEUTICAL SCIENCES

        (Professor PORNANONG ARAMWIT, Ph.D.)

DISSERTATION COMMITTEE

-- Chairman

        (Associate Professor Uraiwan Panich, M.D., Ph.D.)

-- Thesis Advisor

        (Professor PITHI CHANVORACHOTE, Ph.D.)

-- Thesis Co-Advisor

        (Assistant Professor CHATCHAI CHAOTHAM, Ph.D.)

-- Examiner

        (Professor WANCHAI DE-EKNAMKUL, Ph.D.)

-- Examiner

        (Assistant Professor ROSSARIN TANSAWAT, Ph.D.)

-- Examiner

        (WANATCHAPORN ARUNMANEE, Ph.D.)

กีรติ จ้อยจำรัส : ฤทธิ์ต้านออกซิเดชันร่วมกับฤทธิ์ยับยั้งการผลิตเมลานินของเซริซินไฮโดรไลเสทที่เพิ่มประสิทธิภาพด้วยระเบียบ วิธีพื้นผิวตอบสนองในเซลล์ผลิตเมลานินของมนุษย์ ชนิดเอ็มเอ็นที-1. (ANTIOXIDANT WITH ANTIMELANOGENIC ACTIVITIES OF SERICIN HYDROLYSATES OPTIMIZED BY RESPONSE SURFACE METHODOLOGY IN HUMAN MELANIN-GENERATING MNT-1 CELLS) อ.ที่ปรึกษาหลัก : ศ. ภก. ดร.ปิติ จันทร์วรโชติ, อ.ที่ปรึกษาร่วม : ผศ. ภก. ดร.ฉัตรชัย เชาว์ธรรม

โปรตีนเซริซินในน้ำทิ้งจากอุตสาหกรรมไหมก่อให้เกิดมลพิษทางน้ำและปัญหาทางระบบนิเวศ เพื่อเพิ่มมูลค่าทางเศรษฐกิจให้กับ ของเสียชนิดนี้ สภาวะที่เหมาะสมในการย่อยด้วยเอนไซม์เพื่อการผลิตเซริซินไฮโดรไลเสทประสิทธิภาพสูงในการต้านอนุมูลอิสระและยับยั้งการ ผลิตเมลานินได้ถูกค้นหาด้วยระเบียบวิธีพื้นผิวตอบสนอง แผนภาพความสัมพันธ์พื้นผิวตอบสนองแสดงให้เห็นถึงบทบาทที่สำคัญของอุณหภูมิต่อ ความสามารถในการกำจัดอนุมูลอิสระของเซริซินไฮโดรไลเสทที่ทดสอบด้วยวิธี DPPH, FRAP และ ORAC การตรวจสอบด้วยวิธีเปปไทโดมิกซ์ และ SDS-PAGE พบว่าเซริซินที่ย่อยด้วยเอนไซม์อัลคาเลสประกอบด้วยเปปไทด์ที่เกี่ยวข้องกับเซริซินในปริมาณที่แตกต่างและมีขนาดเล็กกว่า เปปไทด์ในเซริซินที่ไม่ผ่านการย่อย การบ่มด้วย 20 มิลลิกรัมต่อมิลลิลิตร ของเซริซินไฮโดรไลเสทที่ดัดแปลงด้วยอัลคาเลสภายใต้สภาวะที่ปรับ ด้วยระเบียบวิธีพื้นผิวตอบสนอง (สัดส่วนเอนไซม์ต่อสารตั้งต้น: 1.5, ค่าความเป็นกรด-ด่าง: 7.5, อุณหภูมิ: 70 องศาเซลเซียส) แสดงให้ถึงฤทธิ์ ต้านอนุมูลอิสระต่อไฮโดรเจนเปอร์ออกไซด์ ความเข้มข้น 1 มิลลิโมลาร์ ที่สูงกว่า ในเซลล์ผิวหนัง ชนิดฮาเคท และเซลล์ผลิตเมลานิน ชนิดเอ็ม เอ็นที-1 เมื่อเปรียบเทียบกับ 5 มิลลิโมลาร์ N-acetyl cysteine ค่าความเข้มข้นที่ยับยั้งการผลิตเมลานินครึ่งหนึ่ง ที่ 9.05 ± 0.66 มิลลิกรัมต่อ มิลลิลิตร ของเซริซินไฮโดรไลเสท ซึ่งต่ำกว่าค่าของเซริซินไม่ดัดแปลง (24.54 ± 0.17 มิลลิกรัมต่อมิลลิลิตร) แสดงถึงประสิทธิภาพของเซริซิน ไฮโดรไลเสทในการยับยั้งการผลิตเมลานิน การได้รับเซริซินไฮโรไลเสท 20 มิลลิกรัมต่อมิลลิลิตรไม่เพียงยับยั้งการทำงานแต่ยังลดการแสดงออก ของโปรตีนไทโรซิเนสในเซลล์เอ็มเอ็นที-1 การตรวจหาปริมาณด้วย RT-PCR พบการลดลงของ mRNA ของ MITF โปรตีนควบคุมการสังเคราะห์ ไทโรซิเนส ซึ่งสอดคล้องกับการลดลงของสัญญาณต้นน้ำชนิด pCREB/CREB ที่ตรวจสอบด้วยวิธี western blot ในเซลล์เอ็มเอ็นที-1 ที่ได้รับเซริ ซินไฮโดรไลเสท 20 มิลลิกรัมต่อมิลลิลิตร เป็นระยะเวลา 12 ชั่วโมง เป็นที่น่าสนใจว่าการได้รับเซริซินที่ดัดแปลงด้วยอัลคาเลสนาน 6-24 ชั่วโมง เพิ่มปริมาณโปรตีน pERK ที่กระตุ้นการทำลายโปรตีน MITF ในเซลล์เอ็มเอ็นที-1 ข้อมูลที่ได้จะช่วยส่งเสริมการนำโปรตีนของเสียจาก อุตสาหกรรมไหมมาใช้หมุนเวียนเป็นสารต้านอนุมูลอิสระและสารยับยั้งการผลิตเมลินินที่มีประสิทธิภาพ

จุฬาลงกรณ์มหาวิทยาลัย
CHULALONGKORN UNIVERSITY

สาขาวิชา	เภสัชศาสตร์และเทคโนโลยี	ลายมือชื่อนิสิต ....
ปีการศึกษา	2564	ลายมือชื่อ อ.ที่ปรึกษาหลัก ....
		ลายมือชื่อ อ.ที่ปรึกษาร่วม ....

6176453033 : MAJOR PHARMACEUTICAL SCIENCES AND TECHNOLOGY

KEYWORD: Sericin, Enzymatic hydrolysis, wastewater, Melanogenesis, MITF, Tyrosinase, Reactive oxygen species, Response surface methodology, Alcalase®

Keerati Joyjamras : ANTIOXIDANT WITH ANTIMELANOGENIC ACTIVITIES OF SERICIN HYDROLYSATES OPTIMIZED BY RESPONSE SURFACE METHODOLOGY IN HUMAN MELANIN-GENERATING MNT-1 CELLS. Advisor: Prof. PITHI CHANVORACHOTE, Ph.D. Co-advisor: Asst. Prof. CHATCHAI CHAOTHAM, Ph.D.

Sericin, a protein presenting in the wastewater from silk industry, causes water pollution and ecological problem. To increase economic value to this waste product, the optimum enzymatic condition that could create sericin hydrolysates with high antioxidant and antimelanogenic capacities was generated through response surface methodology (RSM). Response surface plots demonstrate the major role of temperature on scavenging capacity of sericin hydrolysates assessed via DPPH, FRAP and ORAC assays. Alcalase®-hydrolyzed sericin consisted of sericin-related peptides in differing amounts and smaller sizes compared with unhydrolyzed sericin, as respectively demonstrated by peptidomic and SDS-PAGE analysis. Pre-incubation with 20 mg/mL sericin hydrolysates digested by Alcalase® at RSM-optimized condition (enzyme/substrate ratio: 1.5, pH: 7.5, temperature: 70°C) exhibited higher antioxidant activity against 1 mM hydrogen peroxide in human HaCat keratinocytes and melanin-generating MNT-1 cells when compared with 5 mM N-acetyl cysteine. The lower half maximum inhibitory concentration was 9.05 ± 0.66 mg/mL compared with unhydrolyzed sericin (24.54 ± 0.17 mg/mL) indicated a potent effect of Alcalase®-hydrolyzed sericin on inhibiting melanin production in MNT-1 cells. Not only inhibiting enzymatic activity but also downregulated expression of tyrosinase was evident in MNT-1 cells incubated with 20 mg/mL sericin hydrolysates. Quantitative RT-PCR revealed the decreased mRNA level of MITF, a tyrosinase transcription factor, which correlated with the reduction of pCREB/CREB, an upstream cascade, as assessed by western blot analysis in MNT-1 cells cultured with 20 mg/mL sericin hydrolysates for 12 h. Interestingly, treatment with Alcalase®-hydrolyzed sericin for 6-24 h also upregulated pERK, a molecule that triggers MITF degradation in human melanin-producing cells. The acquired information would facilitate the recycling of waste products from silk industry as an effective antioxidant and antimelanogenic compound.

Field of Study:	Pharmaceutical Sciences and Technology	Student's Signature	
Academic Year:	2021	Advisor's Signature	
		Co-advisor's Signature	

ACKNOWLEDGEMENTS

TABLE OF CONTENTS

LIST OF TABLES

LIST OF FIGURES

Page

CHAPTER 1

INTRODUCTION

Background and rationale

The rapid expansion of industries to supply consumable products, globally unavoidably causes of ecological problems (1). Without proper management, sericin protein presenting in the degumming water used in silk processing results in a high level of chemical oxygen demand (COD), which contributes to water pollution (2). In seeking to recycle the wastewater from silk production, several researchers have discovered the potential benefits of silk sericin (3),(4),(5). Silk protein, which is produced from *Bombyx mori*, comprises with 25-30% sericin protein wrapped around fibroin fiber (6). The globular structure of water-soluble sericin consists of diverse amino acids, among which serine, histidine, glycine, threonine, tyrosine, aspartate and glutamine are predominant (3). Recently, several biological functions of sericin have been reported, including antioxidant and anti-tyrosinase activities (7),(8),(9).

Scavenging activity, or the capability to eliminate the unpaired electron in oxygen and other molecules, is one of the major characteristics of antioxidant compounds (10). Through direct interaction with reactive oxygen species (ROS), antioxidants can restrain oxidative stress and prevent the propagation of oxidative

chain reactions, which otherwise damage cellular organelles (11). Moreover, the application of natural antioxidants has been researched in food, pharmaceutical and cosmetic products (12),(13). It is widely accepted that the antioxidant capacity of natural compounds can be accessed through various *in vitro* assays, including 2,2-diphenyl-1-picrylhydrazyl (DPPH) radical scavenging activity, ferric-reducing antioxidant power (FRAP) and oxygen radical absorbance capacity (ORAC) (14). Based on the donation of a single electron to free radicals and ferric ions (Fe^{3+}), antioxidant activity can be respectively determined using DPPH and FRAP assays (15). Despite their simplicity and repeatability, DPPH and FRAP assays carry the drawback of irrelevance to biological ROS and physiological conditions (16). Therefore, ORAC assay, which generates peroxyl radicals ($ROO^{\cdot}$), is introduced to examine the translocation of hydrogen atoms from antioxidant to oxygen molecules (17). According to diverse mechanisms of action, ROS scavenging activity of antioxidant compounds is recommended to be evaluated through several methods (18),(19),(20).

Intriguingly, the ROS scavenging capacity of peptides, in both natural and hydrolyzed forms, is well established (21),(22),(23). While the antioxidant potential of sericin and sericin hydrolysates has largely been evidenced by DPPH assay (6),(24),(25), the study of scavenging activity of sericin hydrolysates prepared by specific enzymes against diverse free radicals is still limited (26),(27). To optimize conditions in both laboratory and industrial scenarios, response surface methodology (RSM), a type of statistical and mathematical analysis, has been broadly applied (28).

RSM gathers the effects of different independent factors to generate an applicable model for desired output (29). Variables in enzymatic reactions, including pH, temperature and enzyme/substrate ratio are acquired from RSM in this study, and analyzed to discover the optimum conditions for antioxidant activity of sericin hydrolysates assessed via DPPH, FRAP and ORAC assays.

The inhibitory potential of sericin against enzymatic activity of mushroom tyrosinase has been recently indicated (24),(29). Interestingly, anti-tyrosinase activity of sericin and sericin hydrolysates seem to be correlated with their ROS scavenging activity (25). Nevertheless, the effect of sericin hydrolysates on tyrosinase enzyme isolated from human melanin-generating cells has not been investigated. Despite composing of various regulatory proteins, tyrosinase has been considered as a rate limiting enzyme, which catalysts tyrosine amino acid to melanin pigment in melanogenesis pathway. Thus, tyrosinase inhibitors have been widely accepted as effective depigmenting agents in cosmetic application (30). Not only determining color tone but also protecting skin cells from environmental exposures, especially ultraviolet (UV) radiation which is an important role of epidermal melanin. However, the overproduction of melanin, or hyperpigmented condition, also causes many health problems and aesthetic concerns (31). Large number of available whitening cosmetic products reflects health concern in hyperpigmented condition that affects self-confidence and quality of life. Although, various synthetic and natural

hypopigmenting agents have been continuously introduced but most of them own short efficacy and serious side effects (32).

Melanocytes that located at the bottom layer of epidermis are responsible for melanin production through melanogenesis pathway. The expression of tyrosinase, tyrosinase-related protein-1 (TRP-1) and tyrosinase-related protein-2 (TRP-2 or dopachrome tautomerase; Dct) is regulated by microphthalmia-associated transcription factor (MITF) (33). From the fact that the production of melanin is also mediated by cyclic adenosine 3',5'-monophosphate (cAMP), activation of cAMP results in phosphorylation of cAMP response element-binding protein (CREB), which in turn provokes MITF transcription (34). MITF is also post-translationally modulated by mitogen-activated protein kinase (MAPKs)/extracellular signal-regulated protein kinase (ERK) signal. Activated ERK (pERK) triggers proteasomal degradation of MITF consequence with diminished level of tyrosinase and suppression of melanin synthesis (35),(36). According to regulatory role on tyrosinase expression, MITF has been proposed as a novel target for antimelanogenic compound that could provide sustainable effect on preventing melanin production (37),(38).

This study aims to optimize enzymatic condition for preparation of sericin hydrolysates containing high ROS scavenging activity against various free radicals through RSM compared with unhydrolyzed sericin and known antioxidant. Furthermore, antimelanogenic activity and related mechanisms of RSM-optimized sericin hydrolysates were investigated in human melanin-generating cells. The

obtained information would be benefit for recycling and utilizing sericin, a waste product from the silk industry, as a potent antioxidant and hypopigmenting agent for further development of a safe and effective cosmeceutical products.

Research questions

1. Does an optimum enzymatic condition for preparing sericin hydrolysates possess ROS scavenging capacity against various free radicals obtained from RSM?

2. Does RSM optimized-sericin hydrolysates exhibit antimelanogenic activity via modulating MITF in human melanin-generating cells?

Objectives

1. To optimize condition of enzymatic hydrolysis and ROS scavenging activity of sericin hydrolysates through RSM.

2. To investigate antimelanogenic activity and related mechanisms of RSM optimized-sericin hydrolysates in human melanin-generating cells.

Hypotheses

1. The optimum condition for preparation of sericin hydrolysates containing high ROS scavenging activity against various free radicles could be obtained from RSM.

2. RSM optimized-sericin hydrolysates could inhibit melanin synthesis through regulating on MITF-related proteins.

Expected benefits

1. The optimum enzymatic condition for preparing sericin hydrolysates containing potential ROS scavenging activity against diverse free radicals and biological antioxidant activity.

2. The information of antimelanogenic activity and related mechanisms of sericin hydrolysates for further recycling the waste product from silk industry as a cosmeceutical ingredient.

CHAPTER 2

LITERATURE REVIEWS

Silk sericin protein

Silk is a protein fiber spontaneously synthesized during specific lifetime of various animals, including silkworm and spider. In fabric industry, a silkworm, *Bombyx mori*, is a major source of natural silk production. Silk fiber containing in cocoons, which are derived during the end of larval stage of *Bombyx mori*, comprises with 70-80% fibroin, 20-30% sericin and 1-5% other components, including wax, sugars, minerals and pigments (Figure 1) (39),(40). Fibroin is glycoprotein fiber used for producing silk thread while sericin is protein polymer connecting fibroin filaments and protecting cocoons against environmental stimuli (40). In the degumming step of silk processing, sericin that acts as glue protein wrapping around fibroin will be removed from cocoons by boiling in hot water.
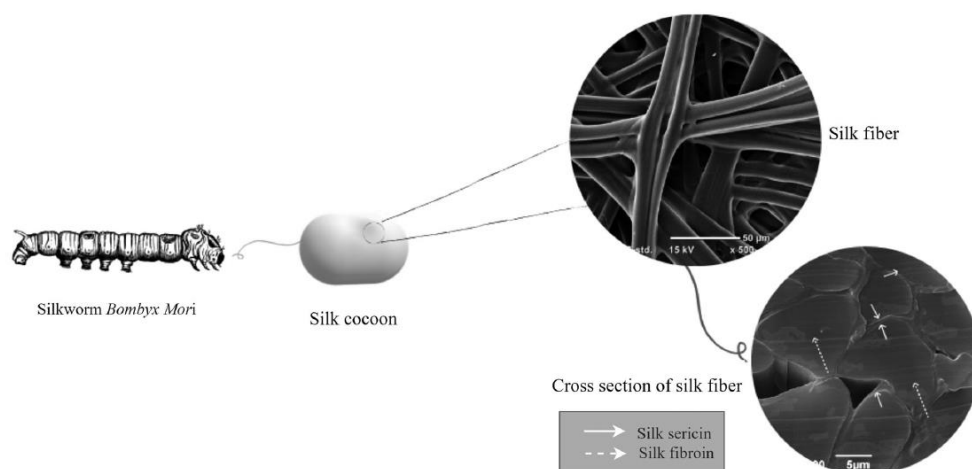
Figure 1 *Cross-sectional image obtained from scanning electron microscopy (SEM) of silk fiber presents sericin (solid arrow) linking each fibroin filament (dash arrow) together. (39).*

Approximately, 50,000 tons of sericin present as a production waste from silk industry all over the world (41). Without proper management, sericin protein presenting in the degumming water results in a high level of chemical oxygen demand (COD), which contributes to water pollution (2). Recently, sericin from industrial waste can be recovered after separation of low molecular weight impurities via dialysis following with further freeze-drying of the solution containing sericin (42). In seeking to recycle the wastewater from silk production, several researchers have discovered the potential benefits of silk sericin (3),(4),(5).

Structure and amino acid composition of silk sericin

Despite composing of polar amino acids, sericin possesses low water solubility, and forms gel at room temperature. Boiling with hot water (≥ 50–60°C) during degumming process activates the transformation of β-sheet, which responses for gel forming, into random coil (amorphous) structure of globular sericin that can increase water solubility (3). Sericin contains different 18 amino acids in which 30-39% serine has been considered as one of the identical characters of sericin (Table 1). Additionally, sericin is constructed by 14-16% glycine, 11-15% asparagine acid, and 8-10% threonine (42). Among these amino acids, polar amino acid accounts for 42.3% while non-polar amino acids are about 12.2% (45). Moreover, inorganic constituents, including carbon, oxygen, nitrogen, and hydrogen also present in sericin (3). According to solubility and location surrounding fibroin, sericin can be differentiated into three types of A, B and C (Figure 2). As an adhesive protein, sericin fasten two strands of fibroin for forming silk filament in cocoons. Presenting in the outer layer, sericin A composing of nitrogen, serine, threonine, glycine and aspartic is soluble in boiling water. Sericin B comprising of nitrogen, serine, threonine, glycine, aspartic and tryptophan locates at the middle layer. For the inner layer attaching closely to fibroin is sericin C, which is insoluble and contain nitrogen, sulphur, serine, threonine, glycine, aspartic, tryptophan and proline (45),(46).
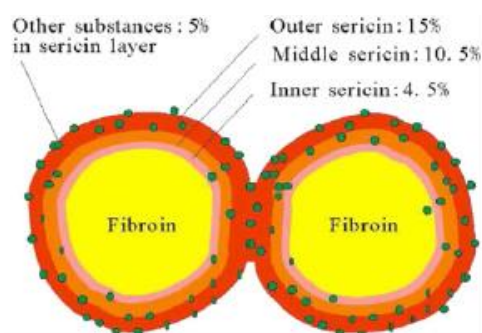
Figure 2 *Diagram illustrates sericin layers wrapping around fibroin (40).*

Table 1 Amino acid composition (mol%) in silk sericin and fibroin proteins (40).

No	Amino acids	S	So	Sm	Si	F
1	Gly	17.85	16.29	16.35	17.87	42.62
2	Ala	6.70	5.20	6.13	11.58	33.38
3	Val*	4.05	3.77	4.27	5.43	2.58
4	Leu*	1.49	1.21	1.77	4.06	0.54
5	Ile*	1.02	0.79	1.17	3.76	0.72
6	Phe*	0.67	0.64	0.66	2.49	0.81
7	Met*	0.31	-	-	0.83	0.15
8	Pro	0.81	-	0.64	-	0.47
9	Thy	3.10	2.87	3.98	4.09	5.84
10	Cys	0.38	0.69	0.95	0.75	0.26
11	Ser	25.50	28.00	25.57	13.32	7.65
12	Thr*	7.47	7.78	8.13	5.66	0.85
13	Asp	18.38	17.97	17.08	15.83	1.79
14	Glu	5.74	6.25	4.65	7.34	1.36
15	His	1.32	1.32	1.69	1.38	0.21
16	Lys*	2.08	3.72	3.16	2.18	0.33
17	Arg	3.12	3.52	3.83	3.41	0.44

S: Sericin, So: Outer sericin, Sm: Middle sericin, Si: Inner sericin, F: Fibroin

* represents essential amino acid

Molecular weight distribution of sericin is variable depending on extraction methods (29),(41). The reported methods for isolating sericin from silk cocoons, include denaturing with boiled detergent or alkaline compounds, enzymatic digestion, steaming, ultrafiltration and infrared ray which present sericin constituents ranged from 10 to 310 kDa (25),(47). Naturally, polypeptide at ~ 400, 250 and 150 kDa have been revealed in silk sericin (42). Teramoto, *et al*. (2005) demonstrated the separated band of protein constituents detected via SDS-PAGE analysis in soluble fraction of sericin at low temperature (Figure 3). Meanwhile, the extraction at high temperature of 121°C provided continuous distribution of sericin proteins range from < 50 to 250 kDa (42). Moreover, the distribution of protein between 5 to 50 kDa had been reported in sericin obtained from spray-drying (45). These modifications of protein distribution pattern could arise from denaturing and transformation of β-sheet to random coil structure during extraction process (48). General information of sericin characteristic is indicated in Table 2.
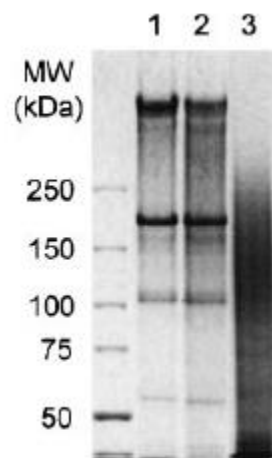
Figure 3 *SDS-PAGE analysis of protein distribution in sericin obtained from 1) water soluble at room temperature, 2) boiling water for 20 min, and 3) autoclave at 121°C for 20 min (41).*

Biological activities and applications of sericin

Biological activities and potential therapeutic applications of sericin have been continuously discovered. Recently, cosmetic products containing sericin as an active ingredient are commercially available. These cosmetic preparations highlight sericin as skin moisturizer, sun protectant, antioxidant, brightening agent and anti-aging substance. Not only aesthetic application but also therapeutic potentials, including anti-bacterial, anti-inflammation and anti-cancer as well as biocompatible and biodegradable property bring attention to biological activity of sericin (Figure 4) (3),(49). It is the fact that amino acid constituents and secondary structure resulted from diverse extraction and modification methods critically influence on biological

activities of sericin (3). Gel forming capability and high glycine and serine containing involve with moisturizing property of sericin (44),(50). Sericin at low molecular weight (<100 kDa) possesses high proliferative effect in human fibroblast (51). However, toxic profile of small size sericin is also demonstrated at high concentration (>100 µg/mL) in both normal and cancer cells (51),(52),(53).

Table 2 *General characters of silk sericin (42)*

Attributes	Properties
Characteristics	White/yellow, water soluble, odor free, and sweet in taste. Moisture content is 10-17%.
Morphology	Wrinkled particles due to collapse of hollow spherical structures on rapid evaluation.
Molecular weight	Ranges from 17100 to 18460 or 90-125 kDa.
Solubility	Insoluble in cold water, soluble in hot water. Solubility increases with addition of polyacrylate and decreases with addition of formaldehyde.
Isoelectric pH	As it contains more of basic amino acids, its isoelectric pH is 4.0.
Sol-gel transition	It gets transformed to fluid at 50-60 °C and returns to gel form on cooling.

Sericin mediates protective effect against UVB-induced cell damage via modulating cellular oxidative stress (54). Intriguingly, greater scavenging activity against reactive oxygen species (ROS) can be achieved after modified structure and component of sericin. Short chain sericin peptide comprising of arginine, valine or

tyrosine indicates the direct inhibition on enzymatic activity of mushroom tyrosinase

(55),(29). Moreover, flavonoids and carotenoid presenting in degumming water also

involve with anti-tyrosinase activity (29).
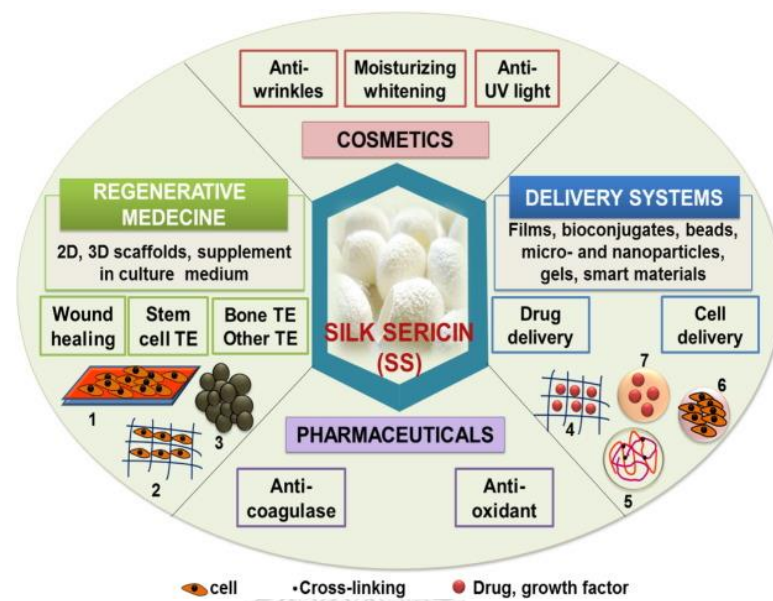
Figure 4 *Potential applications of sericin from silk cocoons. TE: tissue engineering*

(48).

Although the immune modulating effect of sericin is still controversial, many

biomaterials and drug delivery systems have been developed from sericin

(3),(49),(56). According to hydrophilic property and stimulation of collagen synthesis,

the benefits of sericin in tissue engineering have been highlighted (3),(57),(58).

Response to pH adjustment and composing of OH containing amino acid are

principal properties of sericin, which is suitable for drug delivery application (48),(59).

Not only sustain release hydrogel but also conjugation with drugs or other molecules gains attention for development of sericin as drug delivery systems (60),(61),(62),(63),(64).

Furthermore, the benefits of sericin as dietary supplements and food additives are constantly documented. The improvement of glucose and lipid metabolism was demonstrated in high-fat diet rat administrated with sericin (65),(66). Focusing on obesity and cardiovascular disease, supplementation with high sericin containing cocoon extracts significantly reduced plasma cholesterol and triglyceride, and lowered fat weight in high-fat diet mice (67). Surprisingly, very low molecular weight (< 5 kDa) of sericin protein decreased blood pressure through vasodilation (68). It should be noted that chemical reagent as well as extraction and isolation procedure need to be validated for suitable preparation of food grade sericin.

Reactive oxygen species

Reactive oxygen species (ROS) are active substances that highly interact with other molecules consequence with oxidative chain reaction, damaged biological molecules and injured cellular organelles. Both non-free radical and free radical oxygen atom is the active site of ROS. Indeed, reactive nitrogen, reactive sulfur, reactive iron and reactive copper species also play a role in oxidative chain reaction and ROS initiation (69). Despite being harmful at high concentration, low amount of

ROS is essential for mediating cellular signaling pathways. The optimal level of cellular ROS is tightly modulated by intrinsic antioxidant mechanism. As involving in many pathological conditions, the unbalance between generated ROS and cellular antioxidant molecules results in oxidative stress, damaged organelles and eventually cell death (70). Cellular ROS are contributed by endogenous pathways and exogenous stimuli. Exposure to pollutants, toxins, radiations and ozone as well as microbial infections and extensive exercise account for over-production of cellular ROS (71). Superoxide anions ($O_2^{\cdot-}$), hydrogen peroxide (H_2O_2), and hydroxyl radical ($OH^{\cdot}$) are major endogenous ROS generated during cellular metabolism and oxidative phosphorylation in mitochondria (72). Among these, $O_2^{\cdot-}$ and $OH^{\cdot}$ are considered as free radical due to containing an unpaired electron (70). Superoxide anions are initially generated from oxygen molecules, which act as an electron acceptor in mitochondrial electron transport and from the catalytic enzyme reaction of cytoplasmic xanthine oxidase (Figure 5). Then, superoxide dismutase (SOD) converts $O_2^{\cdot-}$ into H_2O_2, which is detoxified to H_2O by glutathione-redox system or catalase. However, H_2O_2 is also being a substrate for generating $OH^{\cdot}$, the most dangerous ROS via Fenton reaction (73),(74),(75). The commonly found endogenous ROS are presented in Table 3 (70).

Table 3 *General endogenous ROS (70)*

Oxidant	Formula	Reaction Equation
Superoxide anion	$O_2^{\cdot-}$	$NADPH + 2O_2 \leftrightarrow NADP^+ + 2O_2^{\cdot-} + H^+$ $2O_2^{\cdot-} + H^+ \rightarrow O_2 + H_2O_2$
Hydrogen peroxide	H_2O_2	Hypoxanthine $+ H_2O + O_2 \leftrightarrows$ xanthine $+ H_2O_2$ xanthine $+ H_2O + O_2 \leftrightarrows$ uric acid $+ H_2O_2$
Hydroxyl radical	$^{\cdot}OH$	$Fe^{2+} + H_2O_2 \rightarrow Fe^{3+} + OH^- + {^{\cdot}OH}$
Hypochlorous acid	HOCl	$H_2O_2 + Cl^- \rightarrow HOCl + H_2O$
Peroxyl radicals	$ROO^{\cdot}$	$R^{\cdot} + O_2 + ROO^{\cdot}$
Hydroperoxyl radical	$HOO^{\cdot}$	$O_2^- + H_2O \leftrightarrows HOO^{\cdot} + OH^-$
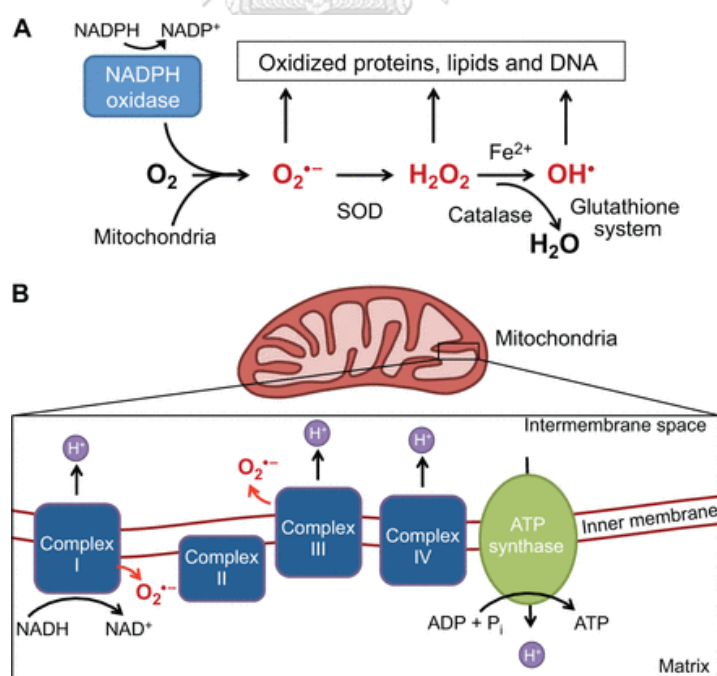
Figure 5 *Generation of major cellular ROS (75).*

To maintain optimal ROS level, which benefits for biological function, cellular redox status is regulated by enzymatic antioxidant and non-enzymatic antioxidant mechanisms. Despite conversion of $O_2^{\cdot-}$ into H_2O_2, SOD is classified as cellular enzymatic antioxidant that covers catalase (CAT) and glutathione redox system related proteins, including glutathione peroxidase (GPx) and glutathione transferase (GST) (70),(73). Meanwhile ascorbic acid (vitamin C), α-tocopherol (vitamin E), glutathione (GSH), β-carotene and uric acid are categorized as non-enzymatic antioxidant molecules (76). These non-enzymatic antioxidant molecules directly interact with an unpaired electron on ROS to terminate the oxidative chain reaction (70). Additionally, vitamin C, vitamin E, carotenoids, and flavonoids are exogenous antioxidants, which can be dietary intake from food (77).

Free radical scavenger

At low concentration, antioxidants are the substances that can inhibit or prevent damage induced by ROS (78). Antioxidants possibly modulate oxidative stress through various machineries, including direct interaction with free radicals, suppression of ROS generation and regulation of antioxidant enzymes (79). Generally, free radical scavengers are defined as small molecules that are able to react with ROS and other free radicals via donating hydrogen atom or acceptance of free electron (10),(80). Moreover, ROS scavengers can synergize function of other free radical scavengers and cellular antioxidant (78). According to physical property and

mode of action, ROS scavengers can be classified as water/lipid-soluble and primary/secondary antioxidant. Because of producing stable radicals, the propagation of oxidative chain reaction can be stopped after the interaction between primary antioxidants and ROS. Meanwhile, secondary antioxidants can facilitate antioxidant mechanism via regenerating primary antioxidant (10). Such recycling of ROS scavengers includes the regeneration of active tocopherols (vitamin E), a lipid-soluble antioxidant, from a phenyl radical by a water-soluble antioxidant vitamin C (Figure 6) (79). Additionally, secondary antioxidants are considerably delay and restrain oxidation, and promote activity of metal ions, singlet oxygen, pro-oxidative enzymes and oxidative molecules through redox reactions (10). It should be noted that despite direct interaction with ROS, not all ROS scavengers efficiently provide stable free radical molecule, or stop oxidative chain reaction (80).
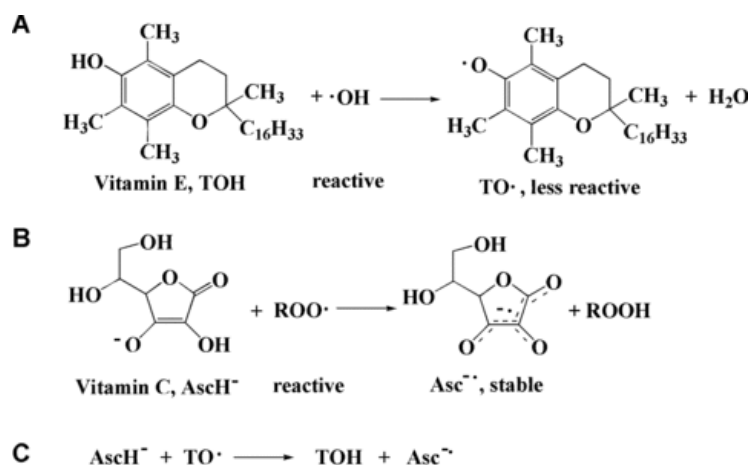
Figure 6 *Scavenging activity of A) vitamin E, a secondary antioxidant, B) vitamin C, a primary antioxidant, and C) the regeneration of vitamin E from a phenyl radical mediated by vitamin C (79).*

Scavenging agents for free radicals and ROS can be intrinsically found in cellular antioxidant such as vitamin C, vitamin E and glutathione, or exogenously obtained from dietary intakes. Recently, therapeutic potentials of free radical scavengers from natural extracts, including plant-derived phenolic compounds and protein hydrolysates obtained from various resources, have been continuously demonstrated (81),(82),(83),(84). These free radical scavengers might compose of aromatic ring in which electron delocalization occurs to create stable free radicals (79).

As mention above, antioxidants (AH) can transfer their hydrogen atom to neutralize free electron presenting in ROS (ROO$^{\bullet}$ and RO$^{\bullet}$) and free radicals (R$^{\bullet}$) as following.

$$R^\bullet + AH \longrightarrow RH + A^\bullet$$

$$ROO^\bullet + AH \longrightarrow ROOH + A^\bullet$$

$$RO^\bullet + AH \longrightarrow ROH + A^\bullet$$
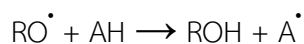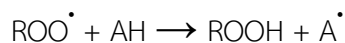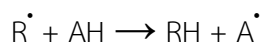
Considering the product of antioxidant ($A^\bullet$), these antioxidant radicals can be inactivated through delocalization of the unpaired electron in aromatic ring, or further accept electron from another free radical to generate non-radical compound as indicted below (85).

$$ROO^\bullet + A^\bullet \longrightarrow ROOA$$

$$RO^\bullet + A^\bullet \longrightarrow ROA$$

$$A^\bullet + A^\bullet \longrightarrow AA$$

According to diverse mechanisms of action, ROS scavenging activity of antioxidant compounds is recommended to be evaluated through several methods (18),(19),(20). It is widely accepted that antioxidant capacities of natural compounds can be accessed through both chemical and biological models. Due to high sensitivity and simple protocol, chemical antioxidant assays are usually performed for screening ROS scavenging activity though there are less relevance to biological ROS and physiological condition. Nevertheless, these assays are required to provide the intrinsic information about free radical scavenging activity of antioxidant compounds. Classification based on scavenging machinery, there are two major

groups of chemical antioxidant assays, including hydrogen atom transfer (HAT) reaction-based assays and single electron transfer (SET) reaction-based assays (10),(79). Antioxidant might eliminate free radicals through both hydrogen donation and transferring electron machinery, however, the major mechanism depends on structure of antioxidant and reaction condition that influences on solubility and partition coefficient of antioxidant (86). Notably, the efficient antioxidant activity also involves with type of ROS, concentration of antioxidant and cellular compartment (87).

Among many free radical scavenging assays, 2,2-diphenyl-1-picrylhydrazyl (DPPH) radical scavenging activity is one of the most recommended assays because of its' simplicity and repeatability (86). In DPPH assay, antioxidant capacity is determined through the capability of transferring electron from stable DPPH free radicals, which are less relevant to biological ROS. Moreover, the inhibitory activity of ROS scavengers against DPPH radicals can be modulated by type of solvent and recentness of DPPH solution (88). Schematic of reaction between DPPH radical and antioxidants (AH) presents in figure 7. It should be noted that antioxidants might also donate hydrogen atom to DPPH radical (89).

Chemical reactions:

$$DPPH^\bullet + ArOH \rightarrow DPPH\text{-}H + ArO^\bullet \qquad \text{(HAT mechanism)}$$

$$DPPH^\bullet + ArOH \rightarrow DPPH + [ArOH]^{\bullet+} \qquad \text{(SET mechanism)}$$

where ArOH: phenolic AO

Mechanism of reaction: HAT

λ = 517 nm

Deep purple   Pale yellow
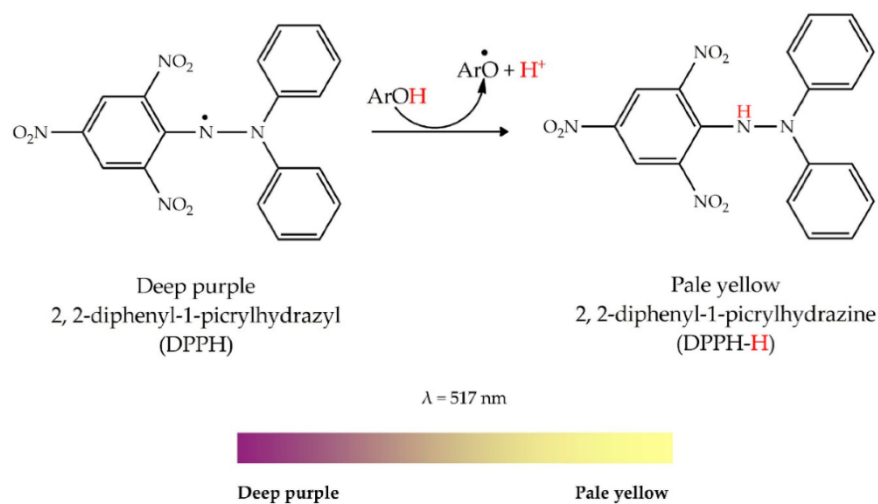
Figure 7 *Reaction diagram of DPPH assay (90).*

Another electron transfer-based assay is ferric-reducing antioxidant power (FRAP) in which capability to reduce ferric ion (Fe^{3+}) to blue colored ferrous (Fe^{2+}) is determined at acidic conditions as indicated in figure 8 (90),(91). Because the reducing power of interested compound is emphasized in testing condition, FRAP assay is commonly used for evaluation of reducing power of biological fluids, foods, and natural extracts (10). Nevertheless, there is less correlation between antioxidant capacity evaluated via FRAP and other chemical assays (86).
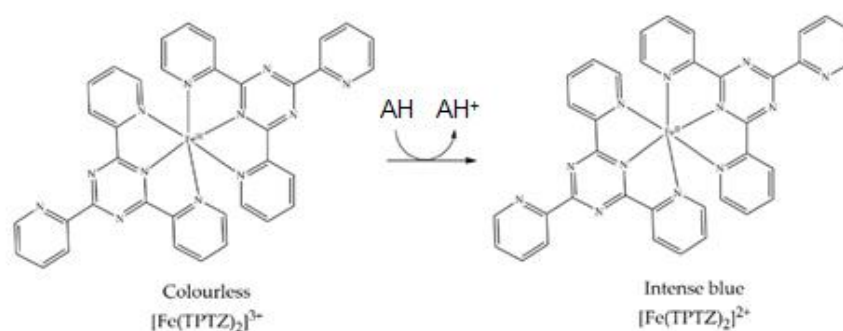
Figure 8 *Schematic of reaction in ferric-reducing antioxidant power (FRAP) assay,*

AH: antioxidant [Adapted from (90)].

Despite their simplicity and repeatability, DPPH and FRAP assays carry the drawback of irrelevance to biological ROS and physiological conditions (16). Therefore, oxygen radical absorbance capacity (ORAC) assay, in which generates peroxyl radicals (ROO$^\bullet$), is introduced to examine the translocation of hydrogen atoms from antioxidant to oxygen molecules (17). Based on donating of hydrogen atom to ROO$^\bullet$, a major ROS damaging lipid component in food and living organism, antioxidant possessing high inhibition in ORAC assay is suggested to be an effectively biological antioxidant (92). The azo compound of 2'-azobis(2-amidinopropane) dihydrochloride (AAPH) is usually used to generate ROO$^\bullet$, which in turn interacts with fluorescent prob. Antioxidant will competitively react with ROO$^\bullet$ in order to delay the decomposition of detecting fluorescent probe (Figure 9) (86),(93). However, the ORAC value of food is recently retracted by USDA (United States Department of Agriculture)

because it does not relate with antioxidant capacity *in vivo* model (10). The

comparison between DPPH, FRAP and ORAC assay summarized in Table 4.
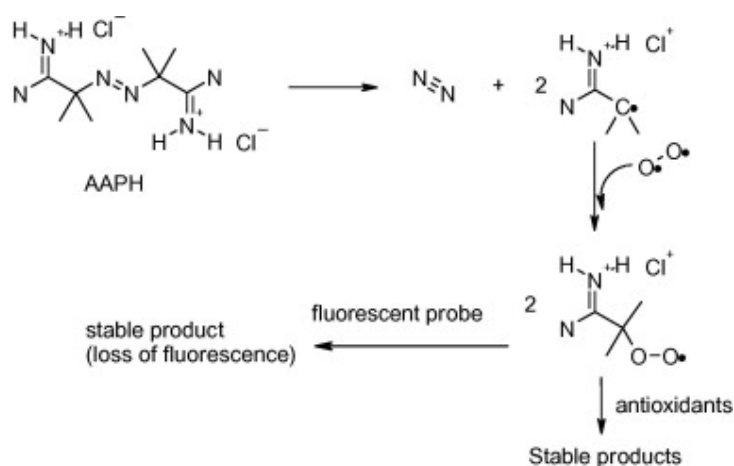
Figure 9 *Reaction diagram of ORAC assay (93).*

Table 4 *Major chemical-based ROS scavenging assay (10)*

Name of assay	Dominating mechanism	Oxidant	Probe	Detection
ROS scavenging assays				
ORAC	HAT	Peroxyl radical generated by AAPH	Fluorescein	Fluorometry
DPPH scavenging	HAT	DPPH radical	DPPH radical	Spectrophotometry or EPR
Redox potential assays				
FRAP	SET	Fe^{3+}	Ferricyanide	Spectrophotometry

<u>Antioxidant peptide</u>

Intriguingly, the ROS scavenging capacity of peptides, in both natural and hydrolyzed forms, is well established (21),(22),(23). It has been revealed that peptide characteristics, including molecular weight, amino acid sequence and hydrophobicity strongly determine its antioxidant potential (94). As a biological macromolecule, protein is one of the targeted molecules damaged by oxidative stress (95). ROS potentially interact with protein at specific amino acids, which can result in both active and stable protein radical. However, antioxidant peptides possess the capability to stabilize free electron and stop oxidative chain reaction (96). Moreover, ROS scavenging capacity of proteins also depends on oxidizable potential of amino acid composition. Among 20 amino acids, nucleophilic sulfur (cysteine and methionine) and aromatic containing amino acid side chains (tryptophan, tyrosine, and phenylalanine) as well as histidine's imidazole-containing amino acids highly interact with free radicals (97). Scavenging activity of amino acids can mediate through both hydrogen atom transfer (HAT) reaction-based assays and single electron transfer (SET). Figure 10 illustrates the ROS scavenging machineries of a) tyrosine b) cysteine and c) histidine containing peptides (98). The amino acids that potentially react with free radicals are also indicated in Table 5.
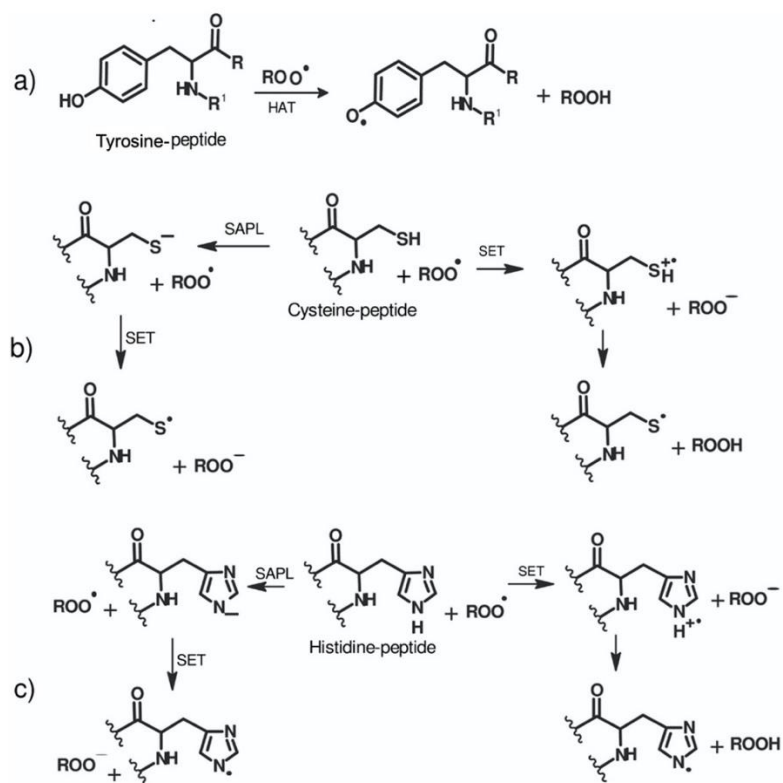
Figure 10 *ROS scavenging machineries of a) tyrosine b) cysteine and c) histidine containing peptides (99).*

Not only type of amino acid but also the location presented in peptide sequence determine their antioxidant potency. Either steric property or electron translocation of R-side chain of adjacent amino acid critically influence on free radical scavenging capacity of antioxidant peptide (99). Moreover, solubility of antioxidant peptide or accessibility of solvent also involves with scavenging activity (97). It has been reported that higher ROS scavenging activity of peptides can be achieved through enzymatic hydrolysis modification which reorganizes their tertiary structure, uncovers R-group, and increases solvent solubility (100).

Table 5 *Amino acids and their products generated from ROS scavenging activities*

(97)

Amino acid	Product	ROS scavenging mechanisms
Cysteine (Cys)	(1) Cystine	(1) Hydrogen abstraction from SH group and subsequent radical dimerization
	(2) Oxy acids	(2) Hydrogen abstraction from SH group, subsequent reaction with oxygen, and isomerization
Methionine (Met)	Methionine sulfoxide	Variety of routes including both radical and non-radical reactions
Tryptophan (Trp)	*N*-formylkynurenine, kynurenine, 5-hydroxytrytophan, 7-hydroxytryptophan	HO$^{\bullet}$ attack or one-electron oxidation of ring
Tyrosine (Tyr)	(1) 3,4-dihydroxy-phenylalanine	(1) HO$^{\bullet}$ attack or one-electron oxidation of aromatic ring
	(2) Di-tyrosine	(2) HO$^{\bullet}$ attack or one-electron oxidation of tyrosine and subsequent radical-radical dimerization; HOCl
	(3) 3-chlorotyrosine	(3) Chlorination of tyrosine as a result of exposure to HOCl or other chlorinating agents
	(4) 3-nitrotyrosine	(4) Reaction of reactive nitrogen species with tyrosine
	(5) Tyrosine hydroperoxide and subsequent cyclicized materials	(5) Formation of tyrosine phenoxyl radical in presence of $O_2^{\bullet-}$

Amino acid	Product	ROS scavenging mechanisms
Phenylalanine (Phe)	(1) o-, m-tyrosine	(1) HO$^\bullet$ attack or one-electron oxidation of aromatic ring. Possibly via reaction nitrogen species
	(2) Dimers of hydroxylated aromatic amino acids	(2) HO$^\bullet$ attack or one electron oxidation before or after dimerization
Histidine (His)	2-oxo-histidine	HO$^\bullet$ attack or one-electron oxidation

It should be noted that maximum antioxidant activity of protein hydrolysates requires suitable molecular distribution (26),(43),(101). Additionally, over-reaction of enzymatic hydrolysis also decreases ROS scavenging activity of peptides. Therefore, the conditions of enzymatic hydrolysis need to be optimized for maximizing free radical scavenging activity of protein hydrolysates (100). Some antioxidant peptides prepared from enzymatic hydrolysis are demonstrated in Table 6.

Table 6 *Protein hydrolysates containing free radical scavenging activity prepared*

from various enzymatic hydrolysis (100)

Sources	Enzymes used for production	Activity
Rice endosperm proteins and frog skin	Neutrase	Inhibits auto-oxidation and has hydroxyl radical-scavenging activity
Peanut proteins	Esperase	Prevents LDL oxidation
Peanut proteins, corn gluten, alfalfa leaves	Alcalase	Controls peroxidation and possesses chelating properties
Yam tubers, zein hydrolysate	Pepsin	Contains radical chelating properties and has DPPH-scavenging activity
Sunflower protein	Pancreatin	Shows copper-chelating activity
Peptide from frog skin	Trypsin	DPPH and superoxide scavenger
Animal proteins	Papain	Inhibition of lipid peroxidation
Animal skin	Chymotrypsin	Has DPPH, superoxide and hydroxyl-scavenging activity
Marine sources	Papain, pepsin	Control oxidation and possess strong chelating properties

Hyperpigmented disorder

Color displaying on various organs in human body, including skin, hair and iris is resulted from the accumulation of cellular pigmented compound called melanin. Not only determination of color tone but also protection skin cells from environmental exposures, especially ultraviolet (UV) radiation which is an important role of epidermal melanin (102). People with light skin tone because of low melanin content is more sensitive to develop skin damage, aging and cancer caused by UV radiation compared to dark-skinned person (103). However, the overproduction of melanin or hyperpigmented condition also causes many health problems, especially aesthetic concern (104). Large numbers of available whitening cosmetic products reflects health concern in hyperpigmented condition that affects self-confidence and quality of life. Although, various synthetic and natural hypopigmenting agents have been continuously introduced but most of them own short efficacy and serious side effects (105). Melanocytes that locate at the bottom layer of epidermis are responsible for melanin production through melanogenesis pathway (106).

Melanocytes

After exposure to melanogenic stimuli, melanogenesis or melanin synthesis pathway is started in melanocytes. Melanocytes are cells that play an important role in melanin synthesis. Melanocytes are developed from melanoblasts in the neural crest during embryogenesis (107). Then, they migrate to various organs throughout the body and develop into melanocytes. Melanoblasts that develop into melanocytes can be found in the basal layer (stratum basale) and hair follicles (Figure 11). Melanocytes contain various protein markers such as melanosomal matrix proteins (Pmel17), melan-A or melanoma antigen recognized by T cells 1 (MART-1), tyrosinase, tyrosinase-related protein 1 (TRP-1), dopachrome tautomerase (Dct) or tyrosinase-related protein 2 (TRP-2) and microphthalmia-associated transcription factor (MITF) (108). Melanocyte has a limb-like structure called dendrite that extends into the stratum spinosum, whereas one melanocyte is surrounded by 36 keratinocytes called the epidermal-melanin unit. In melanocyte, production of melanin occurs in melanosome before being transported to neighboring keratinocytes (109). Normally, the color of the skin depends on the shape, size and type of melanosome as well as the distribution of melanosome in the keratinocytes. People with light skin possess the aggregation of small size melanosomes while melanosomes of browned skin are larger size and thoroughly distribute in keratinocyte. Melanin is responsible for filtering and protecting cells from ultraviolet

radiation. In addition, melanocytes can be found in various parts of the body such as the central nervous system, eyes, ears, mucous membranes and hair (108).
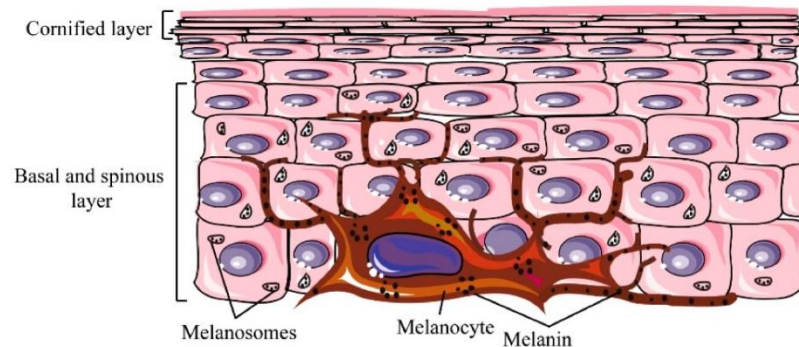
Figure 11 *Melanocytes located in the basal of skin (106).*

Melanogenic signal and regulation

Melanogenesis is a complex pathway occurring in melanosomes. In melanosomes, 2 types of melanin, eumelanin and pheomelanin, are synthesized. Eumelanin is the metabolite of DOPAquinone, which can be integrated with cysteine or glutathione resulting in pheomelanin (Figure 12).

Melanogenesis involves with numerous enzymes including tyrosinase, tyrosinase-related protein 1 (TRP-1), dopachrome tautomerase (Dct) or tyrosinase-related protein 2 (TRP-2). In the first step, tyrosinase enzyme converts tyrosine to L-DOPA, which is further oxidized to DOPAquinone by tyrosinase, again. DOPAquinone is a substrate for generating DOPAchrome that can be transformed into 5,6-dihydroxyindole (DHI) or 5,6-dihydroxyindole-2-carboxylic acid (DHICA). DHI is became

to eumelanin through oxidization by tyrosinase. In addition, Dct converts DOPAchrome into DHICA, which is continuously changed to eumelanin by TRP-1. On the other side, DOPAquinone can be changed to 5-s-cystenyl dopa or glutathionyl dopa in conditions with sulphydryl donor or with glutathione or cysteine, then becomes pheomelanin (110).
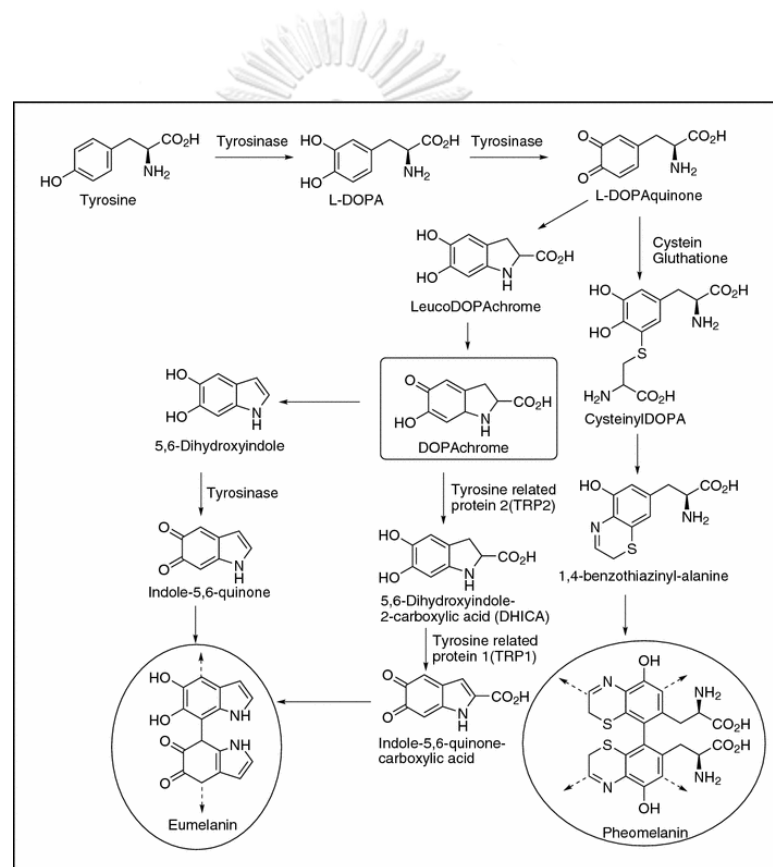
Figure 12 *Melanin synthesis pathway (110).*

Tyrosinase-related protein family (TRPs) consists of 3 enzymes including tyrosinase, TRP1 and Dct. Despite composing of various regulatory proteins, tyrosinase has been considered as a rate limiting enzyme, which catalysts tyrosine amino acid to melanin pigment in melanogenesis pathway. Thus, tyrosinase inhibitors have been widely accepted as effective depigmenting agents in cosmetic application (30). Tyrosinase is an enzyme that is important in controlling melanin synthesis. It is an oxidation enzyme that requires copper ion as structural component at the catalytic site and acting as a cofactor. Tyrosinase involves not only with the initial step during conversion of L-tyrosine to L-DOPA and conversion of L-DOPA to DOPAquinone but also the latter of changing DHI to eumelanin. Meanwhile, Dct and TRP1 modulate the final stages of generating DHICA and eumelanin, respectively in melanin synthesis pathway (111).

Microphthalmia-associated transcription factor

The expression of tyrosinase, TRP-1 and Dct is regulated by microphthalmia-associated transcription factor (MITF) (33). MITF is a transcription factor that is important in controlling the growth and development of various cells, including neural crest that will develop into melanocyte. MITF is a member of Myc-related family of basic helix-loop-helix leucine zipper (bHLH-ZIP) that is important in vertebrates. Among several isoforms, the most important isoform is MITF-M, which controls the transcription of tyrosinase, TRP1 and Dct genes, as well as PKC-b

proteins that are responsible for phosphorylation in the tyrosinase structure. After phosphorylation, pMITF binds to DNA with specific codes such as M- (AGTCATGTGCT) and E- (CATGTG) boxes, which are the starting points for transcription of the target genes including tyrosinase, TRP1 and Dct (112). However, pMITF is often unstable and is simply digested by enzymes in proteasome.

Accumulating evidence reveal that MITF is a novel therapeutic target for treatment of hyperpigmented disorders (113). According to mediating tyrosinase expression, suppression on MITF could give more efficacy on preventing melanin production compared with tyrosinase inhibitors (114). Moreover, recent study reports about the potential side-effect of arbutin, an available tyrosinase inhibitor, that highly disintegrate into cytotoxic compound in a presence of water and oxygen molecule (115). The expression of MITF has been reported to be modulated by cyclic adenosine monophosphate (cAMP)-response element binding protein (CREB). The up-regulation of MITF consequence with stimulation of tyrosinase expression and melanogenesis is mediated by phosphorylated-CREB (pCREB) (116). At normal condition, melanogenesis is triggered by the interaction between α-melanocyte-stimulating hormone (α-MSH) and melanocortin 1 receptor (MC1R) receptors. This signal regulates 3',5'-cyclic adenosine monophosphate (cAMP) and protein kinase A (PKA) which in turn promotes CREB to translocate into nucleus (117). Additionally, glycogen synthase kinase 3β (GSK3β)/β-catenin signal also mediates MITF at transcriptional level (Figure 13) (118).
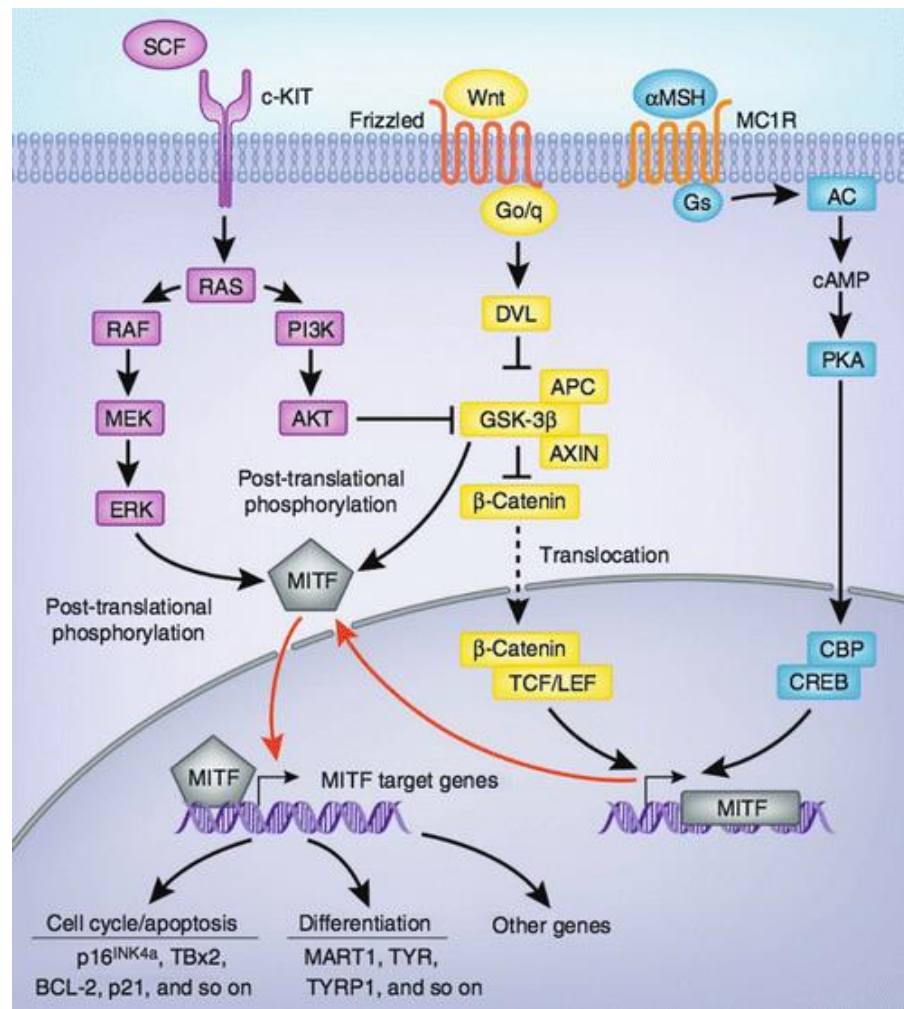
Figure 13 *Melanogenesis signaling pathway (118).*

After translation, the level of MITF is regulated by mitogen-activated protein kinase (MAPKs)/extracellular signal-regulated protein kinase (ERK) signal. The proteasomal degradation of MITF is promoted after phosphorylation by pERK (35),(36). Therefore, the activation of ERK is one of potential target for suppression tyrosinase expression and inhibiting the process of skin pigmentation (37),(38). Interestingly, the cellular oxidative stress also regulates the melanin production in

melanocyte. The level of cellular reactive oxygen species (ROS) associating with stimulation of extracellular-signal-regulated kinase (ERK) pathway modulates melanogenic function of MITF (119). In a current study, the essential oil from *Achillea millefolium* L. that decreased cellular ROS stimulated the phosphorylation of ERK resulting in the inhibition of melanogenesis (120). Moreover, *Oenothera laciniata* Hill extracts suppresses MITF expression through antioxidant capacity (121). Also, chemical substance that has an inhibitory effect on skin pigmentation through suppression on cAMP mechanism, leading to downregulation of MITF. Sargaquinoic acid (SQA) inhibits melanin production through decrease cAMP level and suppresses tyrosinase in B16F10 mouse melanoma cells (122).

Response surface methodology (RSM)

Base on mathematic and statistical analysis of related experimental information, response surface methodology (RSM) is an effective tool for optimization of processing condition in both laboratory and industrial setting. Indeed, the term of "Response surface methodology" is applied for graphical relationship between variable factors and dependent response derived from mathematical fitting (123),(124). Additionally, both chemical and biochemical machineries can be explained via RSM mathematic model (125). Not only inputting several independent variables at the same time but also depicting interrelation as well as generating of

reliable information is major advantage of RSM (125). To maximize the dependent response or optimize the desired outcome without increasing production cost, a multivariate statistical analysis is implemented in RSM (125). Generally, RSM comprises of three simple steps of 1) Identifying independent factors and their variable levels, 2) Selecting and verifying the RSM experimental model and 3) Determining optimized RSM condition (125).

1) *Identifying independent factors and level of variation, an initial and important step for RSM.* The preliminary experiments are essentially required for selecting independent factors and determining the level of variation that critically influence on the interested response. The failure of optimization mostly results from unsuitable selection of variable factors. It is worth noting that because of containing different unit, the variation of independent factors range from -1 to 1 is regularly performed to minimize the relevance of unit parameter. The equation for setting level of variation is indicated as below (125).

$$X = \frac{x - (x_{max} + x_{min})/2}{(x_{max} - x_{min})/2}$$

where X is the coded variable, x is the independent factor while x_{max} and x_{min} are the maximum and minimum values of the independent factor.

2) *Selecting and verifying the RSM experimental model.* A quadratic equation is usually generated from RSM to calculate response variable. A full quadratic equation of secondary model derived from RSM is demonstrated below.

$$y = \beta_0 + \sum_{i=1}^{k} \beta_i x_i + \sum_{i=1}^{k} \beta_{ii} x_i^2 + \sum_{1 \leq i \leq j}^{k} \beta_{ij} x_i x_j + \varepsilon$$

where y is the response variable. β_0, β_i, β_{ii} and β_{ij} sequentially are regression coefficients for intercept, linear, quadratic and interaction coefficients. X_i and X_j are coded variable of independent factors while ε is the residual associated to the experiments (123).

There are many types of available symmetrical response surface designs that are used for evaluating independent factors. Among these, Box–Behnken design is one of symmetrical second-order experimental designs mostly applied for optimization of chemical and physical processes (123). In comparison with full three-level factorial designs, Central composite design and Doehlert design, Box–Behnken design successfully minimizes number of experiments from 3^k (Full three-level factorial design) and $k^2 + k + c_p$ (Central composite design and Doehlert design) to $2k(k-1) + c_p$; where k is the number of factors and c_p is the number of the central points, which is practically investigated the response variable affected by more than 2 independent factors (Figure 14). Additionally, three interval levels (-1, 0, +1) of all independent factors will be equally modified in Box–Behnken design (122).
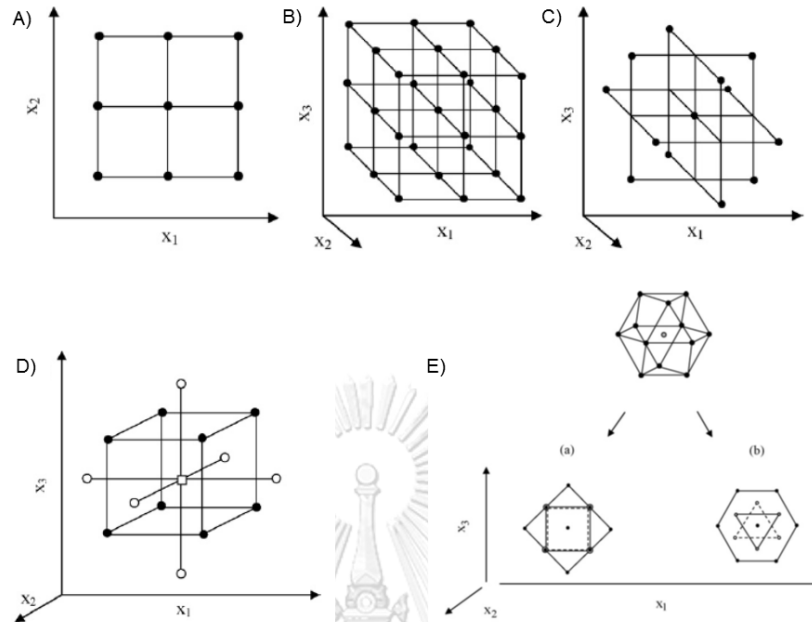
Figure 14 *Three-level factorial design for the optimization of (A) two independent*

factors and three independent factors variables via (B) full three-level factorial

design, (C) Box–Behnken design, (D) Central composite design and (E) Doehlert design

[Adapted from (123)].

To verify the correlation between RSM model and experimental data,

analysis of variance (ANOVA) is performed to evaluate the fitness of quadratic

equation of secondary model derived from RSM (123),(125). The value of

analysis of variance mostly considered for fitness of RSM mathematical model

are summarized in Table 7.

3) *Determining optimized RSM condition.* The relation between independent

factors and response variable can be simply demonstrated via the response

surface plot. It should be noted that if there are three or more independent factors, the three-dimensional visualization possibly illustrates the relationship between an interested response and two variable factors while the other factors are constant value.

Table 7 *Analysis of variance of fitted mathematical model (123),(125).*

Analysis of variance	Optimal range	Remark
Residuals	-	Variation from non-independent factors (e.g. fluctuation of measurement)
Lack of fit	$p > 0.05$ (Non-statistical significance)	
Coefficient of determination (R^2)	Nearly 1.000	Adding a variable to the model will always increase R^2
Adjusted R^2	Nearly 1.000	Comparison model with different number of variables
Predicted R^2	Nearly 1.000	-Prediction of new observation -Usually lower than R^2 however over-fit of model is indicated with extremely low predicted R^2
Regression	$p < 0.05$ (Statistical significance)	

Many types of response surface profile are indicated in figure 15. The maximum and minimum response clearly identified inside experimental setting is

respectively illustrated in response surface plot of figure 15A and figure 15D. Although figure 15B demonstrates the point of maximum response in the experimental region, the less relation between the response and x_2 independent factor evidenced with a plateau curve. Figure 15E shows the points of maximum response, minimum response and intermediate response or saddle point within experiment scenario. Meanwhile, the maximum response locating outside the experimental region could be suggested in surface response plot presented in figure 15C (123),(125). It is the fact that only the fitness of the model, but not actual characters of the system can be interpreted from surface response plot (125). To obtain the condition for desirable response, the optimized independent factors can be resulted from the calculation in a quadratic equation of secondary model derived from RSM. Nevertheless, the optimized condition is essentially ranged in the levels of independent factors (123).
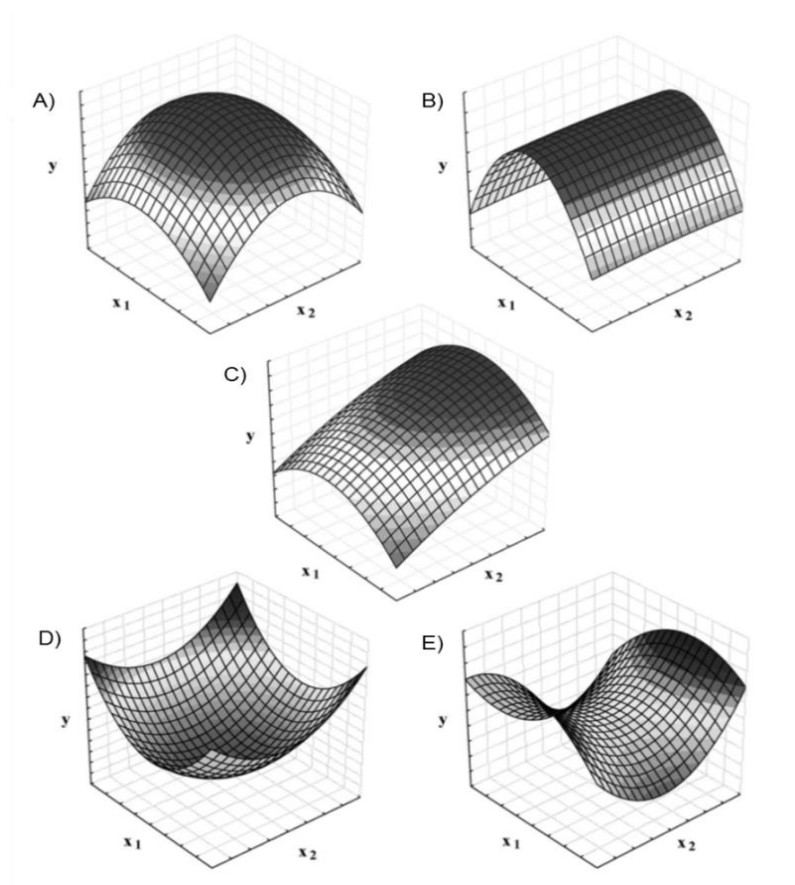
Figure 15 *Different types of surface response plots including (A) Maximum, (B)*

Maximum with plateau, (C) Maximum outside the experimental region, (D) Minimum,

and (E) Saddle responses (124).

CHAPTER 3

MATERIALS AND METHODS

1. Materials

Lyophilized silk sericin powder was kindly prepared and provided by Ruenmai-baimon, LTD., Surin Province, Thailand. Briefly, sericin protein was extracted by boiling uncover cocoon shells in hot water during the degumming process of the silk industry. Then, the degumming wastewater was lyophilized into dry powder prior kept at 4°C. Porcine pancreas trypsin (EC 3.4.21.4), papain (EC 3.4.22.2), Alcalase from *Bacillus licheniformis* (EC 3.4.21.62), 2,2-diphenyl-1-picrylhydrazyl (DPPH), 2,4,6-tri(2-pyridyl)-s-triazine (TPTZ), ferric chloride hexahydrate (FeCl$_3$·6H$_2$O), 37% hydrochloric acid (HCl) solution, fluorescein, 2,2'-azobis-2-methyl-propanimidamide dihydrochloride (AAPH), sodium dodecyl sulfate (SDS), Coomassie brilliant blue R-250, isopropanol, ethanol, acetic acid solution, 2',7'-dichlorofluorescein diacetate (DCFH$_2$-DA), synthetic melanin, bovine serum albumin (BSA), chloroform, 2-propanol, forskolin, 4-butylresorcinol and N-acetyl cysteine (NAC) were purchased from Sigma (St. Louis, MO, USA). A bicinchoninic acid (BCA) protein assay kit, 3-(4,5-Dimethyl-2-thiazolyl)-2,5-diphenyl-2H-tetrazolium bromide (MTT), Luna Universal qPCR Master Mix, RevertAid First Stand cDNA Synthesis Kit and DNase I were procured from Thermo Scientific (Rockford, IL, USA). MilliporeSigma (Burlington, MA, USA) was the

source of 3% w/w hydrogen peroxide (H_2O_2) solution. N, N, N', N'-tetramethylethylenediamine (TEMED), 40% acrylamide/bisacrylamide 37.5:1, Tween 20 and ammonium persulfate were obtained from Bio-Rad (Hercules, CA, USA). GENEzol reagent was purchased from Geneaid Biotech Ltd. (New Taipei City, Taiwan). Antibodies, including mouse monoclonal antibody to MITF, mouse monoclonal antibody to TRP-1, rabbit polyclonal antibody to Dct and rabbit polyclonal antibody to β-actin were purchased from Abcam (Cambridge, UK). Santa Cruz Technology (Dallas, TX, USA) was a source of mouse monoclonal antibody to tyrosinase. Meanwhile, rabbit monoclonal antibody to CREB, rabbit monoclonal antibody to pCREB (phosphorylated-S133), rabbit monoclonal antibody to Erk1/2, rabbit monoclonal antibody to pErk1/2 (phosphorylated-Thr202/Tyr204), rabbit monoclonal antibody to GAPDH, secondary antibody anti-mouse IgG horseradish peroxidase (HRP)-linked and secondary antibody anti-rabbit IgG HRP-linked were bought from Cell Signaling Technology (Denver, MA, USA).

2. Cell culture

Human keratinocytes (HaCaT) and human melanoma MNT-1 cells were obtained from The American Type Culture Collection (ATCC, Manassas, VA, USA). Human keratinocytes were cultured in Dulbecco's Modified Eagle Medium (DMEM), supplemented with 2 mmol/L L-glutamine, 10% (v/v) fetal bovine serum (FBS) and 100 units/mL of penicillin/streptomycin (Gibco, Gaithersburg, MD, USA). Meanwhile,

human melanin-generating MNT-1 cells were cultured in DMEM supplemented with 20% FBS, 10% AIM-V medium (Gibco, Gaithersburg, MD, USA), 2 mmol/L L-glutamine and 100 units/mL of penicillin/streptomycin. Cells that reached 70-80% confluence under 5% CO_2 at 37°C were used in further experiments.

3. Enzymatic hydrolysis of sericin

Three commercial proteases, including trypsin, papain and Alcalase® were chosen to hydrolyze sericin at the optimum conditions recommended by the manufacturers as indicated in Table 8. Briefly, sericin powder was dispersed in de-ionized water at a concentration of 2% w/v. The protein suspension was heated at 95°C for 10 min until complete solubilization before immediate cool down on ice to room temperature. The sericin solution was adjusted to the desired condition depending on used proteases and then hydrolysis experiments were carried out in a 50 mL vessel. To stop the enzymatic reaction, the solution was heated at 100°C for 5 min and quickly chilled on ice to room temperature. After centrifugation at 3,500g for 30 min at 4°C, the supernatant was that were further dialyzed overnight with the phosphate buffer at 4°C before subjected to freeze-drying for collecting the sericin hydrolysates. The hydrolyzed sericin powder was stored at -20°C until use in further experiments.

Table 8 *Optimum enzymatic condition following the manufacturer's instructions*

Protease enzyme	Factors			
	pH	E/S (w/w)	Temperature (°C)	Time (h)
Alcalase[®]	8	2	60	3
Papain	7	2	60	3
Trypsin	8	2	40	3

E/S: Enzyme/Substrate ratio

4. Response surface methodology for optimization of enzymatic hydrolysis conditions

The three independent variables of pH, enzyme/substrate ratio and temperature at three levels were generated in a Box-Behnken design using a trial version of Design-Expert[®] 11 software (Stat-Ease Inc., Minneapolis, MN, USA). The levels and range of each variable are indicated in Table 9. The response data obtained from each designed condition were determined by the following quadratic polynomial equation:

$$Y = \beta_0 + \beta_1 x_1 + \beta_2 x_2 + \beta_3 x_3 + \beta_{11} x_1^2 + \beta_{22} x_2^2 + \beta_{33} x_3^2 + \beta_{12} x_1 x_2 + \beta_{13} x_1 x_3 + \beta_{23} x_2 x_3$$

where Y is the response variable (DPPH, FRAP or ORAC); β_0 is an offset constant; β_1, β_2, and β_3 are linear regression coefficients; β_{11}, β_{22} and β_{33} are quadratic effects; β_{12}, β_{13} and β_{23} represent interaction effects; x_1, x_2 and x_3 represent independent variables in this model.

Table 9 *Independent variables and their levels in Box-Behnken*

Variables	Code	Factors		
		-1	0	1
pH	A	7	8	9
E/S (w/w)	B	1	2	3
Temperature (°C)	C	50	60	70

E/S: Enzyme/Substrate ratio

The analysis of variance (ANOVA) was performed using RSM software Minitab.16 to determine the adequacy of models through lack of fit value, coefficient determination (R^2) and adjusted-R^2 (126). Statistical significance was $p < 0.05$.

5. Molecular weight distribution of sericin hydrolysates

Constituents of hydrolyzed sericin were analyzed via sodium dodecyl sulfate-polyacrylamide gel electrophoresis (SDS-PAGE). Equal amounts of protein mixed with loading dye were heated at 95°C for 5 min and added onto 12% (w/v) gel of SDS-PAGE. The separated protein constituents were stained overnight with Coomassie brilliant blue R-250 solution. The molecular weight distribution of hydrolyzed sericin was clearly observed after destaining the gel with isopropanol: acetic acid: water (10: 10: 80% v/v) solution (127). Additionally, the size distribution profile of RSM-optimized sericin hydrolysates was also generated through fast protein liquid chromatography (FPLC) coupled with HiPrep 16/60 Sephacryl S-200 HR column (GE Healthcare, Stockholm, Sweden). Briefly, sericin hydrolysates at 4 mg/mL was

prepared in Tris-HCl buffer (50 mM Tris–HCl, pH 8.0, 200 mM NaCl) for loading on the

size exclusion chromatography column preequilibrated with Tris-HCl buffer. Then, the

protein sample was eluted with Tris-HCl buffer at a flow rate of 1 mL/min.

Absorbance of the eluent at 214 nm was determined to estimate protein

concentration.

6. Identification of peptide in sericin hydrolysate

Peptidomic analysis was performed at Functional Ingredients and Food

Innovation Research Group, National Center for Genetic Engineering and

Biotechnology, National Science and Technology Development Agency, Pathum

Thani, Thailand through the collaboration with Sittiruk Roytrakul, Ph.D. to identify

peptide components in sericin hydrolysates compared to unhydrolyzed sericin.

1) Liquid chromatography/electrospray ionization-tandem mass spectroscopy

(LC-ESI-MS/MS)

Both sericin hydrolysates and unhydrolyzed sericin was dissolved in 10 mM

ammonium bicarbonate. After subjected to zip-tip purification and dried using a

speed vacuum concentrator, the protein samples were resuspended in 0.1% formic

acid prior to LC-ESI-MS/MS analysis. The protein solutions were injected into an

Ultimate3000 Nano/Capillary LC System (Thermo Scientific, Loughborough, UK)

coupled to a Hybrid quadrupole Q-Tof impact II™ (Bruker Daltonics GmbH, Bremen,

Germany) equipped with a Nano-captive spray ion source. Briefly, 1 μL of peptide

digests were enriched on a µ-Precolumn 300 µm i.d. × 5 mm C18 Pepmap 100, 5 µm, 100 A (Thermo Scientific, Loughborough, UK), separated on a 75 µm I.D. × 15 cm and packed with Acclaim PepMap RSLC C18, 2 µm, 100Å, nanoViper (Thermo Scientific, Loughborough, UK). The C18 column was enclosed in a thermostatted column oven set to 60°C. Solvent A and B containing 0.1% formic acid in water and 0.1% formic acid in 80% acetonitrile, respectively were supplied on the analytical column. A gradient of 5–55% solvent B was used to elute the peptides at a constant flow rate of 300 nL/min for 30 min. Electrospray ionization was carried out at 1.6kV using the CaptiveSpray. Nitrogen was used as a drying gas (flow rate about 50 l/h). Collision-induced-dissociation (CID) product ion mass spectra were obtained using nitrogen gas as the collision gas. Mass spectra (MS) and MS/MS spectra were obtained in the positive-ion mode at 2 Hz over the range (m/z) 150–2200. The collision energy was adjusted to 10 eV as a function of the m/z value. The LC-MS analysis of each sample was done in triplicate.

2) Bioinformatics and data analysis

MaxQuant 1.6.6.0 was used to quantify the peptides in individual samples using the Andromeda search engine to correlate MS/MS spectra to the Uniprot sericin database (128). Label-free quantitation with MaxQuant's standard settings was performed: maximum of two miss cleavages, mass tolerance of 0.6 dalton for main search, unspecific digesting enzyme, oxidation of methionine as variable modifications. Only peptides with a minimum of 7 amino acids, as well as at least

one unique peptide, were required for protein identification. Only proteins with at least two peptides, and at least one unique peptide, were considered as being identified and used for further data analysis. Protein FDR was set at 1% and estimated by using the reversed search sequences. The maximal number of modifications per peptide was set to 5. As a search FASTA file, the proteins present in the sericin proteins downloaded from Uniprot. Potential contaminants present in the contaminants.fasta file that comes with MaxQuant were automatically added to the search space by the software. The level of peptides in each sample were expressed as log2 value.

7. ROS scavenging assay

1) DPPH radical scavenging activity

DPPH radical scavenging activity of sericin hydrolysates was determined according to the method of Agrawal et al. (129). Briefly, 100 μL of sericin hydrolysates was mixed with 100 μL of 0.1 mM DPPH solution in a 96-well plate and incubated at room temperature for 60 min in the dark. The absorbance intensity (Abs) of DPPH radicals was determined using a microplate reader (Anthros, Durham, NC, USA) at 517 nm. The % inhibition of DPPH was calculated as follows:

$$\text{DPPH scavenging inhibition } (\%) = \frac{\text{Abs}(\text{Control}) - \text{Abs}(\text{Sample})}{\text{Abs}(\text{Control})} \times 100$$

2) Ferric reducing antioxidant power (FRAP) assay

FRAP assay was performed to evaluate the ferric reducing antioxidant power of sericin hydrolysates (130). Sericin hydrolysates (50 μL) were allowed to react with 150 μL of 0.3 M FRAP reagent in acetate buffer, pH 3.6 (10 mM TPTZ: 40 mM HCl: 20 mM $FeCl_3 \cdot 6H_2O$ at 10: 1: 1 ratio). The reaction mixture was kept from light at room temperature for 15 min then the absorbance of ferrous ion (Fe^{2+}) complex was examined using a microplate reader (Anthros, Durham, NC, USA) at 595 nm. A calibration curve of Fe^{2+} was used to calculated reducing power, which is presented as Fe^{2+} equivalence/mg of sericin hydrolysates.

3) Oxygen radical absorbance capacity (ORAC) assay

ORAC assay was performed in 75 mM phosphate buffer (pH 7.4). Briefly, the mixture of sericin hydrolysates (25 μL) and fluorescein solution at final concentration of 70 nM (150 μL) in a 96-well clear bottom black plate was preincubated at 37°C for 15 min. Subsequently, 25 μL of AAPH was rapidly added to the mixture to get the final concentration of 12 mM. The plate was shaken for 5 s before measurement of the fluorescence intensity of fluorescein using a CLARIOstar plus microplate reader (BMG LABTECH, Ortenberg, Germany) with excitation wavelength at 485 nm and emission wavelength at 520 nm every 90 s for 150 min. Instead of the testing solution, phosphate buffer solution (PBS) at pH 7.4 was chosen as a blank, while

Trolox was selected as a calibration solution. Fluorescence measurements were normalized to the curve of the PBS blank. The area under the fluorescence decay curve (AUC) was calculated as follows:

$$AUC = 1 + \sum_{i=150}^{i=1.5} f_i/f_0$$

$$net\ AUC = AUC_{antioxidant} - AUC_{blank}$$

where f_0 is the initial fluorescence reading at 0 min, fi is the fluorescence reading at time i min

The regression equation between the net AUC and the Trolox concentration was calculated. ORAC values were expressed as μmol Trolox equivalence (TE)/mg of sericin hydrolysates (130).

8. Determination of cellular ROS level via flow cytometry

Cells seeded at a density of 1×10^5 cells/well in 6-well plates were incubated with 10 μM DCFH$_2$-DA for 30 min at 4°C while kept from light. Then, the cells were washed with PBS and pretreated either with 5 mM NAC, 20 mg/mL Alcalase®-hydrolyzed sericin or 20 mg/mL unhydrolyzed sericin prior to exposure to 1 mM H$_2$O$_2$. After 30 min of treatment with H$_2$O$_2$, the cells were resuspended in PBS and immediately subjected to flow cytometry using Guava easyCyte Benchtop Flow Cytometers (EMD Millipore, Darmstadt, Germany) for measurement of cellular fluorescence intensity of DCF at excitation/emission wavelengths of 488/538 nm.

Cellular ROS level was a relative value of mean fluorescence intensity quantified by Guava InCyte version 3.1 software (EMD Millipore) between specific treatment and untreated control cells.

9. Measurement of melanin content

To evaluate the effect on melanogenesis, the non-toxic concentration range of sericin hydrolysate was determine via MTT viability assay. Melanin-generating MNT-1 cells were incubated with different concentrations of sericin hydrolysate. After 24-72 h, the cells were incubated with 500 µg/ml of MTT solution in PBS (Invitrogen, Carlsbad, CA, USA) for 3 h at 37°C and kept from light. After that, the MTT solution was replaced with DMSO to dissolve the formazan product. The intensity of the absorbance of MTT product was measured at 570 nm using a microplate reader (Anthos, Durham, NC, USA). Cell viability was calculated from absorbance of MTT product, as following equation:

$$\text{Cell Viability} \left(\%\right) = \frac{\text{A570 of treatment}}{\text{A570 of control}} \times 100$$

Sericin hydrolysate at concentrations that did not cause significant reduction of %cell viability compared with untreated control cells were selected for further investigation of antimelanogenic activity. Melanin-generating MNT-1 cells were placed in 24-well plates (1×10^5 cells/well) for 12 h, and then the melanin content was

determined after incubation either with non-toxic concentrations of sericin hydrolysate, forskolin (a melanin stimulator) or 4-butylresorcinol (a tyrosinase inhibitor) for 24-72 h (131),(132). Determination of melanin content was slightly modified from previous study (133). Briefly, the collected cell pellets were washed with PBS (pH 7.4) then incubated with 1 N NaOH in 10% DMSO at 80°C for 2 h. Thereafter, the samples were collected and centrifuged at 15,000 rpm for 30 min to separate the supernatant. The absorbance intensity of melanin content in the supernatant was measured at 490 nm using a microplate reader (Anthos, Durham, NC, USA). The melanin content was calculated by interpolating from standard curve of synthetic melanin. The amount of total protein in the supernatant obtained from bicinchoninic acid (BCA) protein assay kit (Thermo Fisher Scientific, Waltham, MA, USA) was used to compare the melanin content/µg of protein between each sample.

10. Cell-free tyrosinase activity assay

Cell-free tyrosinase activity assay was modified from the previously described method (134). MNT-1 cells were cultured until they reached 70-80% confluence then collected by trypsinization and centrifuged at 5,000 rpm for 5 min at 4°C. The cell pellets were lysed with RIPA buffer containing 1% protease inhibitor cocktail at 4°C and subsequently vortex every 10 min continuously for 1 h. After centrifugation (12,000 rpm for 15 min at 4°C), the supernatant was determined for protein concentration by a BCA assay kit. The sample contains protein 50 ug was incubated

with different concentrations of sericin hydrolysate. After incubation at 37°C for 10 min, added 2 mM of L-DOPA and further incubated for 2 h at 37°C, the resulting of dopachrome was measured using a microplate reader at 490 nm. The tyrosinase activity was calculated as following.

$$\text{Tyrosinase activity (\%)} = \frac{\text{A490 oftreatment}}{\text{A490 of control}} \text{x}100$$

11. Western blot analysis

After indicated treatment, MNT-1 cells were incubated in iced-cold lysis buffer containing 20 mM Tris-HCl (pH 7.5), 150 mM sodium chloride, 10% glycerol, 0.5% triton X-100, 1 mM sodium orthovanadate, 50 mM sodium fluoride, 100 mM phenylmethylsulfonyl fluoride, and protease inhibitor cocktail (Roche Molecular Biochemicals, Indianapolis, IN, USA) for 30 min. Protein concentration was then measured using BCA protein assay kit. Protein 25 ug from cell lysates were separated on 10% SDS-PAGE. Thereafter, proteins were transferred onto a nitrocellulose membrane (Bio-Rad, Hercules, CA, USA). The membranes were blocked with 5% non-fat milk in TBST (25 mM Tris-HCl; pH 7.5, 125 mM NaCl, 0.1% Tween20) for 1 h at room temperature. After washed with TBST for 5 min and incubated with the primary antibody at 4°C overnight, the membranes were washed with TBST for 5 min (3 times) and probed with horseradish peroxide (HRP) secondary antibody for 2 h at

room temperature. The band of interested protein was illustrated by adding of chemiluminescence substrate (Supersignal West Pico; Pierce, Rockford, IL, USA) onto the membrane after washing with TBST for 5 min for 3 times. The band intensity was quantified using analyst/PC densitometric software (Bio-Rad, Hercules, CA, USA).

12. Quantitative real-time PCR

MNT-1 cells (5×10^4 cells/well) in 6 well-plates were treated with different concentrations of sericin hydrolysate for 24 h. Total RNA from the cells was isolated by using GENEzolTM reagent (Geneaid company, Taipei, Taiwan) according to the manufacturer's instruction. cDNA was synthesized by using RevertAid Premium Reverse Transcriptase (Thermo Fisher Scientific, Waltham, MA, USA). The cDNA obtained was amplified by specific forward and reverse primers (Thermo Fisher Scientific, Waltham, MA, USA) as presented in Table 10.

Table 10 The list of primer used for instigation of melanogenesis

Specific gene	Primer
Human GAPDH	- Forward primer: 5′-GAGTCCACTGGCGTCTTCA-3′
	- Reverses primer: 5′-TTCAGCTCAGGGATGACCTT-3′
Human MITF	- Forward primer: 5′-TCATCCAAAGATCTGGGCTATGACT-3′
	- Reverse primer: 5′-GTGACGACACAGCAAGCTCAC-3′
Human tyrosinase	- Forward primer: 5′-TCATCCAAAGATCTGGGCTATGACT-3′
	- Reverse primer: 5′-GTGACGACACAGCAAGCTCAC-3′
Human TRP-1	- Forward primer: 5′-AAGGCTACAACAAAAATCACCAT-3′
	- Reverse primer: 5′-ATTGAGAGGCAGGGAAACAC-3′
Human Dct	- Forward primer: 5′-GCAGCAAGAGATACACAGAAGAA-3′
	- Reverse primer: 5′-TCCTTTATTGTCAGCGTCAGA-3′

Quantitative real-time PCR was performed through a C1000™ Thermal Cycler (Bio-Rad CFX384 real-time pcr system) using Luna$^®$ Universal qPCR Master Mix (M3003) (Biolab, Lawrenceville, GA, USA). Reaction combinations were incubated for 39 cycles of 95°C for 5 sec; 60°C for 30 sec and 65°C for 5 sec. The target mRNA expression was determined as the relative comparison established by the **Δ**Ct method, and the comparative threshold (Ct) of target genes is normalized by **β**-actin (Ct) values. The mRNA expression was calculated from triplicate experiments from which data represents the means ± standard deviation (SD).

13. Statistical analysis

All experimental data were presented as means ± standard error of the mean (SEM). SPSS version 22 (IBM Corp., Armonk, NY, USA) with one-way analysis of variance (ANOVA) followed by Tukey's post-hoc test. Any p-value under 0.05 was considered statistical significance.

Experimental design
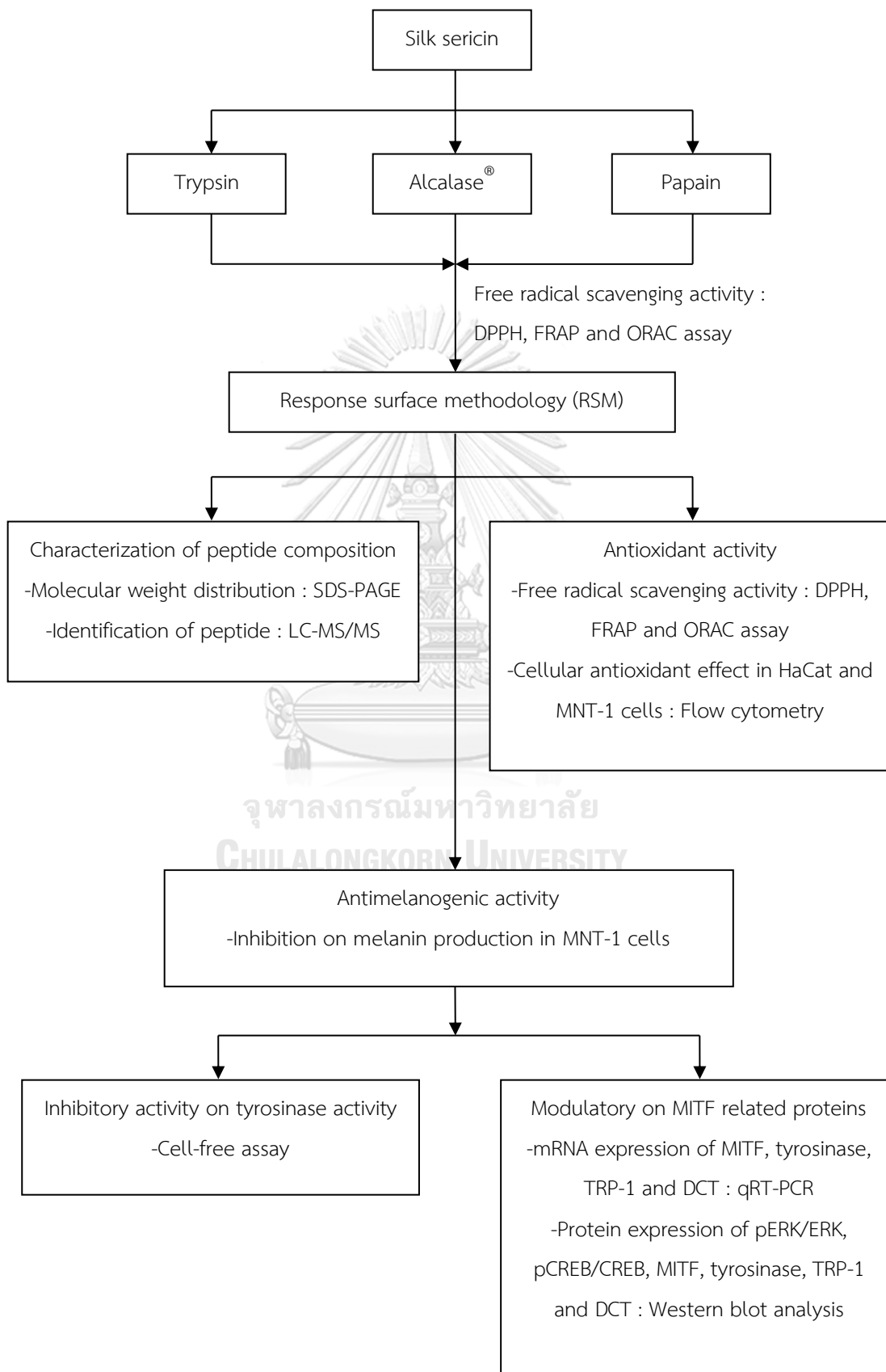
Research framework
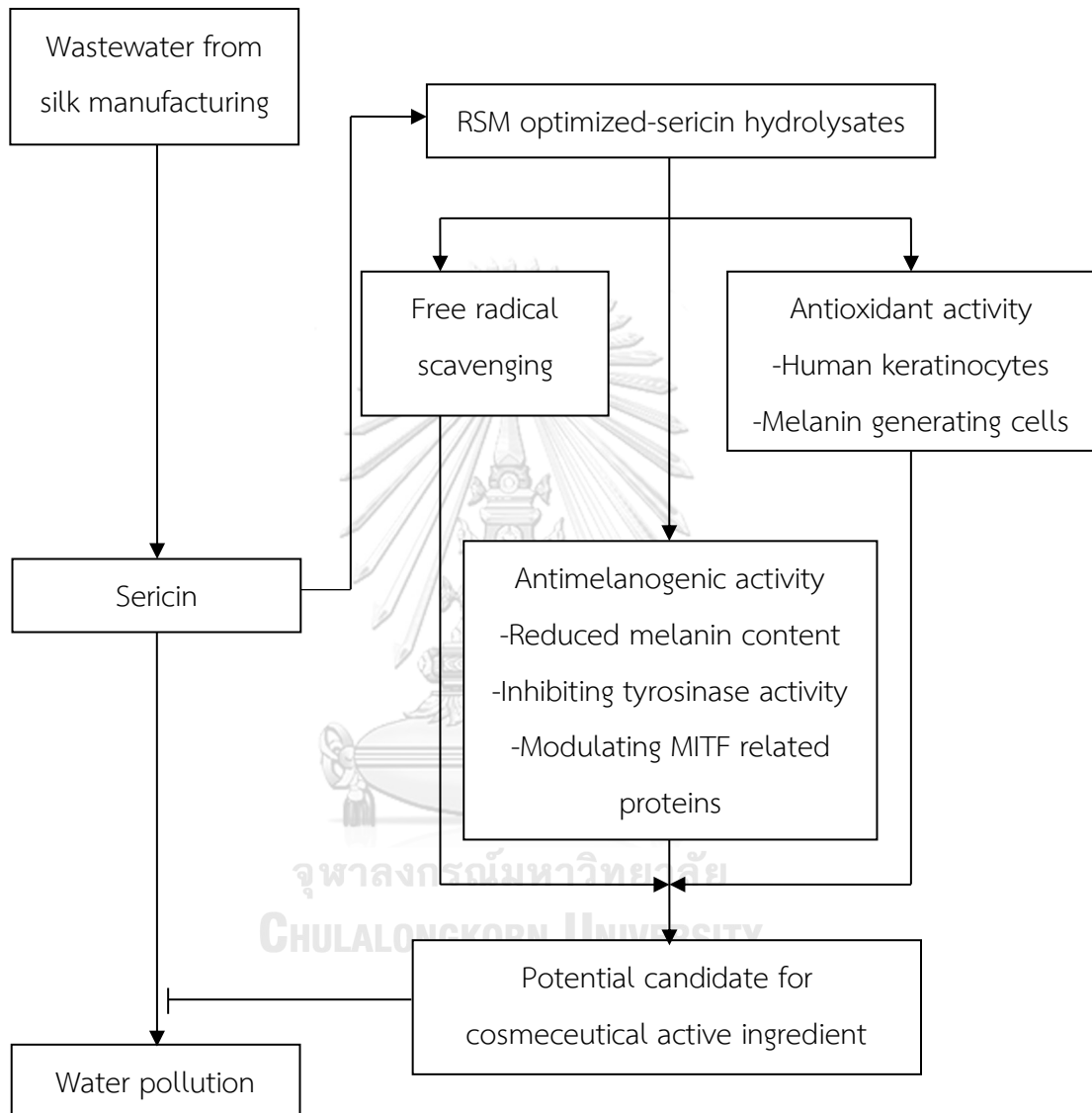
CHAPTER 4

RESULTS AND DISCUSSION

1. ROS scavenging activity of sericin hydrolysates prepared from various protease enzymes

Initially, silk sericin was digested by three commercial proteases to identify the hydrolyzed sericin that possessed the highest antioxidant activity. After 3 h of enzymatic reaction following the manufactures' conditions, SDS-PAGE analysis revealed the alteration of protein constituents in sericin hydrolysates (Figure 16). The absence of high molecular weight (~100–260 kDa) proteins indicated the enzymatic function of Alcalase[®], papain and trypsin in such conditions. Only protein at ~10 kDa was presented in sericin hydrolysates obtained from Alcalase[®] while papain hydrolyzed-sericin consisted with proteins ranging from ~10 to 100 kDa. It should be noted that staining with Coomassie brilliant blue R-250 barely detected protein components in sericin hydrolysates derived from trypsin reaction. Antioxidant activity of the sericin hydrolysates prepared from these three commercial enzymes was then assessed through DPPH, FRAP and ORAC assays. The greater scavenging activity against DPPH and ROO$^•$ radials as respectively indicated by greater % DPPH inhibition and ORAC values was noted in all hydrolyzed sericins compared with undigested sericin (Table 11). Interestingly, only sericin hydrolysates obtained from Alcalase[®]

achieved better Fe^{3+} reducing power, as evidenced by its higher FRAP value when compared with unhydrolyzed sericin. It is worth noting that digestion with papain and trypsin decreased Fe^{3+} reducing power of sericin proteins. Sericin hydrolysates obtained from Alcalase® demonstrated the highest antioxidant capacity in all ROS scavenging assays (DPPH scavenging activity = 19.71 ± 0.13%, FRAP activity = 435.50 ± 10.13 µmol Fe^{2+} eq./mg protein and ORAC value = 4,383.92 ± 12.23 µmol TE/mg protein). Among the three commercial enzymes, the lowest ROS scavenging activities was observed in sericin hydrolysates obtained by using papain. In summary, Alcalase® was selected as the best candidate protease for further optimization of antioxidant activity of sericin hydrolysates.
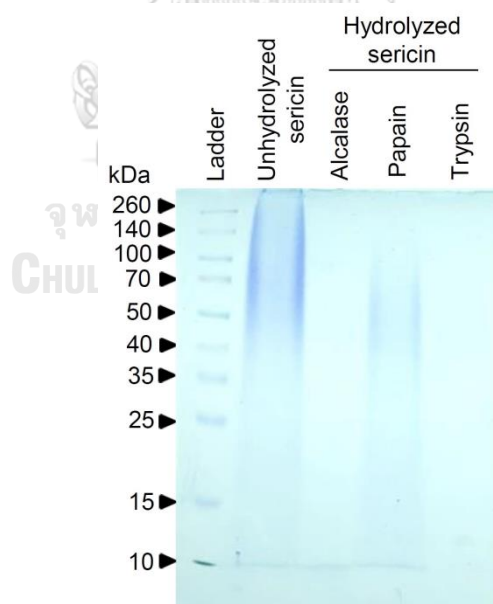
Figure 16 *Distribution of protein composition in sericin hydrolysates prepared from different commercial enzymes in SDS-PAGE analysis.*

Table 11 *Antioxidant activity of hydrolyzed silk sericin from various proteases*

Protease Enzyme	Factors				Response variable		
	pH	E/S (w/w)	Temperature (°C)	Time (h)	DPPH* (% Inhibition)	FRAP value* (μmol Fe^{2+} eq./mg protein)	ORAC value* (μmol TE/mg protein)
- (Unhydrolyzed sericin)	-	-	-	-	9.43 ± 0.10[a]	327.50 ± 11.87[a]	2,767.72 ± 30.97[a]
Alcalase®	8	2	60	3	19.71 ± 0.13[b]	435.50 ± 10.13[b]	4,383.92 ± 12.23[b]
Papain	7	2	60	3	12.64 ± 0.16[c]	274.68 ± 10.47[c]	3,897.33 ± 23.64[c]
Trypsin	8	2	40	3	14.43 ± 0.09[d]	284.51 ± 6.46[c]	4,026.85 ± 20.17[d]

E/S: Enzyme/Substrate ratio, TE: Trolox equivalence

Data is presented as means ± SEM (n=3). a-d values with the same letter denote no significant difference in each assay ($p<0.05$).

* Obtained from three independent experiments

2. Response surface optimization of enzymatic reaction for sericin hydrolysates prepared by using Alcalase®

To investigate the influence of enzymatic conditions on the antioxidant activity of sericin hydrolysates, the independent factors, pH, enzyme/substrate ratio and temperature, were resolved by RSM. The experimental conditions and resultant antioxidant activity generated through Box-Behnken design of RSM are shown in Table 12. From the 17 experimental conditions, the antioxidant responses of sericin hydrolysates ranged as follows: % inhibition on DPPH: 11.21–20.37%, FRAP: 362.03–455.93 μmol Fe^{2+} eq./mg protein and ORAC: 3,568.68–4,597.03 μmol TE/mg protein.

Table 12 *Box-Behnken factorial design of enzymatic hydrolysis and antioxidant*

response

Run	Independent variables			Responses		
	A: pH	B: E/S (w/w)	C: Temperature (°C)	Y_1: DPPH (% Inhibition)	Y_2: FRAP (µmol Fe^{2+} eq./mg sample)	Y_3: ORAC (µmol TE/mg sample)
1	9	2	70	14.67	455.93	4,591.43
2	7	2	70	20.37	449.07	4,504.01
3	8	3	70	18.89	422.03	4,156.45
4	8	2	60	14.83	439.90	4,086.49
5	8	1	50	12.86	364.41	3,617.85
6	8	2	60	14.69	433.76	4,073.43
7	9	3	60	11.21	383.05	4,052.36
8	8	3	50	14.61	404.24	3,568.68
9	9	2	50	13.37	376.95	3,805.73
10	7	3	60	16.87	414.41	3,908.42
11	8	2	60	14.71	443.90	4,086.49
12	7	1	60	13.58	362.03	4,142.16
13	8	2	60	14.15	442.04	4,097.94
14	9	1	60	14.20	445.76	4,283.99
15	7	2	50	12.86	368.64	3,696.03
16	8	1	70	18.31	452.54	4,597.03
17	8	2	60	14.37	449.32	4,064.59

E/S: Enzyme/Substrate ratio, TE: Trolox equivalence

Data were analyzed using model regression analysis with $p < 0.05$ using

Design-Expert[®] 11 software. Polynomial equations were as follows:

$$Y1 = 14.5508 - 1.2788A + 0.3292B + 2.3169C - 1.5689AB - 1.5545AC - 0.2932BC$$
$$- 0.7172A^2 + 0.1325B^2 + 1.4844C^2$$

$$Y2 = 441.784 + 8.4431A - 0.1266B + 33.1675C - 28.7722AB - 0.3609AC -$$
$$17.5847BC - 19.3137A^2 - 21.1577B^2 - 9.8212C^2$$

$$Y3 = 4081.7867 + 60.3617A - 119.3904B + 395.0788C + 0.5267AB - 5.5683AC -$$
$$97.8541BC + 89.6237A^2 - 74.6771B^2 - 22.1088C^2$$

Where Y1 is the response from DPPH, Y2 is the response from FRAP, Y3 is the response from ORAC, A is pH, B is enzyme/substrate ratio and C is temperature.

Following the statistical analysis of the quadratic model of DPPH (Table 13), FRAP (Table 14) and ORAC responses (Table 15), the significance of all models was evidenced with $p < 0.05$. Additionally, both R^2 and adjusted R^2 ranging between 0.9143 and 0.9988 as well as the non-significance ($p > 0.05$) of lack of fit indicated the high accuracy of predicted responses from these quadratic models [130, 131]. Notably, the predicted R^2 is close to 1 in the quadratic model of response of DPPH (0.8829) and ORAC (0.9870) assays, as presented in Tables 14 and 15, respectively, while the predicted R^2 value is about 0.4991 for FRAP response (Table 14). The positive linear effects of pH (A) and temperature (C) were shown to be significant for scavenging activity determined by DDPH, FRAP and ORAC assays. However, the enzyme/substrate ratio (B) was shown to be clearly positive for DDPH and ORAC, but not for FRAP assay. Or to put it conversely, the quadratic effect of the enzyme/substrate ratio (B^2) only significantly affected ORAC and FRAP responses,

while all ROS scavenging activities were found to be modulated by the quadratic effects of pH (A^2) and temperature (C^2).

Table 13 ANOVA for quadratic model of DPPH response

Source	Sum of Squares	df	Mean Square	F-value	*p*-value
Model	87.88	9	9.76	72.96	< 0.0001*
pH (A)	13.08	1	13.08	97.75	< 0.0001*
E/S (B)	0.8671	1	0.8671	6.48	0.0384*
Temperature (C)	42.94	1	42.94	320.87	< 0.0001*
AB	9.85	1	9.85	73.57	< 0.0001*
AC	9.67	1	9.67	72.23	< 0.0001*
BC	0.3439	1	0.3439	2.57	0.1530
A²	2.17	1	2.17	16.19	0.0050*
B²	0.0740	1	0.0740	0.5526	0.4814
C²	9.28	1	9.28	69.32	< 0.0001*
Residual	0.9368	7	0.1338		
Lack of Fit	0.6191	3	0.2064	2.60	0.1895
Pure Error	0.3177	4	0.0794		
Cor Total	88.82	16			
R²	0.9895				
Adjusted R²	0.9759				
Predicted R²	0.8829				
Adeq Precision	32.1496				
C.V.%	2.44				

E/S: Enzyme/Substrate ratio, *p* < 0.05

Table 13 also indicates the interactive effect of two variables on scavenging activity against DPPH radicals. The interaction between pH and enzyme/substrate ratio (AB) and between pH and temperature (AC) clearly affected % inhibition of DPPH of sericin hydrolysates prepared from Alcalase®. Similarly, significant effects on FRAP antioxidant response arose from pH and enzyme/substrate ratio (AB) interaction as well as enzyme/substrate ratio and temperature (BC) interaction (Table 14). Surprisingly, only the interaction between enzyme/substrate ratio and temperature (BC) was significantly positive on scavenging activity against ROO$^\bullet$ (Table 15). Taken together, temperature seems to have the greatest influence on ROS scavenging activity of sericin hydrolysates determined by DPPH, FRAP and ORAC assays, as evidenced in multiple linear regression analysis of linear, quadratic and interactive effects.
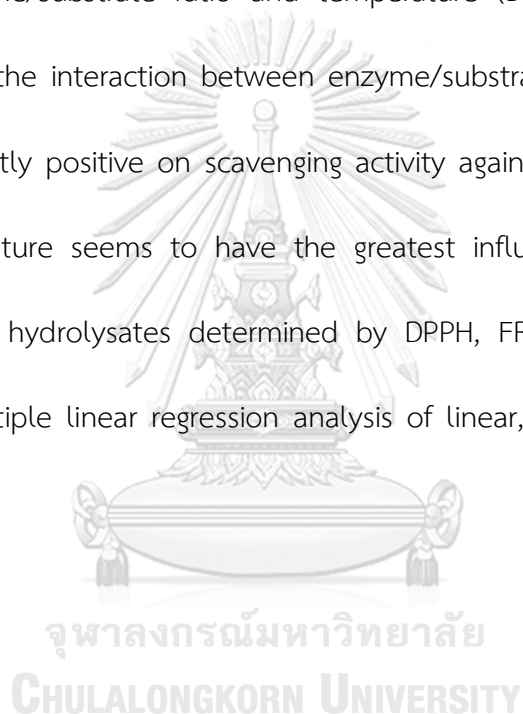
Table 14 *ANOVA for quadratic model of FRAP response*

Source	Sum of Squares	df	Mean Square	F-value	p-value
Model	18183.51	9	2020.39	19.97	0.0003*
pH (A)	570.29	1	570.29	5.64	0.0493*
E/S (B)	0.1283	1	0.1283	0.0013	0.9726
Temperature (C)	8800.69	1	8800.69	87.00	< 0.0001*
AB	3311.35	1	3311.35	32.74	0.0007*
AC	0.5211	1	0.5211	0.0052	0.9448
BC	1236.89	1	1236.89	12.23	0.0100*
A²	1570.61	1	1570.61	15.53	0.0056*
B²	1884.83	1	1884.83	18.63	0.0035*
C²	406.13	1	406.13	4.01	0.0851
Residual	708.09	7	101.16		
Lack of Fit	578.82	3	192.94	5.97	0.0585
Pure Error	129.27	4	32.32		
Cor Total	18891.59	16			
R²	0.9625				
Adjusted R²	0.9143				
Predicted R²	0.4991				
Adeq Precision	13.1588				
C.V.%	2.41				

E/S: Enzyme/Substrate ratio, *p < 0.05

The effect of correlative adjustment of two variables involved in enzymatic reactions on antioxidant activity of sericin hydrolysates prepared by using Alcalase[®] in DPPH, FRAP and ORAC assays is shown in response surface three-dimension graphs (Figure 17). Correspondence with regression analysis of interactive effect, the major influence of temperature (~70°C) during enzymatic process of Alcalase[®] on all ROS scavenging activities are obviously demonstrated in the correlative alteration with both pH (Figure 17b, e and h) and enzyme/substrate ratio (Figure 17c, f and i). The response surface plots also demonstrate that pH variations combined with variations in enzyme/substrate ratio alter only the % inhibition of DPPH free radicals (Figure 17a), but not Fe^{3+} reducing power (Figure 17d) or oxygen radical absorbance capacity (Figure 17g). Meanwhile, the correlative adjustment of enzyme/substrate ratio with other variables plays a minor role in the modulation of all ROS scavenging capacity.

Table 15 *ANOVA for quadratic model of ORAC response*

Source	Sum of Squares	df	Mean Square	F-value	*p*-value
Model	1.48×10^6	9	1.65×10^5	636.50	< 0.0001*
pH (A)	29148.25	1	29148.25	112.31	< 0.0001*
E/S (B)	1.14×10^5	1	1.14×10^5	439.39	< 0.0001*
Temperature (C)	1.24×10^6	1	1.24×10^6	4811.45	< 0.0001*
AB	1.11	1	1.11	0.0043	0.9497
AC	124.03	1	124.03	0.4779	0.5116
BC	38301.75	1	38301.75	147.58	< 0.0001*
A²	33820.70	1	33820.70	130.32	< 0.0001*
B²	23480.70	1	23480.70	90.48	< 0.0001*
C²	2058.09	1	2058.09	7.93	0.0259*
Residual	1816.69	7	259.53		
Lack of Fit	1146.02	3	382.01	2.28	0.2215
Pure Error	670.67	4	167.67		
Cor Total	1.48×10^6	16			
R²	0.9988				
Adjusted R²	0.9972				
Predicted R²	0.9870				
Adeq Precision	83.4263				
C.V.%	0.40				

E/S: Enzyme/Substrate ratio, *p < 0.05

3. ROS scavenging activity of sericin hydrolysates digested using Alcalase® under RSM-optimized conditions

Based on response surface analysis, the optimum conditions for preparation of sericin hydrolysates with maximized antioxidant activity in DPPH, FRAP and ORAC assays was generated through numerical optimization in Design-Expert® 11 software. After 3 h of enzymatic reaction performed according to RSM-optimized conditions at pH 7.5, enzyme/substrate ratio of 1.5 (w/w) and temperature of 70°C, sericin hydrolysates were evaluated for ROS scavenging activity. As presented in Table 16, sericin hydrolysates derived after the reaction of Alcalase® under the RSM-optimized condition possessed antioxidant activity, including % inhibition of DPPH, Fe^{3+} reducing power and oxygen radical absorbance capacity close to predicted values. It is noted that the lower variation between predicted and observed responses in DPPH and FRAP assays is indicated by lower % error range (between 1.46 and 2.50), compared with the 15.91% error in ORAC response.
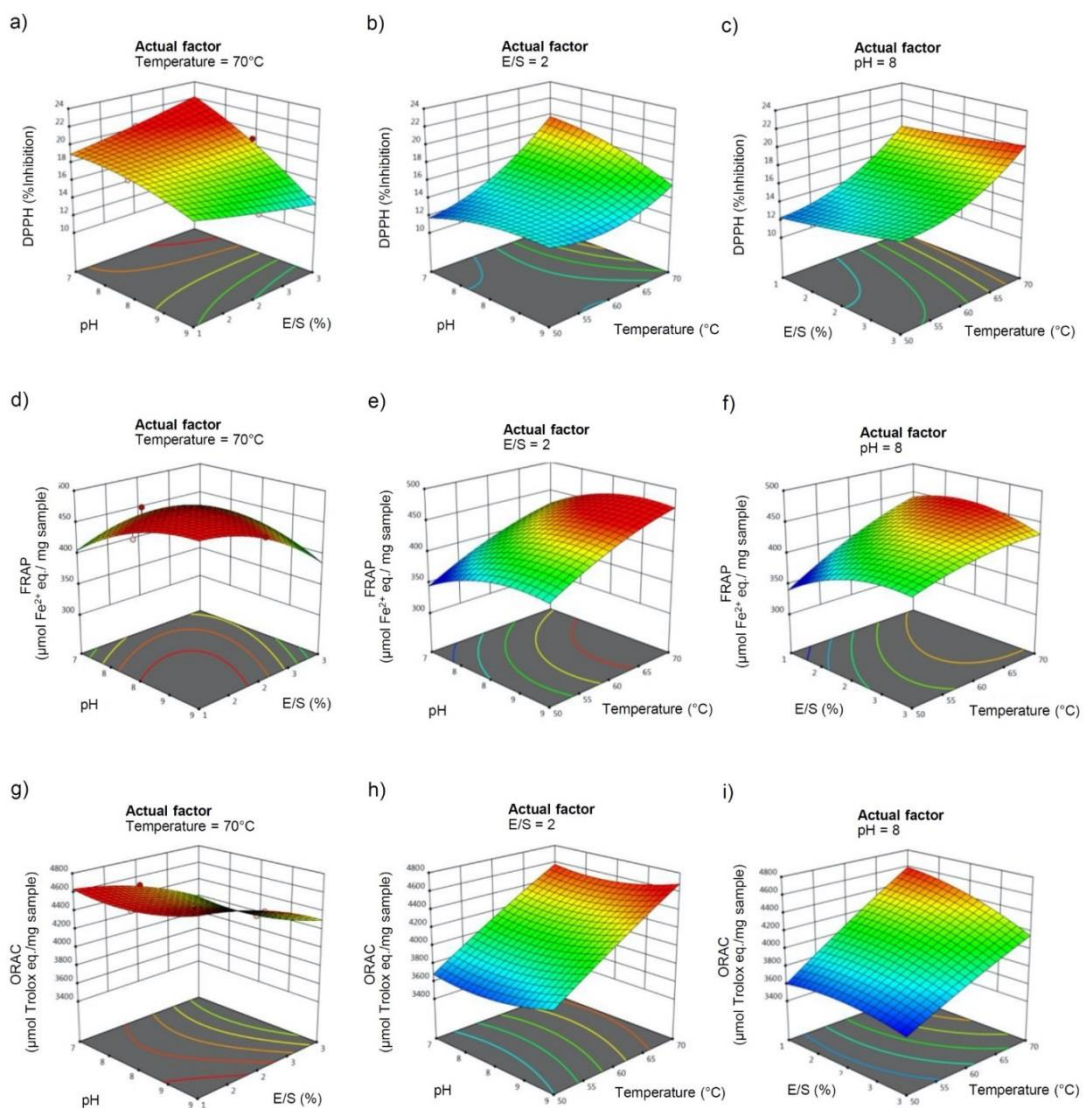
Figure 17 *Response surface plots depicting the effects of pH, enzyme/substrate ratio (E/S) and temperature on antioxidant activity of sericin hydrolysates prepared by using Alcalase[®] against a-c) DPPH free radicals, d-f) ferric ions (Fe^{3+}) and g-i) peroxyl radicals.*

Table 16 *Antioxidant activity of sericin hydrolyzed by Alcalase*[®] *under RSM-*

optimized condition

Optimized condition	Response	Predicted value	Observed value*	% Error
pH: 7.5, E/S: 1.5, Temperature: 70°C Time = 3 h	DPPH (% Inhibition)	19.14	18.65 ± 0.21	2.56
	FRAP (μmol Fe^{2+} eq./mg sample)	455.93	462.31 ± 10.82	1.40
	ORAC (μmol TE/mg sample)	4,532.23	3,811.00 ± 39.37	15.91

E/S: Enzyme/Substrate ratio, TE: Trolox equivalence

*Obtained from three independent experiments

4. Sericin hydrolysates ameliorate H_2O_2-induced oxidative stress in human keratinocytes and melanin-generating cells

The ROS scavenging activity of sericin hydrolysates derived from Alcalase[®] was further evaluated in cell-based assay. Because the potential benefits of sericin are widely recognized in cosmeceuticals (3), the antioxidant activity of sericin hydrolysates obtained from Alcalase[®] was investigated in skin epidermal cells, including human keratinocytes and melanin-generating cells. Flow cytometry histograms illustrate the augmented cellular ROS detected by $DCFH_2$-DA fluorescence probe in keratinocytes (Figure 18a) and melanoma cells (Figure 18c) after exposure to 1 mM H_2O_2 for 30 min. Intriguingly, preculture with 20 mg/mL of Alcalase[®] sericin

hydrolysates for 1 h dramatically reversed cellular oxidative stress induced by H_2O_2. The lower relative ROS levels were indicated in the cells preincubated with sericin hydrolysates compared with the pretreatment either with unhydrolyzed sericin (20 mg/mL) or 5 mM NAC, a well-known antioxidant (Figure 18b and d). It is worth noting that RSM-optimized sericin hydrolysates possess greater % inhibition against H_2O_2 in both HaCaT (99.11 ± 0.54%) and MNT-1 cells (73.25% ± 8.32%) compared with unhydrolyzed sericin (HaCaT: 88.52 ± 2.43%, MNT-1:64.99 ± 7.83%) or NAC (HaCaT: 30.26 ± 7.62%, MNT-1:51.05 ± 7.14%). These results confirm the antioxidant potential of sericin hydrolysates prepared under RSM-optimized conditions for cosmetic application.
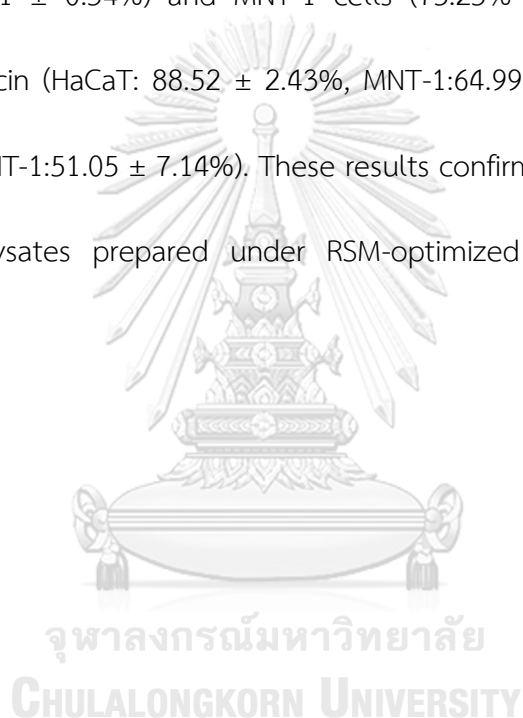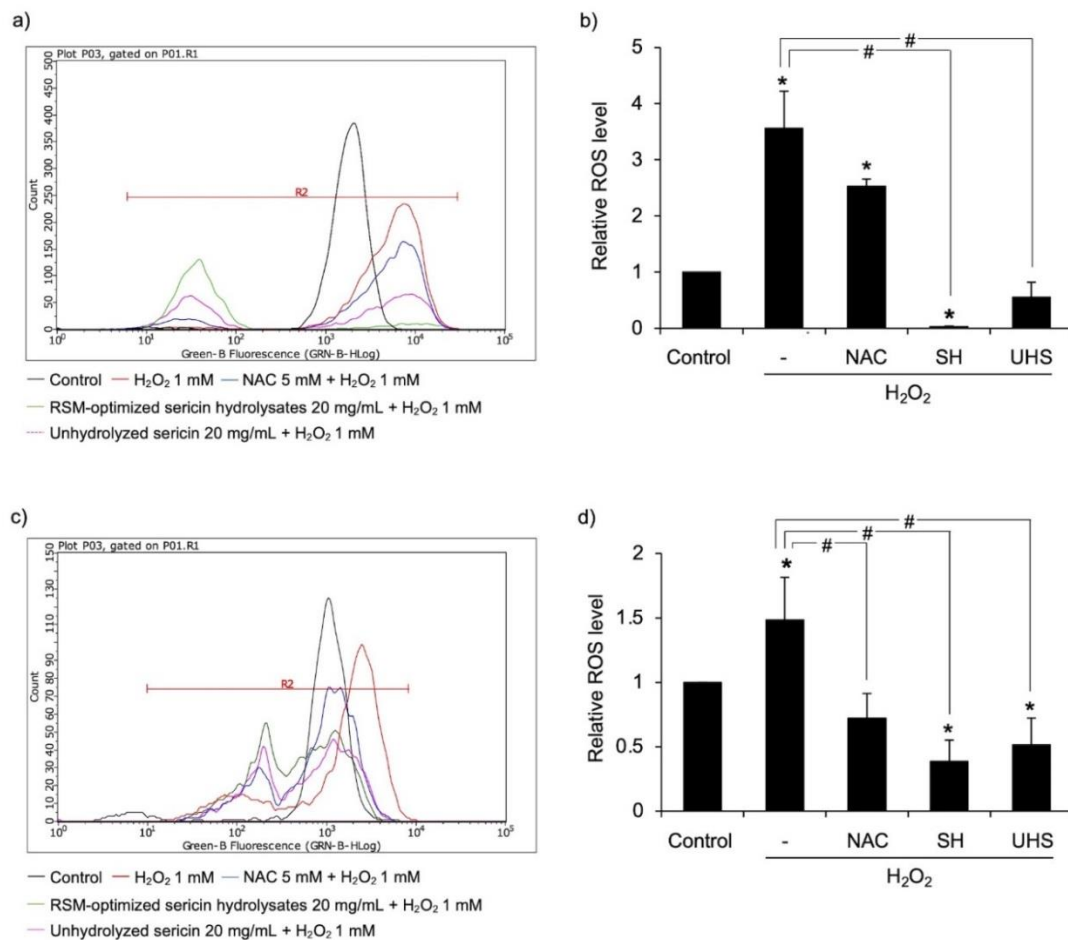
Figure 18 *Cellular antioxidant activity of sericin hydrolysates prepared from*

Alcalase® under RSM optimized conditions. The alteration of cellular ROS levels is

presented in flow cytometry histograms of (a) human keratinocytes and (c) human

melanin generating MNT-1 cells stained with DCFH$_2$-DA fluorescence probe.

Precultures with 5 mM N-acetyl cysteine (NAC), 20 mg/mL unhydrolyzed sericin (UHS)

or 20 mg/mL RSM-optimized sericin hydrolysates (SH) obviously diminished the

relative ROS levels in (b) human keratinocytes and (d) MNT1 cells after exposure to

1 mM hydrogen peroxide (H$_2$O$_2$) for 30 min. Data is presented as means ± SEM from

three independent experiments. *p < 0.05 compared with untreated control cells. [#]p

< 0.05 compared with the cells treated only with H_2O_2.

The size distribution profile was also evaluated in sericin hydrolysates prepared under RSM-optimized condition via size exclusion chromatography using FLPC coupling with HiPrep 16/60 Sephacryl S-200 HR column. Like the distribution pattern observed in SDS-PAGE analysis (Figure 19a), the FPLC chromatogram illustrates that RSM-optimized sericin hydrolysates mainly contained with small protein (~0.2–12 kDa) while the mixture of proteins ranging between 0.2 to higher than 150 kDa was presented in unhydrolyzed sericin (Figure 19b). These results suggest that greater antioxidant activity might result from the protein at low molecular weight composing in RSM-optimized sericin hydrolysates.

จุฬาลงกรณ์มหาวิทยาลัย

CHULALONGKORN UNIVERSITY
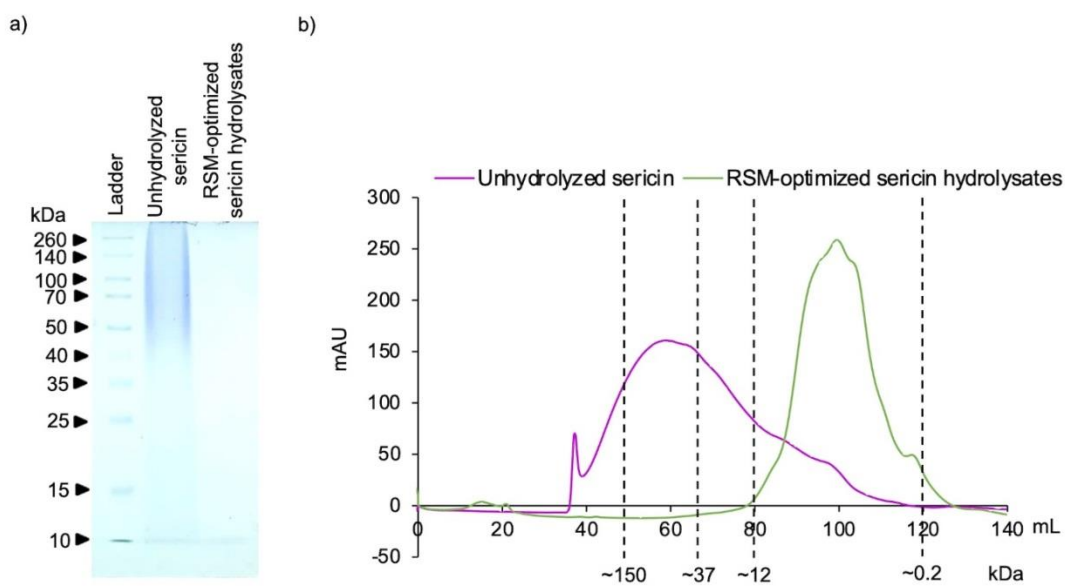
Figure 19 *Molecular weight distribution of protein composition in unhydrolyzed*

sericin and sericin hydrolysates prepared by Alcalase® under RSM optimized

condition in (a) SDS-PAGE analysis and (b) FPLC coupled with HiPrep 16/60

Sephacryl S-200 HR column.

5. Peptide constituents in sericin hydrolysates digested by Alcalase®

The digestion of peptide constituents after enzymatic reaction with Alcalase®

was further evaluated by LC-ESI-MS/MS compared with native peptides present in

unhydrolyzed sericin.

The data obtained from peptidomic analysis indicates the presence of various

sericin-related peptides in the unhydrolyzed sericin, which are proteins made from

wastewater of the silk industry (Figure 20). Though mostly composed of sericin-

derived peptides, the amount of peptide constituents were remarkably different in

the sericin hydrolysates prepared by using Alcalase® compared to unhydrolyzed sericin. These results support the alteration of peptide constituents in sericin hydrolysates digested by Alcalase®.

Protein (Identified sequence)	Unhydrolyzed sericin (LFQ)	Sericin hydrolysates (LFQ)
Sericin (DASSTSSSVSRSHR)	17.09	20.54
Sericin 1 (AAGGATKSG)	43.73	22.31
Sericin 1-like isoform X2 (SQESASYSSSSSSSTEESSSSSSR)	26.16	23.10
Sericin 1-like isoform X3 (GSTERPQPTGHRSAEESS)	18.31	0.00
Sericin 1-like isoform X4 (ESSAEDTKSSNSNVQSDA)	18.21	0.00
Sericin 1-like isoform X5 (NSNVQSDEK)	20.60	0.00
Sericin 1-like isoform X9 (AFGHHQTG)	0.00	19.93
Sericin 1-like isoform X10 (AAGGATKS)	17.52	0.00
Sericin 1B (ADYHNDPNGGSASAGQSR)	0.00	18.36
Sericin 2 (ETETYSDKDAQTSESERTQSKDN)	0.00	11.82
SC element binding protein (DLEEMSVTD)	0.00	17.03
Silk gland factor 1 (AASPTSALQRARNDKTYRR)	0.00	22.47
Silk gland factor 3 (AATTYMPAEM)	21.03	0.00
Homothorax (AAPAHALPGEPLVHK)	20.38	0.00
Extradenticle (AAGLAGLL)	20.21	21.38

LFQ: Relative label-free quantification

Figure 20 *Peptide constituents in sericin hydrolysates prepared by using Alcalase®*

a) The wide range of peptide distribution from 10 to 260 kDa was demonstrated in unhydrolyzed sericin via SDS-PAGE analysis while only peptide at ~10 kDa contained in sericin hydrolysates prepared by using Alcalase®. b) Peptidomic analysis reveals

the alteration of both type and ratio of peptide constituents in sericin after

enzymatic digestion by Alcalase®. The level of peptides in each sample were

expressed as log2 value.

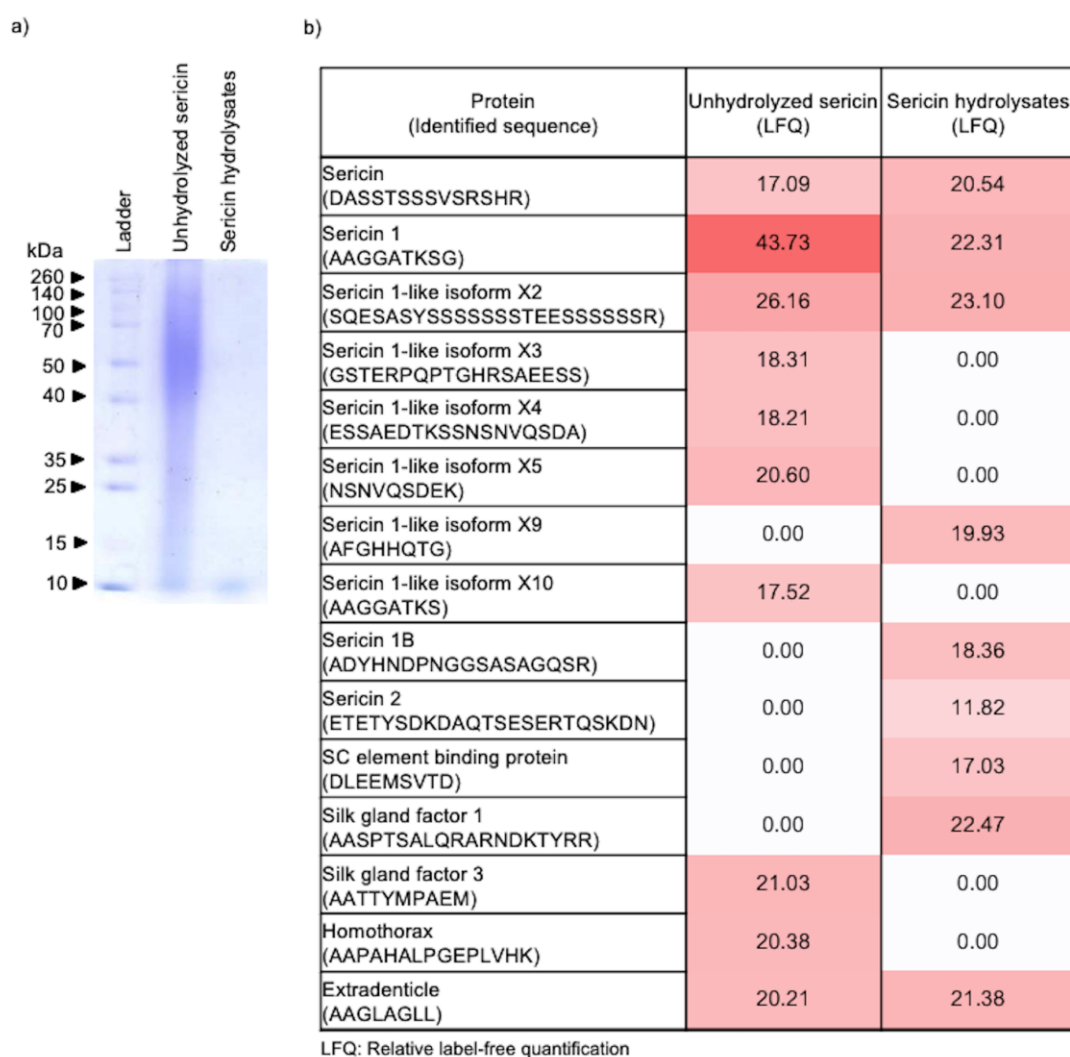## 6. Suppressive effect of sericin hydrolysates on melanin production in human melanin-producing cells

To evaluate the suppressive effect on melanin production, the cytotoxic profile of Alcalase®-hydrolyzed sericin was accessed using MTT viability assay. After culture for 24 h, there was no significant change in MNT-1 cell viability following treatment with 1–20 mg/mL sericin hydrolysates compared with the untreated control cells (Figure 21a). The effect on cell proliferation was further examined in MNT-1 cells incubated with Alcalase®-hydrolyzed sericin at 0–20 mg/mL for 24–72 h. Despite a 24-h treatment with a considerably non-toxic concentration, sericin hydrolysates (20 mg/mL) notably suppressed proliferation in human melanoma MNT-1 cells over a 48–72-h incubation (Figure 21b). Thus, treatment with Alcalase®-hydrolyzed sericin ranging from 0 to 20 mg/mL for 0–24 h was selected as the optimum non-toxic condition for determining antimelanogenic activity in human melanin-producing cells.

Figure 21c shows the gradual increase of melanin production in human melanoma MNT-1 cells after culturing for 6–24 h. The cAMP activator and tyrosinase inhibitor, forskolin and 4-butylresorcinol, were respectively used as positive and

negative controls (131),(132). Surprisingly, incubation for 12 h with either 20 mg/mL

sericin hydrolysates or 4-butylresorcinol (20 µM) comparably decreased cellular

melanin content in human melanin-producing cells (Figure 20d). It is worth noting

that a dose-dependent reduction of melanin content was observed in MNT-1 cells

after a 24-h treatment with sericin hydrolysates at 5–20 mg/mL.

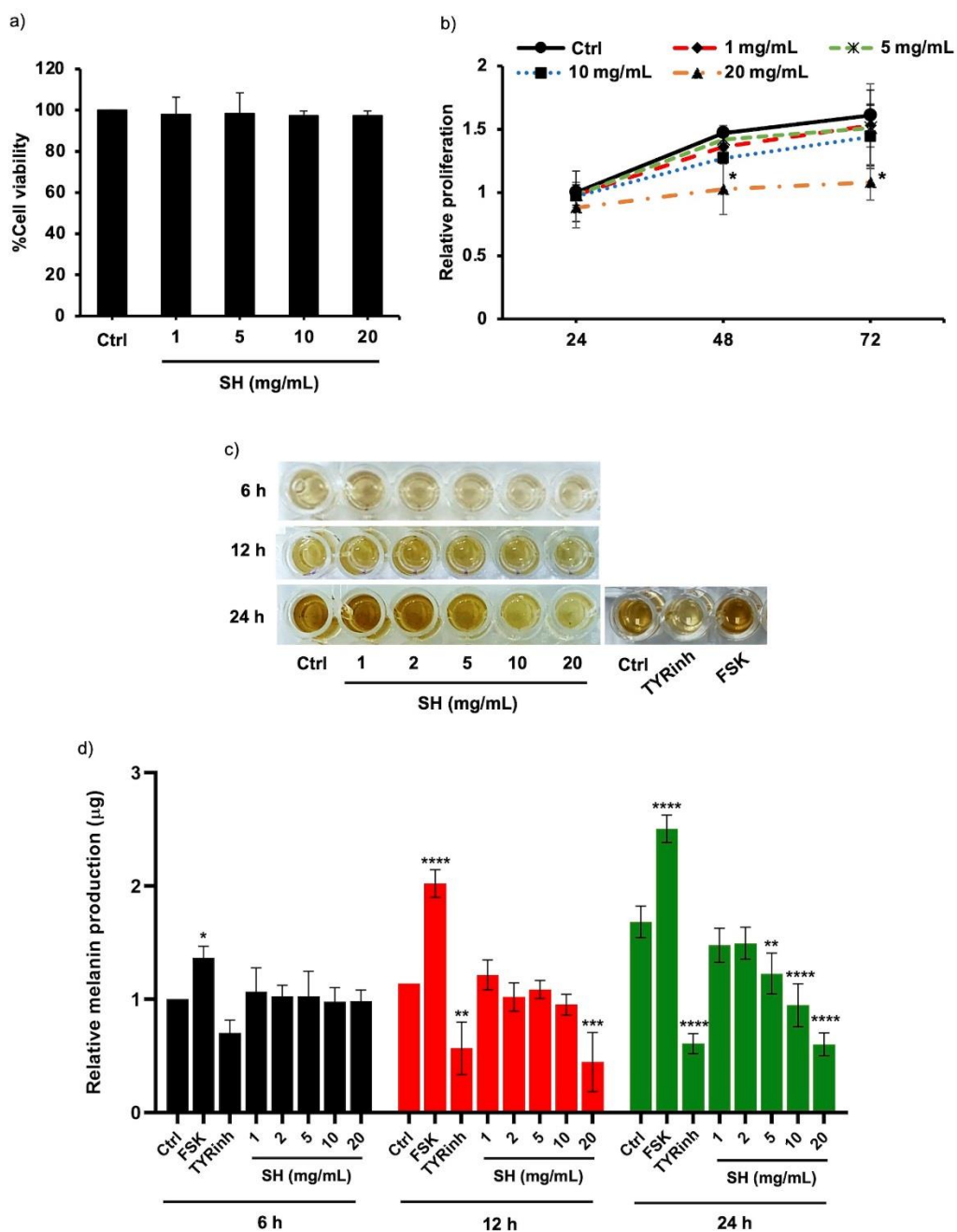*Figure 21* *Inhibitory effect of Alcalase®-hydrolyzed sericin on melanin production*

in human melanin-producing cells a) No significant difference of %cell viability was

detected via MTT assay after 24-h treatment with 1–20 mg/mL sericin hydrolysates

(SH), b) Crystal violet assay indicated low proliferation in human melanoma MNT-1

cells cultured with 20 mg/mL sericin hydrolysates for 48–72 h. c) The cellular

melanin content in MNT-1 cells was gradually increased after culture for 6–24 h in the experiment condition. Tyrosinase inhibitor (TYRinh; 4-butylresorcinol) and forskolin (FSK) were respectively used as a negative control and positive control. d) Sericin hydrolysates prepared by using Alcalase® at 20 mg/mL significantly diminished melanin production in human melanin-producing cells promptly at 12-h treatment and sustainably until 24-h of the incubation time. Data is presented as means ± SEM from three independent experiments. *p < 0.05, **p < 0.01, ***p < 0.005, ****p < 0.001 versus non-treated cells (Ctrl).

The inhibitory effect on melanin production of unhydrolyzed sericin was also performed in human melanoma MNT-1 cells. Compared with sericin hydrolysates prepared by using Alcalase® at the same concentration (1–20 mg/mL), higher melanin content was presented in MNT-1 cells cultured with unhydrolyzed sericin for 24 h (Figure 22a). This corresponded with the half maximum inhibitory concentration (IC_{50}) on melanin production in MNT-1 cells shown in figure 22b. The lower IC_{50} value was demonstrated in sericin hydrolysates at approximately 9.05 ± 0.66 mg/mL compared with an IC_{50} value of 24.54 ± 0.17 mg/mL for the unhydrolyzed sericin-treated group. Taken together, these results clearly demonstrate the potent inhibitory effect of sericin hydrolysates against melanin production in human melanin-producing cells.
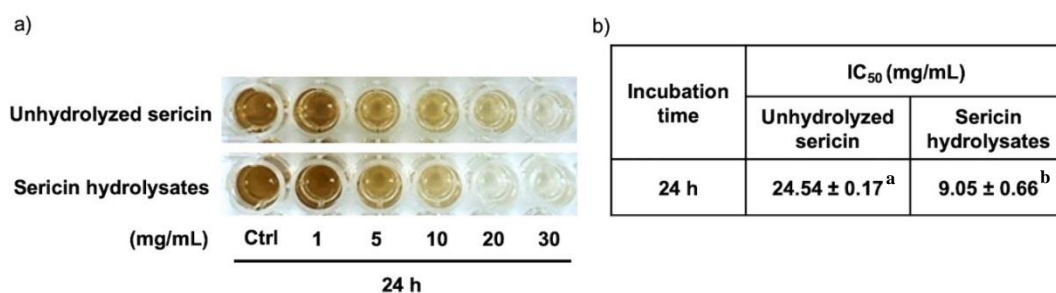
Figure 22 *The more potency of Alcalase®-hydrolyzed sericin on suppression of melanin production when compared with unhydrolyzed sericin was evidenced by a) the lower cellular melanin content and b) half maximum inhibitory concentration (IC$_{50}$) in human melanin-producing cells after 24-h of treatments. Data is presented as means ± SEM (n=3). a-b values with the same letters denote no significant difference (p < 0.05).*

7. Alcalase®-hydrolyzed sericin as a human tyrosinase inhibitor

The role as human tyrosinase inhibitor was determined after adding L-DOPA into the cellular lysate prepared from MNT-1 cells that contain tyrosinase with or without Alcalase®-hydrolyzed sericin. The formed dopachrome, which represents tyrosinase activity, was reduced in a concentration-dependent manner in the reaction containing 1–20 mg/mL sericin hydrolysates (Figure 23). It should be noted that the significant inhibition of human tyrosinase activity was observed only after incubation with 10–20 mg/mL of sericin hydrolysates. Nevertheless, the results confirm a role of Alcalase®-hydrolyzed sericin as an inhibitor against enzymatic activity of human tyrosinase.
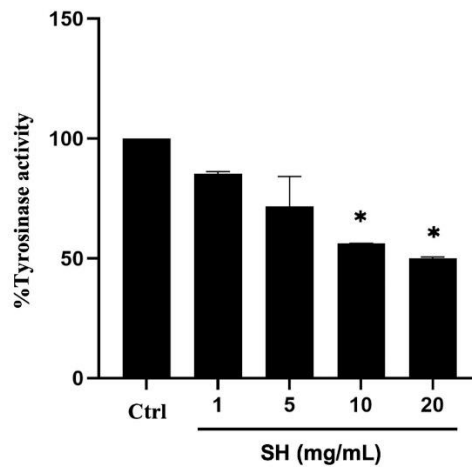
Figure 23 *The enzymatic function of tyrosinase containing in the cellular lysate from human MNT-1 cells was determined after adding of its substrate, L-DOPA (2 mM) with or without sericin hydrolysates (SH) prepared by using Alcalase®. After further incubation at 37°C for 10 min, Alcalase®-hydrolyzed sericin at 10–20 mg/mL significantly inhibited enzymatic activity of human tyrosinase. Data is presented as means ± SEM from three independent experiments. *p < 0.05 versus non-treated cells (Ctrl).*

8. Sericin hydrolysates downregulate tyrosinase expression in human melanin-producing cells

The expression level of tyrosinase, the rate-limiting enzyme in melanogenesis, was further evaluated to clarify the underlying mechanisms of Alcalase®-hydrolyzed sericin in human melanin-producing cells. Quantitative reverse transcription PCR revealed that not only tyrosinase mRNA but also MITF mRNA levels, a tyrosinase transcription factor, were downregulated in MNT-1 cells cultured with 20 mg/mL

sericin hydrolysates for 12 h (Figure 24a). Consequently, the decreased levels of both

MITF (Figure 24b) and tyrosinase proteins (Figure 24c) were detected by western blot

analysis in human melanin-producing cells incubated with sericin hydrolysates (20

mg/mL) for 24 h. It is worth noting that modulation of MITF and tyrosinase expression

levels is well-correlated with the antimelanogenic activity of Alcalase$^{®}$-hydrolyzed

sericin observed in MNT-1 cells after a 24-h treatment.
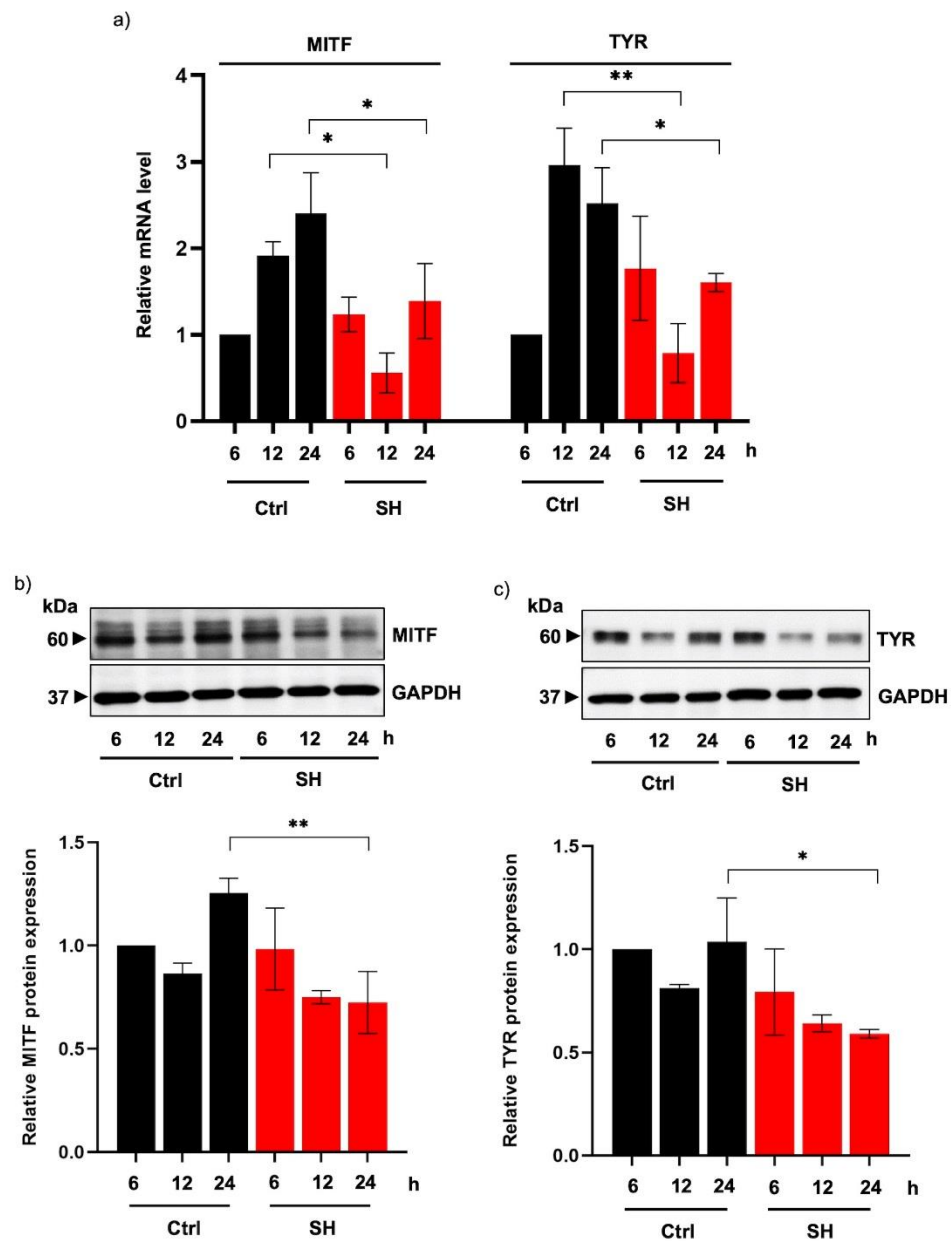
Figure 24 *Diminution of tyrosinase expression in human melanin-producing cells*

cultured with sericin hydrolysates a) Quantitative real-time PCR demonstrated the

decreased mRNA levels of MITF and tyrosinase (TYR) in human MNT-1 cells cultured

with 20 mg/mL sericin hydrolysates (SH) prepared by using Alcalase® for 12–24 h.

Consequently, protein expression levels of b) MITF and c) Tyrosinase was diminished

in sericin hydrolysates-treated human melanin-producing cells after 24-h of incubation time. Data is presented as means ± SEM from three independent experiments. *p < 0.05, **p < 0.01 versus non-treated cells (Ctrl).

9. Alteration of MITF-regulating proteins in human melanin-producing cells cultured with sericin hydrolysates

Based on the decreased expression of MITF mRNA, the modulation of upstream molecules regulating MITF transcription was examined in sericin hydrolysates-treated MNT1 cells. Despite no alteration of pGSK3β/GSK3β (Figure 25a) and β-catenin protein levels (Figure 25b), there was a significant reduction of pCREB/CREB expression in MNT-1 cells incubated with 20 mg/mL sericin hydrolysates for 12 h compared with the untreated control cells (Figure 25c). The suppression of pCREB/CREB cascade was correlated with reduced MITF mRNA level in MNT-1 cells following treatment with sericin hydrolysates for 12 h. Because of the remarked decrease of MITF protein expression at 24 h, the role of Alcalase®-hydrolyzed sericin on regulatory proteins involved in the post-translational regulation of MITF were examined. Figure 25d shows overexpression of pERK, a signaling molecule that promotes MITF degradation, in human melanin-producing cells incubated with 20 mg/mL sericin hydrolysates for 6–24 h. These results suggest that Alcalase®-hydrolyzed sericin mediates MITF expression at both the transcription and post-translational level.
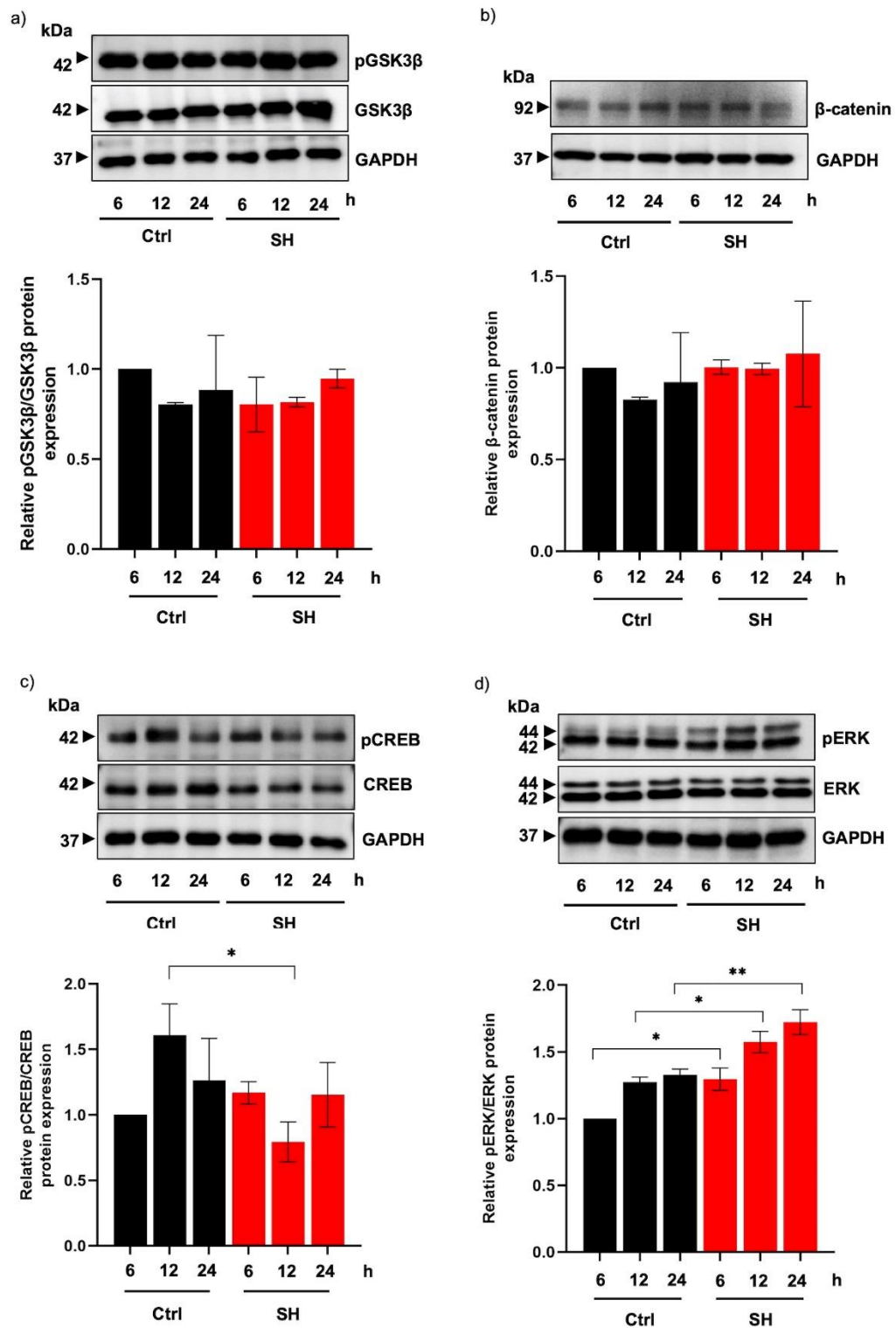
Figure 25 *MITF-regulating proteins modulated by sericin hydrolysates prepared by*

using Alcalase® a-b) There was no alteration of protein involving GSK3β /β -catenin

cascade, c) The decreased expression of pCREB/CREB indicated the restraint on upstream signal regulating MITF transcription in human MNT-1 cells incubated with 20 mg/mL sericin hydrolysates (SH) for 12 h. d) Alcalase®-hydrolyzed sericin (20 mg/mL) upregulated the expression of pERK, a signaling protein triggering MITF degradation, in human melanin-producing cells after the incubation for 6–24 h. Data is presented as means ± SEM from three independent experiments. *p < 0.05, **p < 0.01 versus non-treated cells (Ctrl).

Antioxidant peptides have been well recognized for their therapeutic potential and applicable benefits in diverse applications such as food additives and cosmeceutical ingredients (21),(22),(23). Recently, various uses of sericin protein present in the degumming water used in silk processing have been highlighted (3),(4),(5). Silk sericin has potential for use in recycling industrial waste, but it is also potent for biological activity, which inspires the investigation of its antioxidant activity (7),(8),(9),(26). It has been revealed that peptide characteristics, including molecular weight, amino acid sequence and hydrophobicity strongly determine its antioxidant potential (94). Corresponding with the results presented in this study, enzymatic digestion obviously alters the size distribution patterns (Figure 16) and radical scavenging activity of silk sericin protein (Table 11). Due to the possibility of specific scavenging activity being modulated by the definite features of peptide (94), sericin hydrolysates obtained from trypsin and papain enzymatic reactions demonstrated

lower Fe^{3+} reducing antioxidant power compared with both unhydrolyzed sericin and sericin hydrolysates derived from Alcalase® (Table 11). It should be noted that maximum antioxidant activity of protein hydrolysates requires suitable molecular distribution (26),(43),(101). Sericin hydrolysates obtained from Alcalase® reaction mostly composed with peptides at ~10 kDa meanwhile larger and smaller peptides were respectively found in papain and trypsin hydrolysates (Figure 16). Although the barely detected protein via SDS-PAGE, in which the optimum condition for separating protein needs to be further adjusted in this study, the exclusion chromatography FLPC revealed that Alcalase®-hydrolyzed sericin comtained with peptides lower than ~ 0.2–12 kDa (Figure 19). The substrate specificity to aromatic amino acids as well as the capability to cleave both terminal and non-terminal peptide bond might involve with the size distribution ranging between ~10–100 kDa in sericin hydrolysates derived from papain (135). Despite being an endopeptidase, high containing of lysine and arginine, the specific substrates for trypsin, in silk sericin protein could result in smaller size of sericin hydrolysates digested by trypsin compared to sericin hydrolysates prepared by Alcalase® (136).

Scavenging activity against free radicals, which is one of the important machineries of antioxidant compounds, can be achieved through the translocation of single electrons or hydrogen atoms to free radical molecules (15),(16). Therefore, the antioxidant capability of sericin hydrolysates obtained from three commercial enzymes was evaluated through DPPH and FRAP assays for determination of single

electron donation, as well as ORAC assay for evaluating the translocation of hydrogen atoms herein. When compared with unhydrolyzed, trypsin- and papain-hydrolyzed sericin, Alcalase® sericin hydrolysates possessed the highest scavenging capacity against all three free radicals (Table 11). Alcalase® is widely used for the enzymatic digestion of various proteins for specific purposes because of its broad substrate specificities and commercial availability (137),(138),(139). The obtained results presented in Table 11 concur with a previous study into the highest % inhibiting DPPH and Fe^{3+} reducing power of sericin hydrolysates derived from Alcalase® compared with various protease enzymes (26). In contrast, the reduction of Fe^{3+} reducing power was indicated in trypsin- and papain-hydrolyzed sericin. It is the fact that the less correlation with other antioxidant assays and the underestimating ROS scavenging activity of hydrogen-transferring molecules, especially antioxidant peptide, has been reported as the limitations of FRAP assay (18). Nevertheless, FRAP reducing power is established to represent the capability of antioxidants to maintain cellular redox status and stop oxidative chain reaction in biological sample (88). Taken together with the greater ROS scavenging activity through hydrogen atom translocation assessed via ORAC assay, these data clearly suggest that sericin hydrolysates derived from Alcalase® digestion are a candidate for antioxidant peptides through mediating single electron and hydrogen atom transfer.

In order to maximize the antioxidant activity of Alcalase® sericin hydrolysates, ROS scavenging activities of sericin hydrolysates released from Alcalase® at various

enzymatic conditions were simulated through RSM. Under optimized conditions of pH: 7.5, enzyme/substrate ratio: 1.5 (w/w) and temperature: 70°C obtained from numerical optimization in Design-Expert[®] 11 software, sericin hydrolysates demonstrated scavenging activities assessed through DPPH, FRAP and ORAC assays close to predicted values (Table 16). Response surface models are considered reliable when the response conducted under recommended optimum conditions contains % error from the model-predicted value lower than 5% [140, 141]. For % inhibition of DPPH, the low % error between actual and predicted response of sericin hydrolysates (Table 16) corresponded with the predicted R^2 value obtained from multiple linear regression analysis (Table 13). The predicted R^2, which is usually lower than R^2 value, is a statistical term presenting the suitability of using a regression model for prediction of a new observed response. Despite having the lowest predicted R^2 value (0.4991) among the three regression response models, the greatest correlation between predicted and conducted responses of FRAP assay was obtained from Alcalase[®] sericin hydrolysates. In contrast, the highest difference from the predicted response of sericin hydrolysates prepared by using Alcalase[®] according to RSM conditions was observed in scavenging activity against ROO$^{\bullet}$ (Table 16). Variations in the ORAC response of sericin hydrolysates might result from the fact that only ROO$^{\bullet}$ scavenging activity can be significantly altered through the digestion of all three variables, pH (A), enzyme/substrate ratio (B) and temperature (C), as

evidenced by p being < 0.05 in linear (A, B and C) and quadratic (A^2, B^2 and C^2) effects in Table 15.

Notably, the ROS scavenging activities of % DPPH inhibition, Fe^{3+} reducing power and oxygen radical absorbance capacity were comparable between sericin hydrolysates derived from optimized RSM (Table 16) and the manufacturers' recommended conditions (Table 11). The adjustment of pH and/or temperature according to the active enzymatic conditions of Alcalase$^®$ (pH 6.5-8.5, 60°C) might be considered to minimize the production costs. Because substantial alteration of hydrolyzed proteins was obtained after 3 h of Alcalase$^®$ enzymatic reaction [137], antioxidant sericin hydrolysates should be achieved after at least 3 h of enzymatic digestion. Additionally, the dramatically augmented antioxidant capacity of sericin hydrolysates in H_2O_2-treated human keratinocytes and melanoma cells compared with a well-known antioxidant (NAC) and unhydrolyzed sericin (Figure 17) verify its biological activity. It is worth noting that the secondary structures, particularly β-sheet considerably contribute to free radical scavenging activity and cellular antioxidant potential of unhydrolyzed sericin solution though composing mainly of protein at high molecular weight (Figure 19) (48),(140),(141),(142). Indeed, the highest ratio of β-sheet structure was also revealed in the protein hydrolysates prepared by Alcalase$^®$ compared with various enzymatic digestions (142).

In searching for an effective treatment for hyperpigmented disorders, it is essential to identify compounds that not only exhibit potent efficacy but also have

an acceptable safety profile (32),(143). Recent evidence indicates that MITF, a melanogenic transcription factor, is a novel therapeutic target for modulating melanin synthesis (37),(38). Suppression of MITF correlates with downregulated melanogenesis, a reduction of melanin content, and lightened skin tone (38). While most of available depigmenting agents on the market are tyrosinase inhibitors (30),(144), sericin hydrolysates prepared by using Alcalase® exhibit potent antimelanogenic activity in human melanin-producing cells by acting as human tyrosinase inhibitor (Figure 23) and modulating MITF expression (Figure 24a and b).

Sericin, a natural protein present in degumming water from the silk industry, is recognized for its therapeutic benefits, especially in cosmeceutical applications (48). Nevertheless, a broad peptide composition (~10–250 kDa) hinders sericin from precise therapeutic targeting and lessens its potency (3),(138),(145). Optimal size distribution and specific sequences of amino acids could influence the biological activity of natural proteins (94). Because of the adjustable conditions for producing protein hydrolysates, enzymatic reactions are widely accepted as a method to digest protein structure and composition (146),(147). Among the various proteases, Alcalase®-hydrolyzed proteins exhibited the most promising therapeutic effects (26). As such, the altered pattern of both size (Figure 19a) and peptide component (Figure 20) showed a higher antimelanogenic activity of Alcalase®-hydrolyzed sericin compared with the unhydrolyzed sericin protein (Figure 21). Accounting for the broad substrate specificity, commercial availability (137),(138), and potent antimelanogenic

effects demonstrated in this study, Alcalase® could be considerably suitable for enzymatic digestion of sericin proteins.

The greater activity of the sericin hydrolysates could result from smaller-sized peptides, which readily permeate through cell membranes (148). Despite the diverse types of sericin-related peptides, specific peptides identified by peptidomic analysis in Alcalase®-hydrolyzed sericin likely play an important role in the suppressive effect on melanin production in human melanin-producing cells. Amino acid constituents in peptides critically modulate the inhibitory activity against enzymatic function of tyrosinase. It has been reported that tyrosinase inhibitory peptides should composed with arginine and/or phenylalanine for strong binding with tyrosinase and inhibitory activity. Additionally, hydrophobic amino acids such as valine, alanine and leucine as well as aromatic residual of threonine and tyrosine are also essential for the activity of tyrosinase inhibitory peptides (55),(149). The antimelanogenic potential of sericin was discovered through its activity as a mushroom tyrosinase inhibitor (24),(29). Beside composing of various inhibitory amino acids, serine and threonine containing in sericin was proposed to chelate copper at active site, which involves with the capability of melanin synthesis of mushroom tyrosinase (43). Though mushroom tyrosinase is wildly accepted for screening of tyrosinase inhibitors (150),(151), the difference of structure and amino acid sequence between human and mushroom tyrosinase could result in variable effect of the candidate tyrosinase inhibitors (152),(153). The inhibitory activity against human tyrosinase associated with sericin-

derived peptides (Figure 23), which was first identified in this study, warrants the further development of sericin hydrolysates prepared by using Alcalase® as an effective treatment for hyperpigmented disorders.

Interestingly, the suppressive activities on both the activity (Figure 23) and protein expression of tyrosinase (Figure 24a and c), a rate-limiting enzyme in melanogenesis, indicate the inhibitory effect of Alcalase®-hydrolyzed sericin against melanin production observed in human melanin-producing cells after a 12- and 24-h treatment (Figure 21c and d). It should be noted that the modulated mRNA level should be detected prior the alteration of protein expression. A significant reduction of tyrosinase mRNA and its transcription factor, MITF, were demonstrated in MNT-1 cells cultured with 20 mg/mL sericin hydrolysates at 12 h (Figure 24a). This was correlated with the concomitant reduction of protein levels at a later time point (Figure 24b and c).

The upregulated proteins in the MITF-related pathways result in the overproduction of melanin and cellular hyperproliferation (154). Consequently, depigmenting compounds that target MITF effectively reduce melanin content via restraining melanogenesis-regulated proteins and the proliferation of melanocytes (38),(155). Notably, MNT-1 cells are human melanoma and has been used for evaluating melanogenic effects because of its hyperproliferation and hyperpigmented phenotypes (156),(157). The low proliferation (Figure 21b) as well as decreased expression of MITF and tyrosinase in MNT-1 cells incubated with sericin hydrolysates

(Figure 24) demonstrate the high efficacy of Alcalase®-hydrolyzed sericin against melanogenesis in human melanin-producing cells.

The modulatory role of sericin hydrolysates prepared by using Alcalase® on the upstream signaling cascade that regulates MITF was observed by the reduction of pCREB/CREB level (Figure 25c); however, there was no alteration in the GSK3β/β-catenin signal (Figure 25a and b). The suppression of pCREB/CREB signaling correlated with decreased MITF mRNA level in human melanin-producing cells after treatment with sericin hydrolysates for 12 h. It should be noted that the gradual increase in pCREB/CREB expression level after a 24-h treatment with sericin hydrolysates may have been the result of a positive feedback mechanism from downstream proteins (158). Despite the recovery of the pCREB/CREB signal at the later time point, the low expression of MITF mRNA and protein was sustained up to 24 h of treatment with Alcalase®-hydrolyzed sericin. The protein levels of MITF is post-translationally regulated by pERK through proteasomal degradation (159). The upregulated pERK/ERK pathway in human melanin-generating cells treated with sericin hydrolysates (Figure 25d) would promote the reduction of MITF protein levels concomitantly with downregulated tyrosinase and a reduction of melanin production.

It has been reported that the activation of melanocyte-specific melanocortin-1 receptor (MC1R), a cellular receptor on melanocyte, by α-melanocyte-stimulating hormone (α-MSH), adrenocorticotropic hormone (ACTH) and agonist stimulating

protein (ASP) upregulates melanonegesis through modulating both and pCREB/CREB and pERK/ERK cascades (106). Therefore, the antagonist effect of Alcalase$^{®}$-hydrolyzed sericin against MC1R is worth for further investigation.

REFERENCES

1. Zhu L, Hao Y, Lu Z-N, Wu H, Ran Q. Do economic activities cause air pollution? Evidence from China's major cities. Sustainable Cities and Society. 2019;49:101593.

2. Pakdel E, Wang J, Allardyce BJ, Rajkhowa R, Wang X. Functionality of nano and 3D-microhierarchical TiO2 particles as coagulants for sericin extraction from the silk degumming wastewater. Sep Purif Technol. 2016;170:92-101.

3. Kunz RI, Brancalhão RMC, Ribeiro LdFC, Natali MRM. Silkworm Sericin: Properties and Biomedical Applications. BioMed Research International. 2016;2016:8175701.

4. Cao T-T, Zhang Y-Q. The potential of silk sericin protein as a serum substitute or an additive in cell culture and cryopreservation. Amino Acids. 2017;49(6):1029-39.

5. Liu D, Chen C, Wang D, Chen Z, Song C. Effect of sericin on the p38MAPK signaling pathway and NLRP3 inflammasome in the kidney of type 2 diabetic rats. Exp Ther Med. 2020;20(6):267-.

6. Jena K, Pandey JP, Kumari R, Sinha AK, Gupta VP, Singh GP. Tasar silk fiber waste sericin: New source for anti-elastase, anti-tyrosinase and anti-oxidant compounds. International Journal of Biological Macromolecules. 2018;114:1102-8.

7. Ampawong S, Isarangkul D, Aramwit P. Sericin ameliorated dysmorphic mitochondria in high-cholesterol diet/streptozotocin rat by antioxidative property. Exp Biol Med (Maywood). 2017;242(4):411-21.

8. Ersel M, Uyanikgil Y, Karbek Akarca F, Ozcete E, Altunci YA, Karabey F, et al. Effects of Silk Sericin on Incision Wound Healing in a Dorsal Skin Flap Wound Healing Rat Model. Medical science monitor : international medical journal of experimental and clinical research. 2016;22:1064-78.

9. Manesa KC, Kebede TG, Dube S, Nindi MM. Profiling of Silk Sericin from Cocoons of Three Southern African Wild Silk Moths with a Focus on Their Antimicrobial

and Antioxidant Properties. Materials (Basel, Switzerland). 2020;13(24):5706.

10.   Shahidi F, Zhong Y. Measurement of antioxidant activity. J Funct Foods. 2015;18:757-81.

11.   He L, He T, Farrar S, Ji L, Liu T, Ma X. Antioxidants Maintain Cellular Redox Homeostasis by Elimination of Reactive Oxygen Species. Cellular Physiology and Biochemistry. 2017;44(2):532-53.

12.   E. Obrenovich M, Li Y, Parvathaneni K, B. Yendluri B, H. Palacios H, Leszek J, et al. Antioxidants in Health, Disease and Aging. CNS & Neurological Disorders - Drug Targets. 2011;10(2):192-207.

13.   Ribeiro AS, Estanqueiro M, Oliveira MB, Sousa Lobo JM. Main Benefits and Applicability of Plant Extracts in Skin Care Products. Cosmetics. 2015;2(2).

14.   Gulcin İ. Antioxidants and antioxidant methods: an updated overview. Archives of Toxicology. 2020;94(3):651-715.

15.   Apak R, Özyürek M, Güçlü K, Çapanoğlu E. Antioxidant Activity/Capacity Measurement. 1. Classification, Physicochemical Principles, Mechanisms, and Electron Transfer (ET)-Based Assays. Journal of Agricultural and Food Chemistry. 2016;64(5):997-1027.

16.   Ndhlala AR, Moyo M, Van Staden J. Natural antioxidants: fascinating or mythical biomolecules? Molecules. 2010;15(10):6905-30.

17.   Huang D, Ou B, Prior RL. The Chemistry behind Antioxidant Capacity Assays. Journal of Agricultural and Food Chemistry. 2005;53(6):1841-56.

18.   Ou B, Huang D, Hampsch-Woodill M, Flanagan JA, Deemer EK. Analysis of Antioxidant Activities of Common Vegetables Employing Oxygen Radical Absorbance Capacity (ORAC) and Ferric Reducing Antioxidant Power (FRAP) Assays: A Comparative Study. Journal of Agricultural and Food Chemistry. 2002;50(11):3122-8.

19.   Alam MN, Bristi NJ, Rafiquzzaman M. Review on in vivo and in vitro methods evaluation of antioxidant activity. Saudi Pharmaceutical Journal. 2013;21(2):143-52.

20.   Dienaitė L, Pukalskienė M, Pukalskas A, Pereira CV, Matias AA, Venskutonis PR.

Isolation of Strong Antioxidants from Paeonia Officinalis Roots and Leaves and Evaluation of Their Bioactivities. Antioxidants (Basel, Switzerland). 2019;8(8):249.

21. Wang L, Ding L, Wang Y, Zhang Y, Liu J. Isolation and characterisation of in vitro and cellular free radical scavenging peptides from corn peptide fractions. Molecules. 2015;20(2):3221-37.

22. Jiang B, Zhang X, Yuan Y, Qu Y, Feng Z. Separation of Antioxidant Peptides from Pepsin Hydrolysate of Whey Protein Isolate by ATPS of EOPO Co-polymer (UCON)/Phosphate. Sci Rep. 2017;7(1):13320.

23. Zhang J-B, Zhao Y-Q, Wang Y-M, Chi C-F, Wang B. Eight Collagen Peptides from Hydrolysate Fraction of Spanish Mackerel Skins: Isolation, Identification, and In Vitro Antioxidant Activity Evaluation. Mar Drugs. 2019;17(4):224.

24. Manosroi A, Boonpisuttinant K, Winitchai S, Manosroi W, Manosroi J. Free radical scavenging and tyrosinase inhibition activity of oils and sericin extracted from Thai native silkworms (Bombyx mori). Pharmaceutical Biology. 2010;48(8):855-60.

25. Miguel Mellado GA, Álvarez C. Extraction and antioxidant activity of sericin, a protein from silk. Brazilian Journal of Food Technology. 2020;23.

26. Fan J-B, Zheng L-H, Wang F, Guo H-Y, Jiang LU, Ren F-Z. ENZYMATIC HYDROLYSIS OF SILK SERICIN BY PROTEASES AND ANTIOXIDANT ACTIVITIES OF THE HYDROLYSATES. J Food Biochem. 2010;34(2):382-98.

27. Takechi T, Wada R, Fukuda T, Harada K, Takamura H. Antioxidant activities of two sericin proteins extracted from cocoon of silkworm (Bombyx mori) measured by DPPH, chemiluminescence, ORAC and ESR methods. Biomedical reports. 2014;2(3):364-9.

28. Vázquez JA, Blanco M, Massa AE, Amado IR, Pérez-Martín RI. Production of Fish Protein Hydrolysates from Scyliorhinus canicula Discards with Antihypertensive and Antioxidant Activities by Enzymatic Hydrolysis and Mathematical Optimization Using Response Surface Methodology. Mar Drugs. 2017;15(10):306.

29. Aramwit P, Damrongsakkul S, Kanokpanont S, Srichana T. Properties and antityrosinase activity of sericin from various extraction methods. Biotechnology and Applied Biochemistry. 2010;55(2):91-8.

30. Sarkar R, Arora P, Garg KV. Cosmeceuticals for Hyperpigmentation: What is

Available? J Cutan Aesthet Surg. 2013;6(1):4-11.

31. Pandya AG, Guevara IL. DISORDERS OF HYPERPIGMENTATION. Dermatol Clin. 2000;18(1):91-8.

32. Parvez S, Kang M, Chung H-S, Cho C, Hong M-C, Shin M-K, et al. Survey and mechanism of skin depigmenting and lightening agents. Phytother Res. 2006;20(11):921-34.

33. Hida T, Kamiya T, Kawakami A, Ogino J, Sohma H, Uhara H, et al. Elucidation of Melanogenesis Cascade for Identifying Pathophysiology and Therapeutic Approach of Pigmentary Disorders and Melanoma. International Journal of Molecular Sciences. 2020;21(17).

34. Rodríguez CI, Setaluri V. Cyclic AMP (cAMP) signaling in melanocytes and melanoma. Archives of Biochemistry and Biophysics. 2014;563:22-7.

35. Kim JH, Baek SH, Kim DH, Choi TY, Yoon TJ, Hwang JS, et al. Downregulation of Melanin Synthesis by Haginin A and Its Application to In Vivo Lightening Model. Journal of Investigative Dermatology. 2008;128(5):1227-35.

36. Lee CS, Park M, Han J, Lee J-h, Bae I-H, Choi H, et al. Liver X Receptor Activation Inhibits Melanogenesis through the Acceleration of ERK-Mediated MITF Degradation. Journal of Investigative Dermatology. 2013;133(4):1063-71.

37. Qian W, Liu W, Zhu D, Cao Y, Tang A, Gong G, et al. Natural skin-whitening compounds for the treatment of melanogenesis (Review). Exp Ther Med. 2020;20(1):173-85.

38. Yi X, Zhao G, Zhang H, Guan D, Meng R, Zhang Y, et al. MITF-siRNA formulation is a safe and effective therapy for human melasma. Molecular therapy : the journal of the American Society of Gene Therapy. 2011;19(2):362-71.

39. Arango MC, Montoya Y, Peresin MS, Bustamante J, Álvarez-López C. Silk sericin as a biomaterial for tissue engineering: a review. International Journal of Polymeric Materials and Polymeric Biomaterials. 2021;70(16):1115-29.

40. Cao T-T, Zhang Y-Q. Processing and characterization of silk sericin from Bombyx mori and its application in biomaterials and biomedicines. Materials Science and Engineering: C. 2016;61:940-52.

41. Teramoto H, Nakajima K-i, Takabayashi C. Preparation of Elastic Silk Sericin

Hydrogel. Bioscience, Biotechnology, and Biochemistry. 2005;69(4):845-7.

42. Ghosh S, Rao RS, Nambiar KS, Haragannavar VC, Augustine D, Sowmya SV. Sericin, a dietary additive: Mini review. Journal of Medicine, Radiology, Pathology and Surgery. 2019.

43. Wu J-H, Wang Z, Xu S-Y. Enzymatic production of bioactive peptides from sericin recovered from silk industry wastewater. Process Biochem. 2008;43(5):480-7.

44. Kato N, Sato S, Yamanaka A, Yamada H, Fuwa N, Nomura M. Silk Protein, Sericin, Inhibits Lipid Peroxidation and Tyrosinase Activity. Bioscience, Biotechnology, and Biochemistry. 1998;62(1):145-7.

45. Padamwar M, Pawar AP. Silk sericin and its applications: A review. Journal of Scientific & Industrial Research. 2004;63:323-9.

46. Saha J, Mondal M, Sheikh MR, Habib M. Extraction, Structural and Functional Properties of Silk Sericin Biopolymer from Bombyx mori Silk Cocoon Waste. Journal of Textile Science & Engineering. 2019;09.

47. Kumar P, Kumar D, Sikka P, Dabas P. Sericin supplementation improves semen freezability of buffalo bulls by minimizing oxidative stress during cryopreservation. Animal reproduction science. 2014;152.

48. Lamboni L, Gauthier M, Yang G, Wang Q. Silk sericin: A versatile material for tissue engineering and drug delivery. Biotechnol Adv. 2015;33(8):1855-67.

49. Aramwit P, Siritientong T, Srichana T. Potential applications of silk sericin, a natural protein from textile industry by-products. Waste Management & Research. 2011;30(3):217-24.

50. Voegeli R. Sericin silk protein : unique structure and properties. Cosmetics and toiletries. 1993;108:101-8.

51. Tsubouchi K, Igarashi Y, Takasu Y, Yamada H. Sericin Enhances Attachment of Cultured Human Skin Fibroblasts. Bioscience, Biotechnology, and Biochemistry. 2005;69(2):403-5.

52. Aramwit P, Kanokpanont S, Nakpheng T, Srichana T. The effect of sericin from various extraction methods on cell viability and collagen production. International journal of molecular sciences. 2010;11(5):2200-11.

53. Kaewkorn W, Limpeanchob N, Tiyaboonchai W, Pongcharoen S,

Sutheerawattananonda M. Effects of silk sericin on the proliferation and apoptosis of colon cancer cells. Biological research. 2012;45:45-50.

54.   Zhaorigetu S, Yanaka N, Sasaki M, Watanabe H, Kato N. Inhibitory effects of silk protein, sericin on UVB-induced acute damage and tumor promotion by reducing oxidative stress in the skin of hairless mouse. J Photochem Photobiol B: Biol. 2003;71(1):11-7.

55.   Schurink M, van Berkel WJH, Wichers HJ, Boeriu CG. Novel peptides with tyrosinase inhibitory activity. Peptides. 2007;28(3):485-95.

56.   Aramwit P, Towiwat P, Srichana T. Anti-inflammatory Potential of Silk Sericin. Nat Prod Commun. 2013;8(4):1934578X1300800424.

57.   Teramoto H, Kameda T, Tamada Y. Preparation of Gel Film from Bombyx mori Silk Sericin and Its Characterization as a Wound Dressing. Bioscience, Biotechnology, and Biochemistry. 2008;72(12):3189-96.

58.   Mandal BB, Priya AS, Kundu SC. Novel silk sericin/gelatin 3-D scaffolds and 2-D films: Fabrication and characterization for potential tissue engineering applications. Acta Biomater. 2009;5(8):3007-20.

59.   Kundu SC, Dash BC, Dash R, Kaplan DL. Natural protective glue protein, sericin bioengineered by silkworms: Potential for biomedical and biotechnological applications. Prog Polym Sci. 2008;33(10):998-1012.

60.   Wang Z, Zhang Y, Zhang J, Huang L, Liu J, Li Y, et al. Exploring natural silk protein sericin for regenerative medicine: an injectable, photoluminescent, cell-adhesive 3D hydrogel. Sci Rep. 2014;4:7064-.

61.   Parisi OI, Fiorillo M, Scrivano L, Sinicropi MS, Dolce V, Iacopetta D, et al. Sericin/Poly(ethylcyanoacrylate) Nanospheres by Interfacial Polymerization for Enhanced Bioefficacy of Fenofibrate: In Vitro and In Vivo Studies. Biomacromolecules. 2015;16(10):3126-33.

62.   Zhang Y-Q, Ma Y, Xia Y-Y, Shen W-D, Mao J-P, Xue R-Y. Silk sericin–insulin bioconjugates: Synthesis, characterization and biological activity. Journal of Controlled Release. 2006;115(3):307-15.

63.   Aramwit P, Ekasit S, Yamdech R. The development of non-toxic ionic-crosslinked chitosan-based microspheres as carriers for the controlled release of silk sericin.

Biomedical Microdevices. 2015;17(5):84.

64. Khampieng T, Aramwit P, Supaphol P. Silk sericin loaded alginate nanoparticles: Preparation and anti-inflammatory efficacy. International Journal of Biological Macromolecules. 2015;80:636-43.

65. Limpeanchob N, Trisat K, Duangjai A, Tiyaboonchai W, Pongcharoen S, Sutheerawattananonda M. Sericin Reduces Serum Cholesterol in Rats and Cholesterol Uptake into Caco-2 Cells. Journal of Agricultural and Food Chemistry. 2010;58(23):12519-22.

66. Okazaki Y, Kakehi S, Xu Y, Tsujimoto K, Sasaki M, Ogawa H, et al. Consumption of sericin reduces serum lipids, ameliorates glucose tolerance and elevates serum adiponectin in rats fed a high-fat diet. Biosci Biotechnol Biochem. 2010;74(8):1534-8.

67. Seo C-W, Um IC, Rico CW, Kang MY. Antihyperlipidemic and Body Fat-Lowering Effects of Silk Proteins with Different Fibroin/Sericin Compositions in Mice Fed with High Fat Diet. Journal of Agricultural and Food Chemistry. 2011;59(8):4192-7.

68. Onsa-Ard A, Shimbhu D, Tocharus J, Sutheerawattananonda M, Pantan R, Tocharus C. Hypotensive and vasorelaxant effects of sericin-derived oligopeptides in rats. ISRN Pharmacol. 2013;2013:717529-.

69. Poljsak B, Šuput D, Milisav I. Achieving the balance between ROS and antioxidants: when to use the synthetic antioxidants. Oxid Med Cell Longev. 2013;2013:956792-.

70. Birben E, Sahiner UM, Sackesen C, Erzurum S, Kalayci O. Oxidative stress and antioxidant defense. The World Allergy Organization journal. 2012;5(1):9-19.

71. Poljšak B, Jamnik P, Polona, Raspor P, Peter, Pesti M, et al. Oxidation-antioxidation-reduction processes in the cell : impacts of environmental pollution. 2011.

72. Liu Z, Ren Z, Zhang J, Chuang C-C, Kandaswamy E, Zhou T, et al. Role of ROS and Nutritional Antioxidants in Human Diseases. Front Physiol. 2018;9:477-.

73. Zuo L, Zhou T, Pannell BK, Ziegler AC, Best TM. Biological and physiological role of reactive oxygen species – the good, the bad and the ugly. Acta Physiologica.

2015;214(3):329-48.

74. Snezhkina AV, Kudryavtseva AV, Kardymon OL, Savvateeva MV, Melnikova NV, Krasnov GS, et al. ROS Generation and Antioxidant Defense Systems in Normal and Malignant Cells. Oxid Med Cell Longev. 2019;2019:6175804-.

75. Bigarella CL, Liang R, Ghaffari S. Stem cells and the impact of ROS signaling. Development (Cambridge, England). 2014;141(22):4206-18.

76. Kharrazi H, Vaisi-Raygani A, Rahimi Z, Tavilani H, Aminian M, Pourmotabbed T. Association between enzymatic and non-enzymatic antioxidant defense mechanism with apolipoprotein E genotypes in Alzheimer disease. Clin Biochem. 2008;41(12):932-6.

77. Willett WC. The Mediterranean diet: science and practice. Public Health Nutr. 2006;9(1a):105-10.

78. Bouayed J, Bohn T. Exogenous antioxidants--Double-edged swords in cellular redox state: Health beneficial effects at physiologic doses versus deleterious effects at high doses. Oxid Med Cell Longev. 2010;3(4):228-37.

79. Lü J-M, Lin PH, Yao Q, Chen C. Chemical and molecular mechanisms of antioxidants: experimental approaches and model systems. Journal of cellular and molecular medicine. 2010;14(4):840-60.

80. Benzie IFF. Evolution of antioxidant defence mechanisms. Eur J Nutr. 2000;39(2):53-61.

81. Kim S-K, Kim Y-T, Byun H-G, Nam K-S, Joo D-S, Shahidi F. Isolation and Characterization of Antioxidative Peptides from Gelatin Hydrolysate of Alaska Pollack Skin. Journal of Agricultural and Food Chemistry. 2001;49(4):1984-9.

82. Soobrattee MA, Neergheen VS, Luximon-Ramma A, Aruoma OI, Bahorun T. Phenolics as potential antioxidant therapeutic agents: Mechanism and actions. Mutation Research/Fundamental and Molecular Mechanisms of Mutagenesis. 2005;579(1):200-13.

83. Mendis E, Rajapakse N, Kim S-K. Antioxidant Properties of a Radical-Scavenging Peptide Purified from Enzymatically Prepared Fish Skin Gelatin Hydrolysate. Journal of Agricultural and Food Chemistry. 2005;53(3):581-7.

84. Ao J, Li B. Amino acid composition and antioxidant activities of hydrolysates and

peptide fractions from porcine collagen. Food Sci Technol Int. 2012;18(5):425-34.

85. Shahidi F, Zhong Y. Lipid oxidation and improving the oxidative stability. Chemical Society Reviews. 2010;39(11):4067-79.

86. Prior RL, Wu X, Schaich K. Standardized Methods for the Determination of Antioxidant Capacity and Phenolics in Foods and Dietary Supplements. Journal of Agricultural and Food Chemistry. 2005;53(10):4290-302.

87. Shahidi F, Zhong Y. Revisiting the Polar Paradox Theory: A Critical Overview. Journal of Agricultural and Food Chemistry. 2011;59(8):3499-504.

88. Dawidowicz AL, Wianowska D, Olszowy M. On practical problems in estimation of antioxidant activity of compounds by DPPH method (Problems in estimation of antioxidant activity). Food Chem. 2012;131(3):1037-43.

89. Pisoschi AM, Cheregi MC, Danet AF. Total Antioxidant Capacity of Some Commercial Fruit Juices: Electrochemical and Spectrophotometrical Approaches. Molecules. 2009;14(1).

90. Bibi Sadeer N, Montesano D, Albrizio S, Zengin G, Mahomoodally MF. The Versatility of Antioxidant Assays in Food Science and Safety—Chemistry, Applications, Strengths, and Limitations. Antioxidants. 2020;9(8).

91. Antolovich M, Prenzler PD, Patsalides E, McDonald S, Robards K. Methods for testing antioxidant activity. Analyst. 2002;127(1):183-98.

92. Becker E, Nissen L, Skibsted L. Antioxidant evaluation protocols: Food quality or health effects. European Food Research and Technology. 2004;219:561-71.

93. Zulueta A, Esteve MJ, Frígola A. ORAC and TEAC assays comparison to measure the antioxidant capacity of food products. Food Chem. 2009;114(1):310-6.

94. Karamać M, Kosińska-Cagnazzo A, Kulczyk A. Use of Different Proteases to Obtain Flaxseed Protein Hydrolysates with Antioxidant Activity. International journal of molecular sciences. 2016;17(7):1027.

95. Rokita SE. Radical-Mediated Protein Oxidation: From Chemistry to Medicine. Michael J. Davies , Roger T. Dean. The Quarterly Review of Biology. 1999;74(1):114-5.

96. Østdal H, Davies MJ, Andersen HJ. Reaction between protein radicals and other biomolecules. Free Radical Biology and Medicine. 2002;33(2):201-9.

97. Elias RJ, Kellerby SS, Decker EA. Antioxidant Activity of Proteins and Peptides. Critical Reviews in Food Science and Nutrition. 2008;48(5):430-41.

98. Villamil O, Váquiro H, Solanilla JF. Fish viscera protein hydrolysates: Production, potential applications and functional and bioactive properties. Food Chem. 2017;224:160-71.

99. Tadesse SA, Emire SA. Production and processing of antioxidant bioactive peptides: A driving force for the functional food market. Heliyon. 2020;6(8):e04765.

100. Sohaib M, Anjum FM, Sahar A, Arshad MS, Rahman UU, Imran A, et al. Antioxidant proteins and peptides to enhance the oxidative stability of meat and meat products: A comprehensive review. International Journal of Food Properties. 2017;20(11):2581-93.

101. Thongsook T, Tiyaboonchai W. Inhibitory effect of sericin on polyphenol oxidase and its application as edible coating. International Journal of Food Science & Technology. 2011;46:2052-61.

102. Brenner M, Hearing VJ. The protective role of melanin against UV damage in human skin. Photochemistry and photobiology. 2008;84(3):539-49.

103. Alaluf S, Atkins D, Barrett K, Blount M, Carter N, Heath A. Ethnic Variation in Melanin Content and Composition in Photoexposed and Photoprotected Human Skin. Pigment Cell Research. 2002;15(2):112-8.

104. ElObeid AS, Kamal-Eldin A, Abdelhalim MAK, Haseeb AM. Pharmacological Properties of Melanin and its Function in Health. Basic Clin Pharmacol Toxicol. 2017;120(6):515-22.

105. Lee SY, Baek N, Nam T-g. Natural, semisynthetic and synthetic tyrosinase inhibitors. Journal of Enzyme Inhibition and Medicinal Chemistry. 2016;31(1):1-13.

106. D'Mello SAN, Finlay GJ, Baguley BC, Askarian-Amiri ME. Signaling Pathways in Melanogenesis. International journal of molecular sciences. 2016;17(7):1144.

107. Thomas AJ, Erickson CA. The making of a melanocyte: the specification of

melanoblasts from the neural crest. Pigment Cell & Melanoma Research. 2008;21(6):598-610.

108. Cichorek M, Wachulska M, Stasiewicz A, Tymińska A. Skin melanocytes: biology and development. Postepy dermatologii i alergologii. 2013;30(1):30-41.

109. Ando H, Niki Y, Ito M, Akiyama K, Matsui MS, Yarosh DB, et al. Melanosomes Are Transferred from Melanocytes to Keratinocytes through the Processes of Packaging, Release, Uptake, and Dispersion. Journal of Investigative Dermatology. 2012;132(4):1222-9.

110. Sansinenea E, Ortiz A. Melanin: a photoprotection for Bacillus thuringiensis based biopesticides. Biotechnology Letters. 2015;37(3):483-90.

111. Pillaiyar T, Manickam M, Jung S-H. Recent development of signaling pathways inhibitors of melanogenesis. Cellular Signalling. 2017;40:99-115.

112. Levy C, Khaled M, Fisher DE. MITF: master regulator of melanocyte development and melanoma oncogene. Trends Mol Med. 2006;12(9):406-14.

113. Jian D, Jiang D, Su J, Chen W, Hu X, Kuang Y, et al. Diethylstilbestrol enhances melanogenesis via cAMP-PKA-mediating up-regulation of tyrosinase and MITF in mouse B16 melanoma cells. Steroids. 2011;76(12):1297-304.

114. Alam MB, Bajpai VK, Lee J, Zhao P, Byeon J-H, Ra J-S, et al. Inhibition of melanogenesis by jineol from Scolopendra subspinipes mutilans via MAP-Kinase mediated MITF downregulation and the proteasomal degradation of tyrosinase. Sci Rep. 2017;7(1):45858.

115. Hu Z-M, Zhou Q, Lei T-C, Ding S-F, Xu S-Z. Effects of hydroquinone and its glucoside derivatives on melanogenesis and antioxidation: Biosafety as skin whitening agents. J Dermatol Sci. 2009;55(3):179-84.

116. Chang T-S. Natural Melanogenesis Inhibitors Acting Through the Down-Regulation of Tyrosinase Activity. Materials. 2012;5(9):1661-85.

117. Niu C, Aisa HA. Upregulation of Melanogenesis and Tyrosinase Activity: Potential Agents for Vitiligo. Molecules. 2017;22(8):1303.

118. Dobry AS, Fisher DE. The Biology of Pigmentation. In: Fisher DE, Bastian BC, editors. Melanoma. New York, NY: Springer New York; 2019. p. 21-50.

119. Arck PC, Overall R, Spatz K, Liezman C, Handjiski B, Klapp BF, et al. Towards a "free radical theory of graying": melanocyte apoptosis in the aging human hair follicle is an indicator of oxidative stress induced tissue damage. The FASEB Journal. 2006;20(9):1567-9.

120. Peng H-Y, Lin C-C, Wang H-Y, Shih Y, Chou S-T. The melanogenesis alteration effects of Achillea millefolium L. essential oil and linalyl acetate: involvement of oxidative stress and the JNK and ERK signaling pathways in melanoma cells. PLoS One. 2014;9(4):e95186-e.

121. Ko H-H, Chang Y-T, Kuo Y-H, Lin C-H, Chen Y-F. Oenothera laciniata Hill Extracts Exhibits Antioxidant Effects and Attenuates Melanogenesis in B16-F10 Cells via Downregulating CREB/MITF/Tyrosinase and Upregulating p-ERK and p-JNK. Plants. 2021;10(4).

122. Azam MS, Kwon M, Choi J, Kim H-R. Sargaquinoic acid ameliorates hyperpigmentation through cAMP and ERK-mediated downregulation of MITF in α-MSH-stimulated B16F10 cells. Biomed Pharmacother. 2018;104:582-9.

123. Bezerra MA, Santelli RE, Oliveira EP, Villar LS, Escaleira LA. Response surface methodology (RSM) as a tool for optimization in analytical chemistry. Talanta. 2008;76(5):965-77.

124. Yolmeh M, Jafari SM. Applications of Response Surface Methodology in the Food Industry Processes. Food and Bioprocess Technology. 2017;10(3):413-33.

125. Baş D, Boyacı İH. Modeling and optimization I: Usability of response surface methodology. J Food Eng. 2007;78(3):836-45.

126. Mang DY, Abdou AB, Njintang NY, Djiogue EJM, Loura BB, Mbofung MC. Application of desirability-function and RSM to optimize antioxidant properties of mucuna milk. Journal of Food Measurement and Characterization. 2015;9(4):495-507.

127. Laemmli UK, Favre M. Maturation of the head of bacteriophage T4: I. DNA packaging events. Journal of Molecular Biology. 1973;80(4):575-99.

128. Tyanova S, Temu T, Sinitcyn P, Carlson A, Hein MY, Geiger T, et al. The Perseus computational platform for comprehensive analysis of (prote)omics data. Nature

Methods. 2016;13(9):731-40.

129. Agrawal H, Joshi R, Gupta M. Isolation, purification and characterization of antioxidative peptide of pearl millet (Pennisetum glaucum) protein hydrolysate. Food Chem. 2016;204:365-72.

130. Silva FGDe, Hernández-Ledesma B, Amigo L, Netto FM, Miralles B. Identification of peptides released from flaxseed (Linum usitatissimum) protein by Alcalase® hydrolysis: Antioxidant activity. LWT - Food Science and Technology. 2017;76:140-6.

131. McNaughton BR, Gareiss PC, Jacobs SE, Fricke AF, Scott GA, Miller BL. A potent activator of melanogenesis identified from small-molecule screening. ChemMedChem. 2009;4(10):1583-9.

132. Kolbe L, Mann T, Gerwat W, Batzer J, Ahlheit S, Scherner C, et al. 4-n-butylresorcinol, a highly effective tyrosinase inhibitor for the topical treatment of hyperpigmentation. J Eur Acad Dermatol Venereol. 2013;27(s1):19-23.

133. Kang SJ, Choi BR, Lee EK, Kim SH, Yi HY, Park HR, et al. Inhibitory Effect of Dried Pomegranate Concentration Powder on Melanogenesis in B16F10 Melanoma Cells; Involvement of p38 and PKA Signaling Pathways. International journal of molecular sciences. 2015;16(10):24219-42.

134. Oh T-I, Yun J-M, Park E-J, Kim Y-S, Lee Y-M, Lim J-H. Plumbagin Suppresses α-MSH-Induced Melanogenesis in B16F10 Mouse Melanoma Cells by Inhibiting Tyrosinase Activity. International journal of molecular sciences. 2017;18(2):320.

135. Berger A, Schechter I. Mapping the active site of papain with the aid of peptide substrates and inhibitors. Philosophical Transactions of the Royal Society of London B, Biological Sciences. 1970;257(813):249-64.

136. Sprang SR, Fletterick RJ, Gráf L, Rutter WJ, Craik CS. Studies of Specificity and Catalysis in Trypsin by Structural Analysis of Site-Directed Mutants. Critical Reviews in Biotechnology. 1988;8(3):225-36.

137. Puangphet A, Tiyaboonchai W, Thongsook T. Inhibitory effect of sericin hydrolysate on polyphenol oxidase and browning of fresh-cut products. International Food Research Journal. 2015;22:1623-30.

138. da Silva JDF, Correa APF, Kechinski CP, Brandelli A. Buffalo cheese whey hydrolyzed with Alcalase as an antibrowning agent in minimally processed apple. Journal of food science and technology. 2018;55(9):3731-8.

139. Kubglomsong S, Theerakulkait C, Reed RL, Yang L, Maier CS, Stevens JF. Isolation and Identification of Tyrosinase-Inhibitory and Copper-Chelating Peptides from Hydrolyzed Rice-Bran-Derived Albumin. Journal of agricultural and food chemistry. 2018;66(31):8346-54.

140. Yuan H, Lv J, Gong J, Xiao G, Zhu R, Li L, et al. Secondary structures and their effects on antioxidant capacity of antioxidant peptides in yogurt. International Journal of Food Properties. 2018;21(1):2167-80.

141. Jandaruang J, Siritapetawee J, Thumanu K, Songsiriritthigul C, Krittanai C, Daduang S, et al. The Effects of Temperature and pH on Secondary Structure and Antioxidant Activity of Crocodylus siamensis Hemoglobin. The Protein Journal. 2012;31(1):43-50.

142. Zhu Y, Zhao X, Zhang X, Liu H, Ao Q. Amino acid, structure and antioxidant properties of Haematococcus pluvialis protein hydrolysates produced by different proteases. International Journal of Food Science & Technology. 2021;56(1):185-95.

143. Alexis A. New and Emerging Treatments for Hyperpigmentation. Journal of drugs in dermatology : JDD. 2014;13:382-5.

144. Galappatthy P, Rathnayake D. Depigmenting Agents. In: Kumarasinghe P. (eds) Pigmentary Skin Disorders. Updates in Clinical Dermatology. Springer, Cham. 2018.

145. Omar A, Gao Y, Wubulikasimu A, Arken A, Aisa HA, Yili A. Effects of trypsin-induced limited hydrolysis on the structural, functional, and bioactive properties of sericin. RSC Advances. 2021;11(41):25431-40.

146. Panyam D, Kilara A. Enhancing the functionality of food proteins by enzymatic modification. Trends in Food Science & Technology. 1996;7(4):120-5.

147. Tavano OL. Protein hydrolysis using proteases: An important tool for food biotechnology. Journal of Molecular Catalysis B: Enzymatic. 2013;90:1-11.

148. Yang NJ, Hinner MJ. Getting across the cell membrane: an overview for small

molecules, peptides, and proteins. Methods Mol Biol. 2015;1266:29-53.

149.   Yap P-G, Gan C-Y. Multifunctional Tyrosinase Inhibitor Peptides with Copper Chelating, UV-Absorption and Antioxidant Activities: Kinetic and Docking Studies. Foods. 2021;10(3):675.

150.   Zhou S, Sakamoto K. Pyruvic acid/ethyl pyruvate inhibits melanogenesis in B16F10 melanoma cells through PI3K/AKT, GSK3β, and ROS-ERK signaling pathways. Genes Cells. 2019;24(1):60-9.

151.   Kim J-K, Park K-T, Lee H-S, Kim M, Lim Y-H. Evaluation of the inhibition of mushroom tyrosinase and cellular tyrosinase activities of oxyresveratrol: comparison with mulberroside A. Journal of Enzyme Inhibition and Medicinal Chemistry. 2012;27(4):495-503.

152.   Lai X, Soler-Lopez M, Wichers HJ, Dijkstra BW. Large-Scale Recombinant Expression and Purification of Human Tyrosinase Suitable for Structural Studies. PLoS One. 2016;11(8):e0161697.

153.   Mann T, Gerwat W, Batzer J, Eggers K, Scherner C, Wenck H, et al. Inhibition of Human Tyrosinase Requires Molecular Motifs Distinctively Different from Mushroom Tyrosinase. Journal of Investigative Dermatology. 2018;138(7):1601-8.

154.   Goding C, Meyskens FL, Jr. Microphthalmic-associated transcription factor integrates melanocyte biology and melanoma progression. Clinical Cancer Research. 2006;12(4):1069-73.

155.   Kang W, Choi D, Park S, Park T. Carvone Decreases Melanin Content by Inhibiting Melanoma Cell Proliferation via the Cyclic Adenosine Monophosphate (cAMP) Pathway. Molecules. 2020;25(21):5191.

156.   Kleszczyński K, Kim T-K, Bilska B, Sarna M, Mokrzynski K, Stegemann A, et al. Melatonin exerts oncostatic capacity and decreases melanogenesis in human MNT-1 melanoma cells. Journal of Pineal Research. 2019;67(4):e12610.

157.   Netcharoensirisuk P, Umehara K, De-Eknamkul W, Chaotham C. Cajanin Suppresses Melanin Synthesis through Modulating MITF in Human Melanin-Producing Cells. Molecules. 2021;26(19):6040.

158.   Lin CB, Babiarz L, Liebel F, Kizoulis M, Gendimenico GJ, Seiberg M, et al.

Modulation of Microphthalmia-associated Transcription Factor Gene Expression Alters Skin Pigmentation. Journal of Investigative Dermatology. 2002;119(6):1330-40.

159.   Nishio T, Usami M, Awaji M, Shinohara S, Sato K. Dual effects of acetylsalicylic acid on ERK signaling and Mitf transcription lead to inhibition of melanogenesis. Molecular and Cellular Biochemistry. 2016;412(1):101-10.

APPENDICES

APPENDIX 1

Relative ROS level in human keratinocyte HaCat cells and melanoma MNT-1 cells precultured with unhydrolyzed (UHS) sericin, sericin hydrolysates (SH), or N-acetyl cysteine (NAC) for 1 h prior exposure to 1 mM hydrogen peroxide (H_2O_2) for 30 min

Treatment	Relative ROS level	
	HaCat	MNT-1
Control	1.00 ± 0.00	1.00 ± 0.00
1 mM H_2O_2	3.56 ± 0.66*	1.48 ± 0.33*
5 mM NAC + 1 mM H_2O_2	2.53 ± 0.13*	0.72 ± 0.19[#]
20 mg/mL SH + 1 mM H_2O_2	0.03 ± 0.01*, [#]	0.39 ± 0.16*, [#]
20 mg/mL UHS + 1 mM H_2O_2	0.56 ± 0.26[#]	0.51 ± 0.21*, [#]

Data represent means ± SEM of three independent experiments.

*$p < 0.05$ compared with untreated control cells.

[#]$p < 0.05$ compared with the cells treated only with H_2O_2.

APPENDIX 2

Percentage of viability in MNT-1 cells assessed by MTT assay after incubation with 0-20 mg/mL sericin hydrolysates (SH) for 24 h

Treatment	Percentage of cell viability
Control	100.00 ± 0.00
1 mg/mL SH	96.23 ± 9.56
5 mg/mL SH	96.54 ± 11.34
10 mg/mL SH	95.73 ± 3.65
20 mg/mL SH	95.08 ± 4.12

Data represent means ± SEM of three independent experiments.

*p < 0.05 compared with untreated control cells.

APPENDIX 3

Relative proliferation in MNT-1 cells assessed by crystal violet assay after incubation with 0-20 mg/mL sericin hydrolysates (SH) for 24-48 h

Treatment	Relative proliferation		
	24 h	48 h	72 h
Control	1.00 ± 0.00	1.48 ± 0.02	1.56 ± 0.16
1 mg/mL SH	1.03 ± 0.16	1.37 ± 0.07	1.43 ± 0.24
5 mg/mL SH	1.11 ± 0.06	1.40 ± 0.04	1.40 ± 0.19
10 mg/mL SH	0.98 ± 0.20	1.25 ± 0.09	1.32 ± 0.90
20 mg/mL SH	0.96 ± 0.08	0.99 ± 0.23*	1.00 ± 0.14*

Data represent means ± SEM of three independent experiments.

*$p < 0.05$ compared with untreated control cells at the same time point.

จุฬาลงกรณ์มหาวิทยาลัย

CHULALONGKORN UNIVERSITY

APPENDIX 4

Relative melanin level in MNT-1 cells after incubation with sericin hydrolysates (SH), 4-butylresorcinol or forskolin for 6-24 h.

Treatment	Relative melanin level		
	6 h	12 h	24 h
Control	1.00 ± 0.00	1.14 ± 0.00	1.69 ± 0.14
1 mg/mL SH	1.06 ± 0.21	1.22 ± 0.13	1.48 ± 0.15
5 mg/mL SH	1.03 ± 022	1.09 ± 0.08	1.23 ± 0.18**
10 mg/mL SH	0.98 ± 0.12	0.95 ± 0.09	0.95 ± 0.19****
20 mg/mL SH	0.98 ± 0.10	0.45 ± 0.26***	0.60 ± 0.10****
20 µM 4-butylresorcinol	0.70 ± 0.11*	0.57 ± 0.23**	0.61 ± 0.09****
10 µM forskolin	1.36 ± 0.10	2.02 ± 0.12****	2.51 ± 0.12****

Data represent means ± SEM of three independent experiments.

*$p < 0.05$, **$p < 0.01$, ***$p < 0.005$, ****$p < 0.001$ compared with untreated control cells at the same time point.

APPENDIX 5

Percentage of tyrosinase activity containing in the cellular lysate from human MNT-1 cells with various concentrations of sericin hydrolysates (SH)

Treatment	Percentage of tyrosinase activity
Control	100.00 ± 0.00
1 mg/mL SH	85.35 ± 0.78
5 mg/mL SH	71.77 ± 12.35
10 mg/mL SH	56.17 ± 0.05*
20 mg/mL SH	49.97 ± 0.63*

Data represent means ± SEM of three independent experiments.

*$p < 0.05$ compared with untreated control cells.

APPENDIX 6

Relative mRNA levels of MITF and tyrosinase assessed by qRT-PCR in MNT-1 cells cultured with 20 mg/mL sericin hydrolysates (SH) for 6-24 h.

mRNA	Treatment	Relative mRNA level		
		6 h	12 h	24 h
MITF	Control	1.00 ± 0.00	1.91 ± 0.16	2.40 ± 0.47
	20 mg/mL SH	1.23 ± 0.20	0.56 ± 0.23*	1.39 ± 0.43*
Tyrosinase	Control	1.00 ± 0.00	2.96 ± 0.43	2.53 ± 0.41
	20 mg/mL SH	1.77 ± 0.60	0.78 ± 0.34**	1.60 ± 0.10*

Data represent means ± SEM of three independent experiments.

*$p < 0.05$, **$p < 0.01$ compared with untreated control cells at the same time point.

จุฬาลงกรณ์มหาวิทยาลัย

CHULALONGKORN UNIVERSITY

APPENDIX 7

Relative protein levels of MITF-related proteins assessed by western blotting in MNT-1 cells cultured with 20 mg/mL sericin hydrolysates (SH) for 6-24 h.

Protein	Treatment	Relative mRNA level		
		6 h	12 h	24 h
MITF	Control	1.00 ± 0.00	0.86 ± 0.05	1.26 ± 0.07
	20 mg/mL SH	0.98 ± 0.20	0.75 ± 0.30	0.72 ± 0.15**
Tyrosinase	Control	1.00 ± 0.00	0.81 ± 0.02	1.04 ± 0.21
	20 mg/mL SH	0.79 ± 0.21	0.64 ± 0.04	0.59 ± 0.02*
pGSK3β/GSK3β	Control	1.00 ± 0.00	0.80 ± 0.01	0.88 ± 0.30
	20 mg/mL SH	0.80 ± 0.15	0.82 ± 0.03	0.95 ± 0.05
β-catenin	Control	1.00 ± 0.00	0.83 ± 0.01	0.92 ± 0.27
	20 mg/mL SH	1.00 ± 0.04	0.99 ± 0.03	1.07 ± 0.29
pCREB/CREB	Control	1.00 ± 0.00	1.61 ± 0.24	1.26 ± 0.32
	20 mg/mL SH	1.17 ± 0.08	0.79 ± 0.15*	1.15 ± 0.25
pERK/ERK	Control	1.00 ± 0.00	1.27 ± 0.04	1.33 ± 0.04
	20 mg/mL SH	1.30 ± 0.08*	1.57 ± 0.08*	1.72 ± 0.09**

Data represent means ± SEM of three independent experiments.

*$p < 0.05$, **$p < 0.01$, ***$p < 0.005$, ****$p < 0.001$ compared with untreated control cells at the same time point.

VITA

NAME	KEERATI JOYJAMRAS
DATE OF BIRTH	2 March 1985
PLACE OF BIRTH	Bangkok, Thailand
INSTITUTIONS ATTENDED	1. 2018 - present
	Ph.D. student in Pharmaceutical Sciences and Technology Programme,
	Faculty of Pharmaceutical Sciences, Chulalongkorn University, Bangkok,
	Thailand
	2. 2010 - 2015
	Master of Science in Biomedical Sciences,
	Faculty of Science, Rangsit University, Pathumthani, Thailand
	3. 2003 - 2008
	Bachelor of Science in Chemistry,
	Faculty of Science and Technology, Valaya Alongkorn Rajabhat University,
	Pathumthani, Thailand
HOME ADDRESS	12/327 Moo.4, Beungyitho, Thanyaburi, Pathumthani, Thailand, 12130
PUBLICATION	Keerati Joyjamras, Chatchai Chaotham & Pithi Chanvorachote (2022) Response surface optimization of enzymatic hydrolysis and ROS scavenging activity of silk sericin hydrolysates, Pharmaceutical Biology, 60:1, 308-318, DOI: 10.1080/13880209.2022.2032208
	Keerati Joyjamras, Ponsawan Netcharoensirisuk, Sittiruk Roytrakul, Pithi Chanvorachote & Chatchai Chaotham. (2022). Recycled Sericin Hydrolysates Modified by Alcalase® Suppress Melanogenesis in Human Melanin-Producing Cells via Modulating MITF, International Journal of Molecular Sciences 23, no. 7: 3925. https://doi.org/10.3390/ijms23073925